2012

# Studies on a dirhodium tetraphosphine hydroformylation catalyst

Darina Polakova
*Louisiana State University and Agricultural and Mechanical College*, darinca99@hotmail.com

# STUDIES ON A DIRHODIUM TETRAPHOSPHINE HYDROFORMYLATION CATALYST

A Dissertation

Submitted to the Graduate Faculty of the
Louisiana State University and
Agricultural and Mechanical College
in partial fulfillment of the
requirements for the degree of
Doctor of Philosophy
in

The Department of Chemistry

by
Darina Polakova
MSc., Czech Technical University, 2000
May 2012

ACKNOWLEDGEMENTS

I thank Prof. George G. Stanley for letting me be a part of his research group. He has had a lot of patience with me and I learned much from him. Also his help during FT-IR experiments is highly appreciated.

I thank to former and current Stanley group members Dr. Catherine Alexander, Marc Peterson, Bill Schreiter, Rider Barnum, Katerina Kalachnikova, Gregory McCandless, Cierra Duronslet and Ranelka Fernando. Thank you for your help and for not killing me when things went wrong. Catherine and Marc taught me how to synthesize the catalyst and operate high-pressure equipment. Bill provided much advice. I could not do this work without Rider Barnum, who cooperated with me on the FT-IR studies and also fixed many issues with the Parr autoclaves. I really enjoyed working with him.

I thank Dr. W. Dale Travelean, my NMR guru, without whom this work would not be possible. I also thank my committee members Dr. Julia Y. Chan, Dr. Andrew W. Maverick, Dr. William Crowe and Dr. James Board for many useful ideas and particularly Dr. Chan for encouragement over the years.

I thank Melissa Menard and her family for teaching me to eat crawfish and snowballs, ride a four-wheeler, to survive a hurricane and many other useful skills and activities. I enjoyed all of it. I also thank Udaya Rodrigo and fellow international students for help during my first year in Louisiana.

Last, but not least I thank my parents Jitka Polakova and Milan Polak, and my grandparents Drahoslava Heldova and the late Metodej Held for their support over the years. I thank my husband Greg Schelonka for love and understanding as well as his parents for patience and support.

TABLE OF CONTENTS

## ABSTRACT

The dirhodium tetraphosphine catalyst $[Rh_2(nbd)_2(rac\text{-et,ph-}P_4)](BF_4)_2$ was investigated in acetone and water/acetone in order to explain better hydroformylation results in the latter solvent. In-situ NMR spectroscopy showed slower degradation in water/acetone. Less tendency to form penta/hexacarbonyl complexes in water/acetone was shown by $^{31}P\{^1H\}$ NMR and FT-IR. A pH decrease and hydroformylation studies in presence of a base indicated formation of a monocationic monohydride species. A new reaction mechanism was suggested that takes into account the observed differences from the acetone solvent system.

The presence of water enabled production of hydride species when the dirhodium catalyst was exposed to CO gas. We believe this was caused by water-gas shift chemistry ($H_2O + CO \longrightarrow H_2 + CO_2$). However, a subsequent experiment in a Parr autoclave showed that the process was not fast or efficient enough to serve as a hydrogen source for hydroformylation.

The cationic character of the dirhodium catalyst was utilized for its attachment to the surface of silica gel. The purpose of immobilization is to enable easy separation of the catalyst from hydroformylation products. At room temperature in dichloromethane solution the immobilization was successful, but during hydroformylation conditions in acetone, the catalyst was released into solution.

CHAPTER 1: INTRODUCTION TO HYDROFORMYLATION

## 1.1 General Hydroformylation Background

Hydroformylation enables conversion of an alkene into an aldehyde. Presence of CO, $H_2$ and a metal carbonyl catalyst is necessary for the process. Otto Roelen discovered the homogeneous catalytic process in 1938.[1] The hydroformylation of a generic alkene is shown in Figure 1.1. Both linear and branched aldehydes are produced, while the linear product is usually more valuable to industry. The linear to branched ratio (L:B) is dependent upon the steric factors of the catalyst, with bulkier ligands favoring linear aldehydes (up to a point). Alkene isomerization and hydrogenation are examples of side reactions that can occur simultaneously with hydroformylation and should generally be minimized.

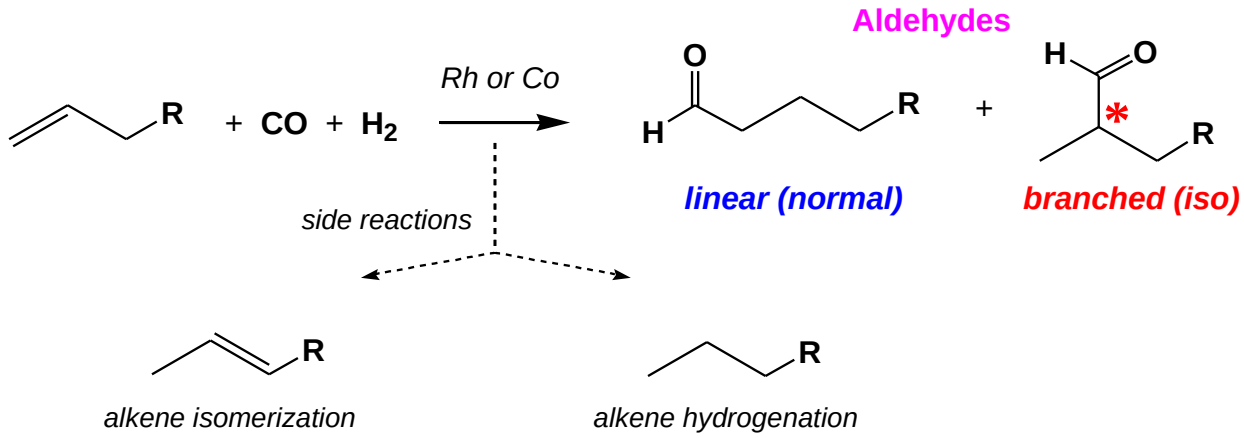


**Figure 1.1**. General scheme for hydroformylation of 1-alkene.

In industry, the aldehydes obtained by hydroformylation are usually converted into other products. Hydrogenation of the aldehydes to alcohols is a common practice for the production of solvents, plasticizers, and detergents.[2] Aldehydes are also commonly converted to amines, carboxylic acids, acroleins, diols, acetals, and ethers.[1]

The two most important industrial hydroformylation processes are the production of butyraldehyde from propylene and the hydroformylation of longer chain alkenes like 1-hexene

and 1-octene. Approximately four million tons of butyraldehyde are produced annually[3] and transformed either into 1-butanol which is used as solvent or into 2-ethylhexanol via an aldol condensation and hydrogenation. 2-ethylhexanol is used to produce plasticizers for PVC production.[2-3] Hydroformylation of terminal olefins, for example 1-octene, leads to fatty alcohols used in the production of detergents and adipate esters used as plasticizers and high temperature lubricants.[2]

Hydroformylation as an industrial process was started by Ruhrchemie in 1940s.[2] The active catalyst species is $HCo(CO)_4$; Heck and Breslow[4] published the hydroformylation mechanism for this catalyst in 1961. The process requires temperatures in range 150-180 °C and pressures 20-30 MPa.[1] As a result, this original process is often referred to as the high-pressure unmodified cobalt process. In 1966, Shell started using $Co_2(CO)_8$ modified with a proprietary bulky and electron-rich phosphine. The phosphine ligand helps stabilize the $HCo(CO)_3(PR_3)$ catalyst so that lower pressures (5-15 MPa) can be used relative to the unmodified cobalt technology.[1]

The next major advance occurred when Wilkinson determined that Rh complexes modified with phosphine ligands were far more active than cobalt and could be run under very mild conditions.[5] In 1976 the $Rh/PPh_3$ technology was first used commercially by Union Carbide[2] and is currently the main industrial hydroformylation process. Reaction conditions include temperature ranges of 60-120 °C and pressure ranges of 1-5 MPa.[1]

In 1984[2] Rhone Poulenc/Ruhrchemie started a biphasic hydroformylation process using rhodium and a water soluble ligand m-triphenylphosphinetrisulfonate TPPTS (Figure 1.2).[6] The main advantage of this process is easy separation of the catalyst from the product, but it can be used only for hydroformylation of alkenes with shorter chains due to solubility reasons.

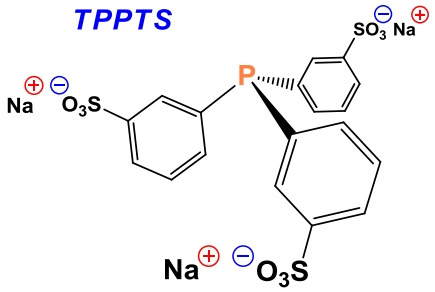


**Figure 1.2.** A water soluble ligand tris-(*m*-sulfonyl)triphenylphosphine ligand (TPPTS).

Currently industrial processes for hydroformylation of propene are based on phosphine-modified rhodium, while Co catalyzed systems are still used for the hydroformylation of internal[7] and higher molecular weight alkenes. Other metals could be used for hydroformylation, however the activity for unmodified monometallic catalysts decreases in the order Rh >> Co > Ir, Ru > Os > Pt > Pd > Fe > Ni.[2] Hydroformylation plants, therefore, use homogeneous monometallic catalysts based on Rh or Co.

The mechanism of hydroformylation employing a Rh catalyst is depicted in Figure 1.3. Excess $PPh_3$ ligand is usually used to hinder $PPh_3$ dissociation and to stabilize the selective catalyst species[8] $HRh(CO)(PPh_3)_2$. The mechanism starts with dissociation of CO from $HRh(CO)_2(PPh_3)_2$ that leads to formation of $HRh(CO)(PPh_3)_2$. This complex can coordinate the alkene and form the alkyl complex $RRh(CO)_2(PPh_3)_2$. Alkyl formation is followed by coordination of CO. Insertion of CO results in formation of acyl complex $R(O=)CRh(CO)(PPh_3)_2$. Oxidative addition of hydrogen is followed by a reductive elimination of the aldehyde product. The key catalyst species is regenerated by coordination of CO. The rate determining step is presumably the oxidative addition of hydrogen to the complex.[1]

Deactivation of the catalyst is a problem. Species with bridging phosphides are formed that are not active for hydroformylation. The initial degradation step is the oxidative insertion of Rh into the P-C bond of $PPh_3$ (Figure 1.4).[1]

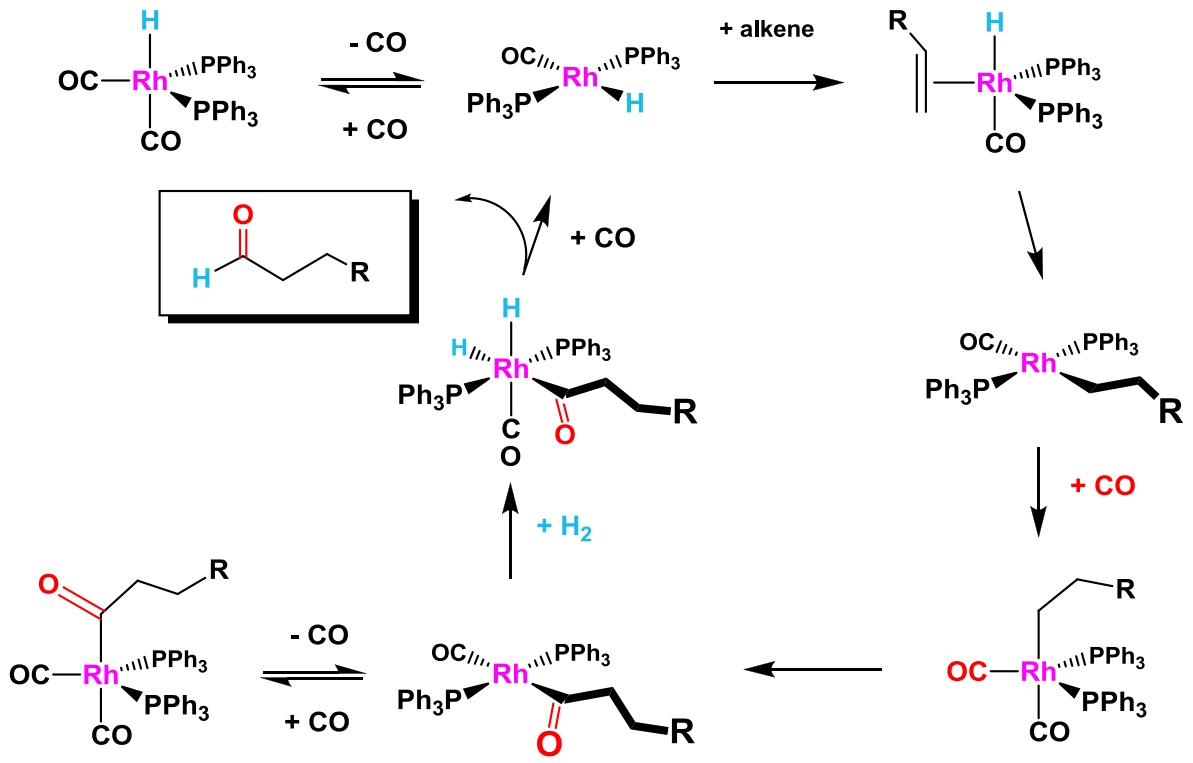


**Figure 1.3.** Core mechanism for hydroformylation with the $Rh/PPh_3$ catalyst.

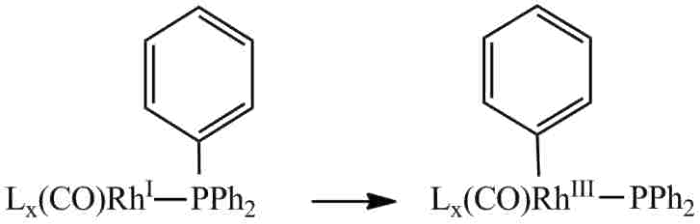


**Figure 1.4.** Degradation of $Rh/PPh_3$ catalyst.[1] The phosphide formed goes on to make phosphide-bridged Rh dimers and clusters that are inactive for hydroformylation.

Monophosphines are not the only phosphine ligand type investigated for hydroformylation purposes. Rhodium with diphosphine ligands BISBI, Naphos and Xantphos showed faster hydroformylation of 1-hexene and gave significantly higher L:B product ratio than $Rh/PPh_3$.[9] The diphosphine ligands are shown in Figure 1.5. However, these ligands suffer from Rh-induced phosphine cleavage reactions that severely limit their commercial use. Triphosphine

ligands, for example triphos $MeC(CH_2PPh_2)_3$, were also investigated for hydroformylation purposes, but do not form good catalysts. Better stereochemistry control of the catalyst complex was expected from the triphosphine ligands compared to diphosphines that should result in improved hydroformylation regiochemistry. However, this is not the case due to the dissociation of one of the arms of the triphosphine ligand from the Rh center, i.e. "arm-off" process.[10]

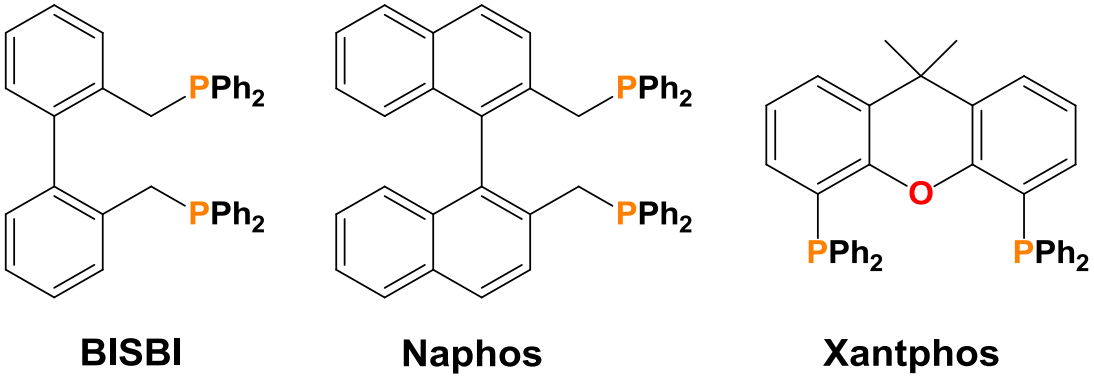


**Figure 1.5.** Diphosphine ligands.

### 1.2 Dirhodium Catalyst Based on a Tetraphosphine Ligand et,ph-P4

Laneman and coworkers designed the ligand $Et_2PCH_2CH_2P(Ph)CH_2P(Ph)CH_2CH_2PEt_2$ (et,ph-P4) in 1988 to bridge and chelate two metal atoms.[11] The tetraphosphine ligand is shown in Figure 1.6. Since the internal phosphines are chiral, racemic (*R*,*R* and *S*,*S*) and meso (*R*,*S*) diastereomers exist.

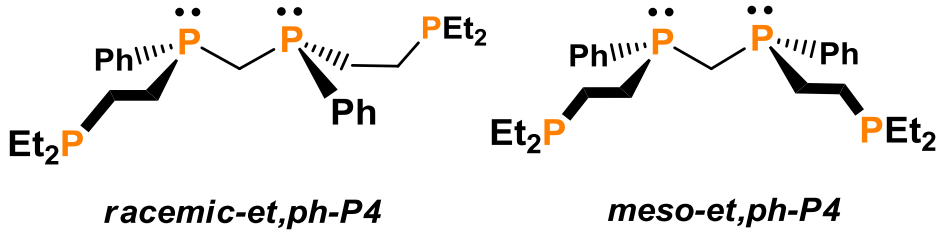


**Figure 1.6.** *Rac*- and *meso*-et,ph-P4 ligands.

The motivation for the work was to study the possibility of bimetallic cooperativity that could produce a better catalyst system relative to monometallic complexes. Cooperation between

the two metal centers is expected to occur due to the bridging tetraphosphine ligand that can hold the metal centers in close proximity. Bimetallic cooperativity in homogeneous catalysis has been an area of interest for quite some time, because it can enable different reaction pathways[12] with a substrate relative to the monometallic complexes. Prior to et,ph-P4, a hexatertiary phosphine ligand was designed and studied along with a number of bimetallic complexes based on it (Figure 1.7). However, due to steric hindrance effects and coordination of the metal centers by three phosphine ligands no catalytic reactions were observed. Therefore, attention was focused on the synthesis of the less hindered and more "open" tetraphosphine ligand.[11]

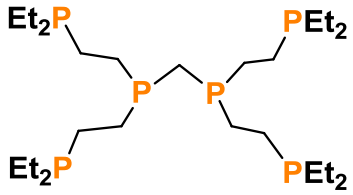


**Figure 1.7.** A hexatertiary phosphine ligand.

Et,ph-P4 is synthesized in several steps shown in Figure 1.8. The bridging bis(phosphino)methane intermediate, $Ph(H)PCH_2P(H)Ph$, is prepared by reaction of phenylphosphine ($PhPH_2$), KOH (to deprotonate the $PhPH_2$), and dichloromethane in dimethylformamide (DMF). The produced bis(phosphine)methane reacts quantitatively with two equivalents of $R_2PCH{=}CH_2$ under UV irradiation (Xenon lamp) to produce et,ph-P4.[13] The catalyst precursor for hydroformylation, $[Rh_2(nbd)_2(\textit{rac}\text{-et,ph-P}_4)](BF_4)_2$, is formed when et,ph-P4 reacts with two equivalents of $[Rh(nbd)_2]BF_4$ (nbd = norbornadiene) as shown in Figure 1.9.[13]

$[Rh_2(nbd)_2(\textit{rac}\text{-et,ph-P}_4)](BF_4)_2$ catalyst has been used for the hydroformylation of the following alkenes: ethylene, propylene, 1-butene, 1-pentene, 1-hexene, 1-heptene and 1-octene. Lower activity and increased isomerization was reported for alkenes with an odd number of carbons. Other substrates investigated are ethyl vinyl ether, butyl vinyl ether, vinyl phenyl ether,

N-methyl-N-vinylacetamide, N,N-dimethylacrylamide, acrylamide, 2,3-dihydrofuran. While none of these substrates was significantly hydroformylated, isoprene and 1,3-butadiene did not produce any aldehyde at all. Hydroformylation of norbornadiene and allyl alcohol were also previously attempted.[14]

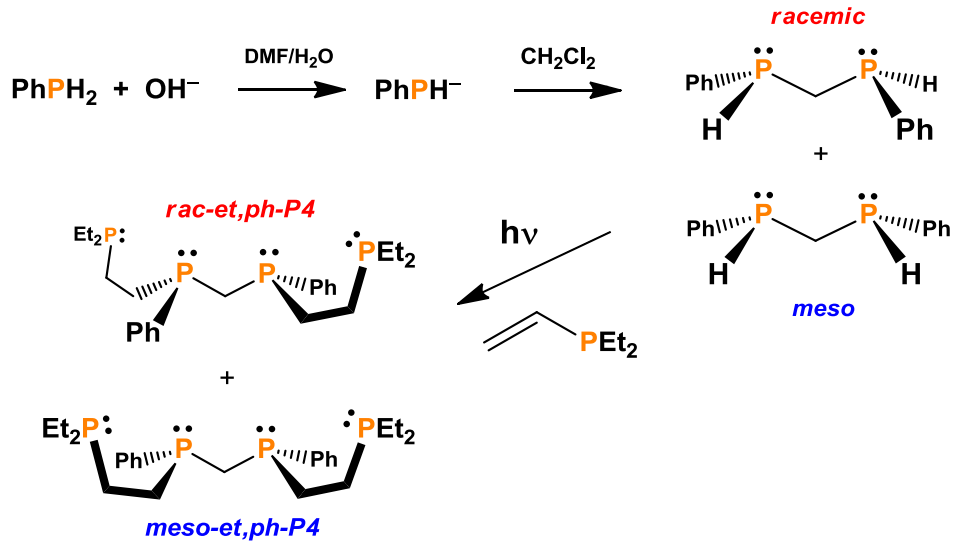


**Figure 1.8.** Ligand synthesis.

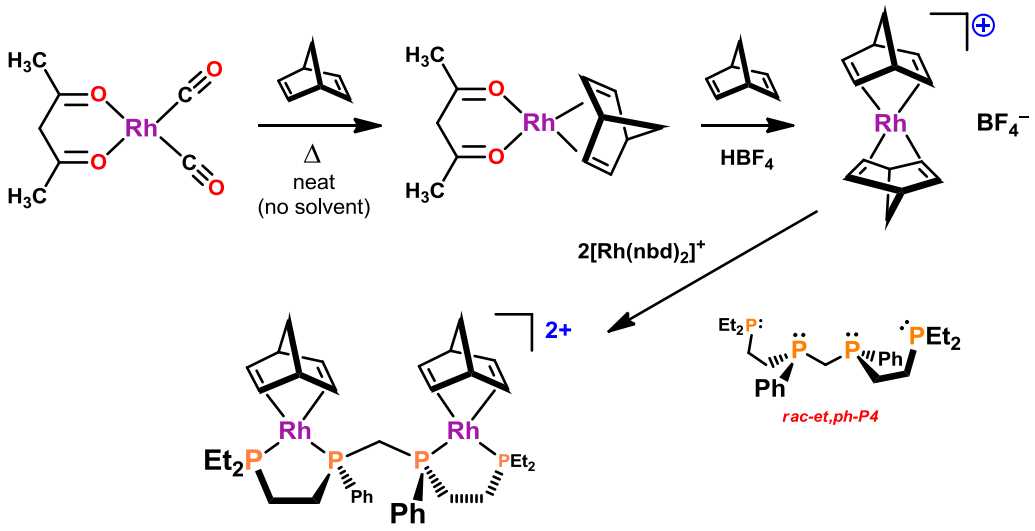


**Figure 1.9**. Preparation of the catalyst precursor $[Rh_2(nbd)_2(rac\text{-et,ph-P}_4)](BF_4)_2$.

Prof. Stanley's proposed bimetallic hydroformylation mechanism for a generic 1-alkene in acetone is shown in Figure 1.10. The proposed key hydride species that reacts with alkene is

$[Rh_2H_2(\mu\text{-}CO)_2(rac\text{-}et,ph\text{-}P_4)]^{2+}$ (**2** in Figure 1.10). It forms from the catalyst precursor under $H_2$/CO pressure.[15] Bimetallic cooperativity occurs when a hydride is transferred from one Rh center to another (structures A, 2* and 2) in order to have one hydride on each metal center. Bimetallic cooperativity also occurs for the reductive elimination of aldehyde from structure D.

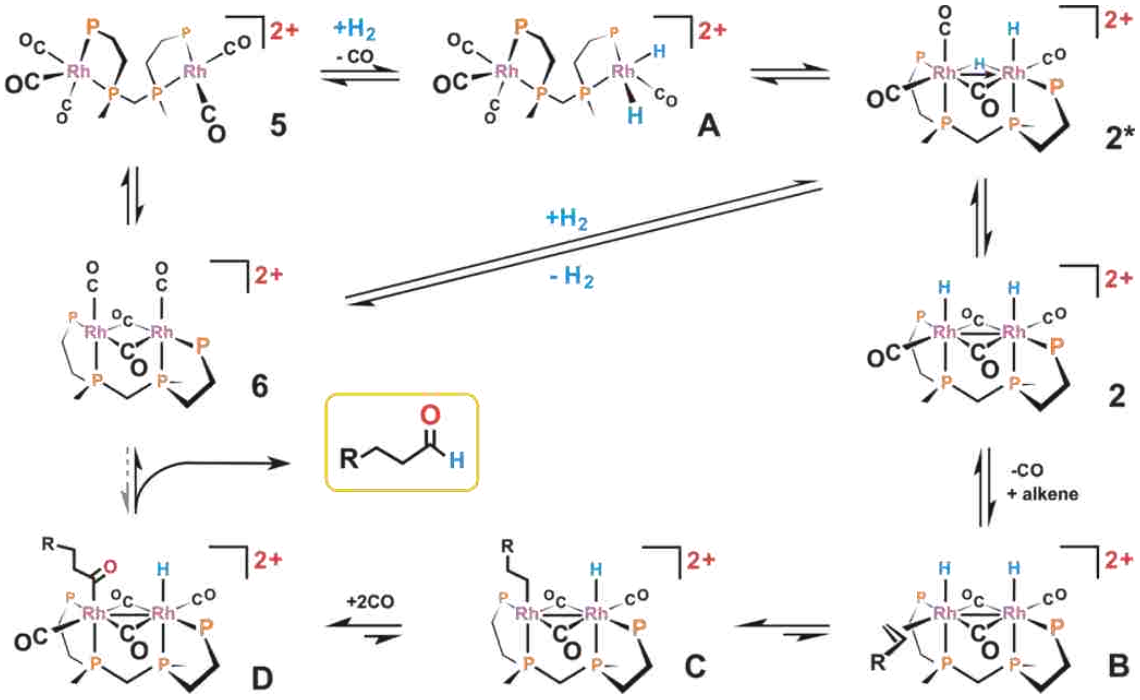


**Figure 1.10.** Proposed mechanism for the bimetallic[13] catalyst $[Rh_2H_2(\mu\text{-}CO)_2(et,ph\text{-}P_4)]^{2+}$.

Performance of the dirhodium catalyst compared to the industrial catalyst was previously reported for hydroformylation of 1-hexene. The results are shown in Table 1.1.

**Table 1.1.** Comparison of catalysts for hydroformylation of 1-hexene in acetone.[16]

| Catalyst | Initial TOF ($min^{-1}$)[a] | L:B ratio | Isomerization (%) | Hydrogenation (%) |
|---|---|---|---|---|
| $Rh_2(nbd)_2(rac\text{-}et,ph\text{-}P_4)^{2+}$ | 10.6(5) | 27.5(8) | 8(1) | 3.4(3) |
| $Rh(acac)(CO)_2$/(0.82M $PPh_3$) | 9(1) | 17(2) | 2.5(4) | 2.8(3) |
| $Rh_2(nbd)_2(meso\text{-}et,ph\text{-}P_4)^{2+}$ | 0.9(1) | 14(2) | 4.1(7) | 2.3(3) |

[a] TOF = turnover frequency; reaction conditions: 90 °C, 90 psig 1:1 $H_2$/CO, 1 mM catalyst; 1 M alkene.

Table 1.1 shows that the *racemic* form of the bimetallic catalyst gives higher linear-to-branched ratio for the aldehyde product than the commercially used $Rh/PPh_3$ system, while the *meso-* form is the worst of the three catalysts under study.[16]

All the data collected so far support bimetallic cooperativity in the hydroformylation mechanism for the *rac*-dirhodium catalyst. After addition of small amounts of $PPh_3$ to the dirhodium catalyst in acetone Aubry and Monteil observed a decrease both in the activity of the catalyst as well as a dramatic drop in aldehyde regioselectivity.[17] This is exactly opposite to the monometallic $Rh/PPh_3$ catalyst system, where an excess of the phosphine ligand improves the performance of the catalyst. Other experiments were performed with the biphosphine ligands: $Et_2PCH_2CH_2PEt_2$ (depe), $Et_2PCH_2CH_2(Me)Ph$ (depmpe), $Et_2PCH_2CH_2PPh_2$ (dedppe) and $Ph_2PCH_2CH_2PPh_2$ (dppe) (Figure 1.11), which represent half of the bimetallic catalyst and cover a range of steric and electronic factors.[16]

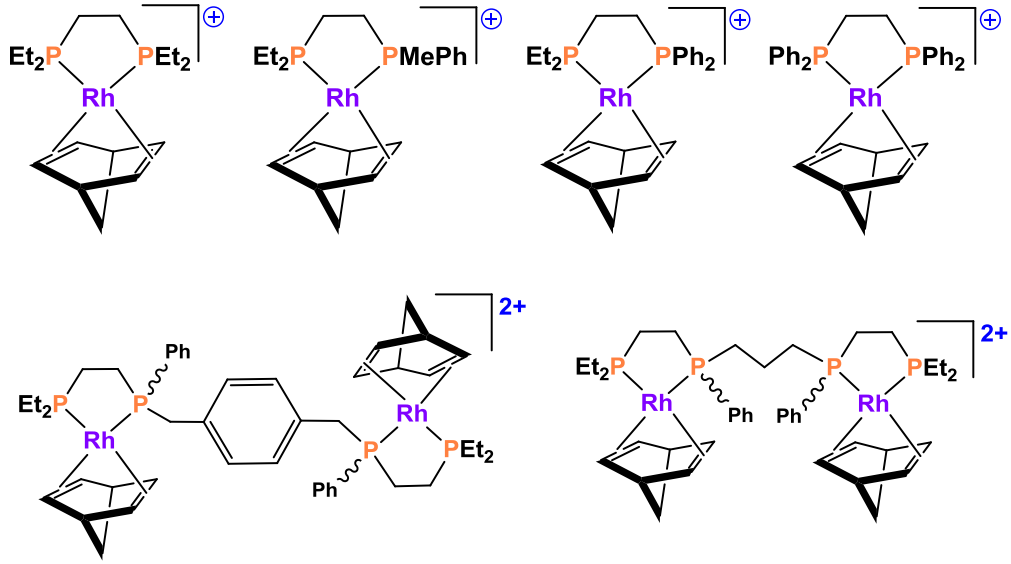


**Figure 1.11.** Monometallic and bimetallic variations of $[Rh_2(nbd)_2(et,ph\text{-}P_4)](BF_4)_2$.

All four monometallic systems showed extremely poor hydroformylation results. The last, but probably the most convincing were experiments with tetraphosphine ligands that

increased the distance between the Rh centers. The methylene bridge in the tetraphosphine ligand was substituted by either a *p*-xylene spacer (et,ph-P4-*p*-xylylene) or 1,3-propylene spacer (et,ph-P4-propylene). Dirhodium complexes with these "spaced" tetraphosphine ligands also proved to be extremely poor hydroformylation catalysts.[16]

Novella Bridges and David Aubry found that the addition of 30% water (by volume) to the acetone solvent improved both the selectivity and activity of the dirhodium catalyst.[9] The initial motivation was to create a polar solvent system that could allow the non-polar heptaldehyde product to phase separate out. Separation of products and homogeneous catalysts remains a serious problem for large-scale industrial reactions. Although it was found that the product did nicely phase separate from the water/acetone solvent, unfortunately the dirhodium catalyst is more soluble in the aldehyde product phase than in acetone/water. The reaction mixture after hydroformylation is shown in figure 1.12. The bottom yellow phase contains acetone and water and a small amount of catalyst, while the top phase is formed by aldehyde products and a considerably higher concentration of the rhodium tetraphosphine complexes.[18]

**Figure 1.12.** The two phases after hydroformylation.[18]

Previous hydroformylation and NMR studies have indicated that the dirhodium catalyst suffers from a serious fragmentation problem.[9, 15] However, it is a different fragmentation

problem relative to that seen in monometallic Rh/phosphine catalyst systems where Rh-induced phosphine-phenyl and phosphine-benzyl ring cleavage reactions lead to inactive phosphide-bridged Rh dimers and clusters. The dirhodium catalyst fragments by losing one of the Rh centers, which results in inactive monometallic or double-P4 ligand coordinated bimetallic systems that are very poor hydroformylation catalysts. The proposed scheme for the bimetallic fragmentation is shown in Figure 1.13. The first step is the dissociation of the $PEt_2$-chelate arm and CO addition to produce complex **A.** The lower electron-density on A promotes the reductive elimination of $H_2$, leading to complex **B** that does not have any hydride ligands and is inactive for hydroformylation. A rhodium atom can be lost[13] from the complex B, giving complexes **2** and **3** (Figure 1.13). The structure of **3** is extremely tentative and will be discussed in a later chapter.

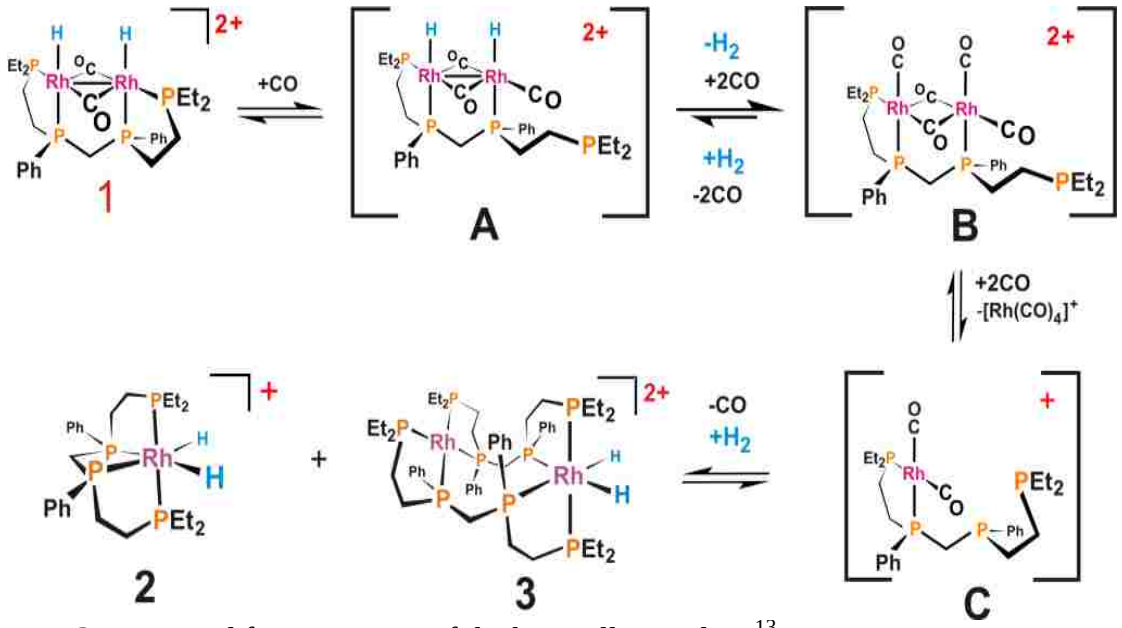


**Figure 1.13.** Proposed fragmentation of the bimetallic catalyst.[13]

A new tetraphosphine ligand et,ph-P4-Ph was developed by Alexander Monteil to reduce the dissociation of a $PEt_2$ chelate arm mentioned above (Figure 1.14).[19] Unfortunately, separation of the *racemic*- and *meso*-diastereomers of the new ligand has been so far unsuccessful. As a

result, the dirhodium complex of et,ph-P4-Ph has not yet been investigated for hydroformylation. Currently there is work in progress to improve the synthesis of et,ph-P4-Ph and to work out its separation and purification.

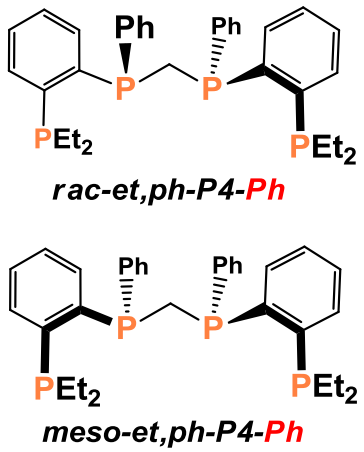


**Figure 1.14.** Et,ph-P4-Ph.[19]

In conclusion, the *rac*-dirhodium catalyst shows excellent catalytic performance comparable to the best industrial Rh/phosphine-based catalyst, but it is more difficult to prepare, it is more expensive, and it suffers from a different type of fragmentation that nonetheless still leads to catalyst deactivation. The advantages of the *rac*-dirhodium catalyst include: highly effective bimetallic cooperativity, lack of need for excess ligand, no rhodium-induced P-C bond cleavage reactions (fragmentations), and the possibility of highly tunable and efficient asymmetric hydroformylation.

Concerning stability, the dirhodium catalyst showed a very different type of fragmentation than the monometallic catalyst. One of the aims of this thesis is to spectroscopically investigate the dirhodium catalyst in 30% water/acetone and compare it to the known behavior in acetone. While Aubry[9] and Bridges did the initial research on the better catalyst performance in water/acetone and proposed reasons for this, it turns out that the reasons are considerably different from those initially proposed. High-pressure nuclear magnetic

resonance (NMR, Chapter 2) and Fourier transform infrared spectroscopy (FT-IR, Chapter 3) are employed to explain the effect and possible differences in hydroformylation mechanism compared to the acetone solvent (Chapter 6).

Water has also been studied as possible source of hydride necessary for the production of the hydroformylation active species instead of hydrogen gas (Chapter 4). This is the water-gas shift reaction (WGSR), when water and carbon monoxide can react in the presence of a suitable catalyst to produce hydrogen and carbon dioxide. Some rhodium phosphine complexes were reported being active for WGSR.[20]

Another research direction was an attempt to immobilize the dirhodium catalyst on the surface of silica gel (Chapter 5). The immobilization could enable easier separation of the catalyst from the reaction mixture and recycling the catalyst. Difficulties for the immobilization of monometallic Rh were already reported.[21] Due to its cationic character, the tetraphosphine dirhodium catalyst could be immobilized on a silica surface via hydrogen bonding of the $BF_4^-$ anions to the surface Si-OH groups. Similar immobilization was already performed for a $BF_4^-$ salt of palladium.[22]

### 1.3 References


1. Cornils, B.; Herrmann, W.A. *Applied Homogeneous Catalysis with Organometallic Compounds*. Wiley: 2002.
2. Whyman, R. *Applied Organometallic Chemistry and Catalysis*. Oxford University Press: 2001.
3. Parshall, G. W. *Homogeneous Catalysis: The Applications and Chemistry of Catalysis by Soluble Transition Metal Complexes*. Wiley: 1992.
4. Heck, R. F.; Breslow, D. S. *J. Am. Chem. Soc.* **1961,** *83* (19), 4023-4027.
5. (a) Brown, C. K.; Wilkinson, G. *J. Chem. Soc. A* **1970**, 2753-2764; (b) Brown, C. K.; Wilkinson, G., *Tetrahedron Lett.* **1969,** *10*, 1725-1726; (c) Evans, D.; Osborn, J. A.; Wilkinson, G., *J. Chem. Soc. A* **1968**, 3133-3142.
6. Kohlpaintner, C. W.; Fischer, R. W.; Cornils, B. *Appl. Catal. A-Gen.* **2001,** *221* (1-2), 219-225.

7. Leeuwen, P. W. N. M. v.; Claver, C. *Rhodium Catalyzed Hydroformylation*. Kluwer: 2000.

8. Pruett, R. L.; Smith, J. A. *J. Org. Chem.* **1969,** *34* (2), 327-330.

9. Aubry, D. A.; Bridges, N. N.; Ezell, K.; Stanley, G. G. *J. Am. Chem. Soc.* **2003,** *125* (37), 11180-11181.

10. (a) Bianchini, C.; Meli, A.; Peruzzini, M.; Vizza, F.; Fujiwara, Y.; Jintoku, T.; Taniguchi, H. *J. Chem. Society Chem. Comm.* **1988,** (4), 299-301; (b) Bianchini, C.; Frediani, P.; Sernau, V. *Organometallics* **1995,** *14* (12), 5458-5459; (c) Bianchini, C.; Frediani, P.; Meli, A.; Peruzzini, M.; Vizza, F. *Chem. Ber. Recueil* **1997,** *130* (11), 1633-1641.

11. Laneman, S. A.; Fronczek, F. R.; Stanley, G. G. *J. Am. Chem. Soc.* **1988,** *110* (16), 5585-5586.

12. (a) Lorenzini, F.; Hindle, K. T.; Craythorne, S. J.; Crozier, A. R.; Marchetti, F.; Martin, C. J.; Marr, P. C.; Marr, A. C. *Organometallics* **2006,** *25* (16), 3912-3919; (b) Davis, A. L.; Goodfellow, R. J. *Chem. Soc. Dalton Trans.* **1993,** (15), 2273-2278.

13. Alexander, C. T., PhD Thesis, Louisiana State University, 2009.

14. Train, S., PhD Thesis, Louisiana State University, Baton Rouge, 1994.

15. Matthews, R. C.; Howell, D. K.; Peng, W. J.; Train, S. G.; Treleaven, W. D.; Stanley, G. G. *Angew. Chem. Int. Ed.* **1996,** *35* (19), 2253-2256.

16. Broussard, M. E.; Juma, B.; Train, S. G.; Peng, W. J.; Laneman, S. A.; Stanley, G. G. *Science* **1993,** *260* (5115), 1784-1788.

17. Aubry, D. A.; Monteil, A. R.; Peng, W. J.; Stanley, G. G. *C. R. Chimie* **2002,** *5* (5), 473-480.

18. Aubry, D., PhD Thesis, Louisiana State University, 2004.

19. Monteil, A., PhD Thesis, Louisiana State University, 2006.

20. Kubiak, C. P.; Eisenberg, R. *J. Am. Chem. Soc.* **1980,** *102* (10), 3637-3639.

21. Sandee, A. J.; Reek, J. N. H.; Kamer, P. C. J.; van Leeuwen, P. *J. Am. Chem. Soc.* **2001,** *123* (35), 8468-8476.

22. Wiench, J. W.; Michon, C.; Ellern, A.; Hazendonk, P.; Iuga, A.; Angelici, R. J.; Pruski, M. *J. Am. Chem. Soc.* **2009,** *131* (33), 11801-11810.

# CHAPTER 2: HIGH-PRESSURE NMR STUDIES

## 2.1. Previous Assignments in Acetone

High-pressure NMR spectroscopy is a technique used to study the mechanism of reactions that take place under gas pressure. Since the samples have to be under high-pressure during NMR measurement, special NMR tubes of various designs were developed for this use.[1] Our studies are in the range of 90 to 300 psig and for this fairly low set of pressures a commercial Wilmad "high-pressure" NMR tube is used.

NMR studies on various rhodium phosphine[1-2] and phosphite[3] systems related to catalysis have been reported. One of the most studied monophosphine ligands is triphenylphosphine ($PPh_3$). When $HRh(CO)(PPh_3)_3$ was placed under CO atmosphere, Brown and Kent observed mainly complex $HRh(CO)_2(PPh_3)_2$ that exists in two isomers.[2b] Bianchini was able to detect four resting states for the same catalyst precursor.[2c] Rhodium complexes with diphosphine ligands, for example BISBI and Xantphos, were also studied by NMR for hydroformylation purposes. These studies are valuable because they can provided information about the orientation of the diphosphine in the complex, which can be either diequatorial or equatorial-apical. It also brings information about the effect of phosphine basicity and bite-angle when the ligands were modified.[4] Rhodium complexes with triphosphine ligands as $MeC(Ch_2PPh_2)_3$ and $PhP(CH_2CH_2PPh_2)_2$ were also investigated by NMR for hydroformylation applications[5] and studies of rhodium complex with a tetraphosphine ligand Tetraphos were published in connection to hydrogenation.[6]

The *rac*-dirhodium tetraphosphine hydroformylation catalyst in acetone was previously investigated via NMR. Even though the main purpose of my work is to concentrate on the acetone/water solvent system, the results in acetone need to be discussed in order to put the

current studies in context. I will summarize here briefly the previous experiments and structural assignment of the complexes in acetone by Rhonda Matthews[7] and Petia Gueorguieva.[8] Results of my experiments in acetone, which focused mainly on one of the degradation products, are summarized in Section 2.2. Results in water/acetone are described in Section 2.3.

The *rac*-dirhodium tetraphosphine catalyst in acetone was previously investigated via $^{31}P\{^{1}H\}$, $^{1}H$, $^{31}P\{^{1}H\}$-$^{31}P\{^{1}H\}$ correlation spectroscopy (COSY), heteronuclear broad-band and selective decoupling experiments $^{1}H\{^{31}P\}$NMR, nuclear Overhauser effect (NOE), and heteronuclear multiple bond correlation spectroscopy (HMBC).[7a, 8]

$^{1}H$ and $^{31}P$ NMR spectroscopy were used because the dirhodium tetraphosphine catalyst contains hydrides and phosphorus atoms. $^{31}P$ NMR spectra are usually collected in broad-band $^{1}H$ decoupled mode so only P-P and Rh-P couplings appear in such spectra. Unfortunately, $^{31}P\{^{1}H\}$ NMR spectrum of $[Rh_2(nbd)_2(rac\text{-et,ph-}P_4)](BF_4)_2$ is quite complicated because there are several species present at the same time. Homonuclear $^{31}P\{^{1}H\}/^{31}P\{^{1}H\}$ COSY is quite useful in this case because phosphorus atoms that belong to one particular species will appear as connected cross-peaks.

Figure 3.1 shows a $^{31}P\{^{1}H\}$ spectrum of a dirhodium catalyst in acetone at 250 psig $H_2$/CO recorded by Petia Gueorguieva.[8] There are several species present, including the key hydride-containing catalyst species, the $[Rh_2(CO)_5(rac\text{-et,ph-P4})]^{2+}$ resting state of the catalyst, and degradation products.

The $^{31}P$ peaks at 59.9 and 72.4 ppm appeared immediately after pressurizing the tube with $H_2$/CO gas and showed connectivity in the homonuclear $^{31}P\{^{1}H\}$ COSY spectrum. The structure was assigned as an open mode pentacarbonyl complex $[Rh_2(CO)_5(rac\text{-et,ph-P4})]^{2+}$ that

is in a rapid CO-based equilibrium with the tetra- and hexa-carbonyl complexes. This structure has been confirmed by X-ray analysis of the crystals grown from dichloromethane solvent.[7a]

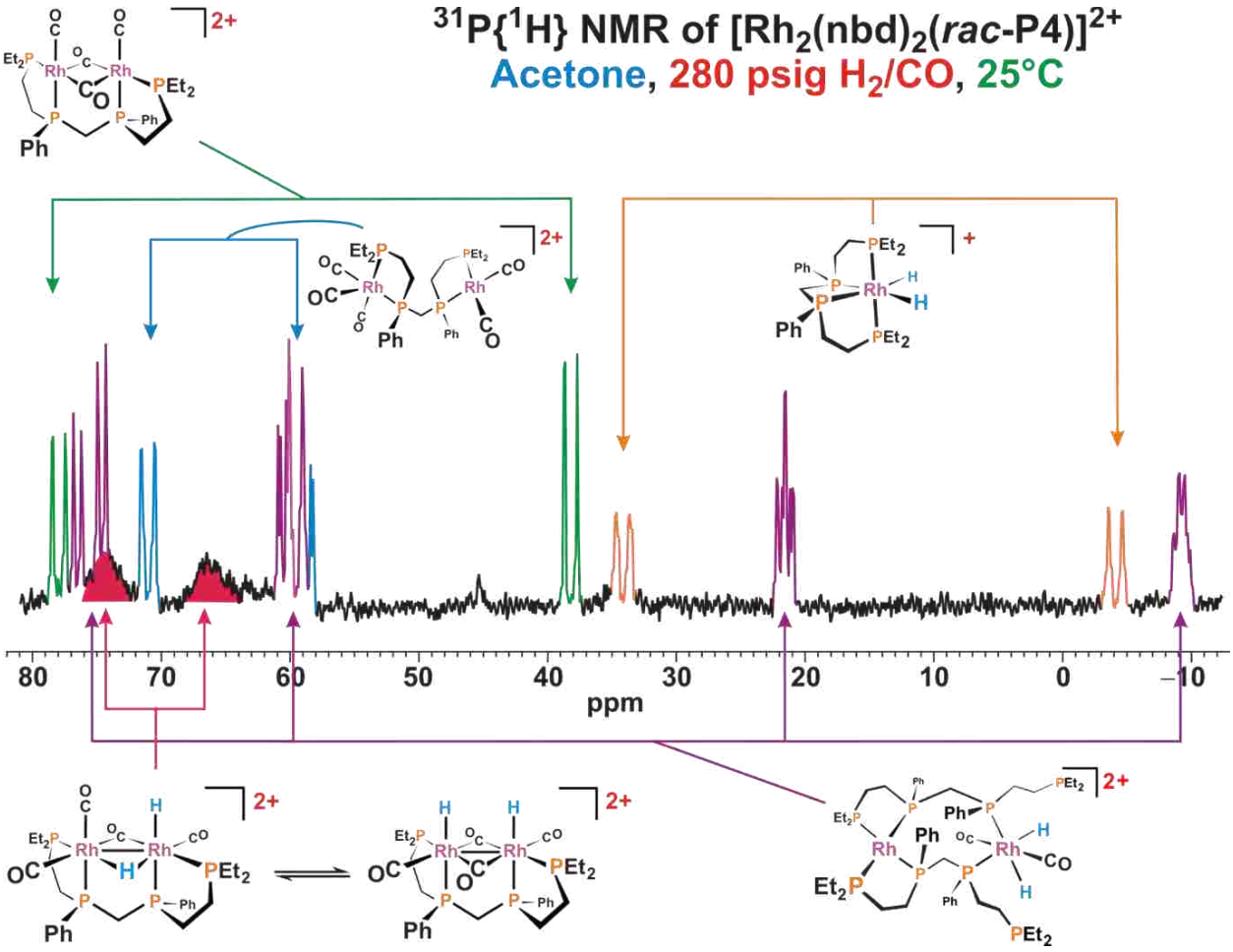


**Fig. 2.1.** $^{31}P\{^{1}H\}$ NMR of $[Rh_2(nbd)_2(rac\text{-et,ph-P4})](BF_4)_2$ under 250 psig $H_2/CO$.[8]

The broad $^{31}P$ peaks at 68 and 75 ppm in $^{31}P\{^{1}H\}$ spectrum also appeared immediately after pressurizing the tube, but did not show any correlation in $^{31}P\{^{1}H\}$ COSY. Moreover, $^{1}H$ NMR showed two broad hydride species after filling the tube with $H_2/CO$ gas at room temperature. Based on the results of $^{31}P\{^{1}H\}$ NMR, variable temperature $^{1}H$ NMR, $^{31}P\{^{1}H\}$COSY and NOE experiments, an equilibrium between complexes $[Rh_2H_2(CO)_2(\mu\text{-}CO)_2(rac\text{-et,ph-P4})]^{2+}$ and $[Rh_2(\mu\text{-}H)(\mu\text{-}CO)H(CO)_3(rac\text{-et,ph-P4})]^{2+}$ was proposed.[8] The

complex $[Rh_2H_2(CO)_2(\mu\text{-}CO)_2(rac\text{-et-ph-P4})]^{2+}$ is believed to be the key complex at higher temperatures that reacts with alkene.

The peaks at 77.4 and 39.0 did not show any correlations in $^{31}P\{^1H\}$ COSY, but always appear together and in the same intensity ratio, which indicates that they are related. Even though the peaks do not show correlation to any hydrides in $^1H$ NMR, this species does not form when $[Rh_2(CO)_4(rac\text{-et,ph-P4})]^{2+}$ is placed under CO pressure, which means that it must be related in some way to the hydride complexes. This is also supported by the fact that the peaks are not present immediately after filling the tube. The structure of the complex was assigned as a closed mode tetracarbonyl complex $[Rh_2(CO)_2(\mu\text{-}CO)_2(et,ph\text{-}P4)]^{2+}$.[7a] Bridging carbonyls have only been observed in the FT-IR studies when $H_2$ is present. We have proposed that conversion from the open-mode carbonyl complex $[Rh_2(CO)_5(rac\text{-et,ph-P4})]^{2+}$ can only occur after $H_2$ addition. Molecular modeling studies performed by Prof. Stanley indicate a very low rotational energy barrier for the formation of bridged hydride and carbonyl complexes once $H_2$ has oxidatively added to one of the rhodium centers.

The peaks at −3.3 and 35.0 ppm in the $^{31}P\{^1H\}$ NMR showed a correlation in the $^{31}P\{^1H\}$ COSY spectrum. The upfield peaks at −3.3 ppm are proposed to be due to the four-membered bis(phosphine)methane chelate ring[9] and phosphines *trans* to the hydrides. It was indeed found by a selective decoupling experiment that the above peaks in a $^{31}P$ spectrum correlate to a pseudo-decet hydride at −18.3 ppm in the $^1H$ NMR.[7a] The hydride pattern also collapsed to a doublet of doublets during broad-band phosphorus decoupling in dichloromethane. A symmetrical species with two types of phosphorus atoms and two hydrides $[RhH_2(\kappa^4\text{-}rac\text{-et,ph-P4})]^+$ was proposed as the structure (Figure 2.2). This assignment is supported by the fact that the $^{31}P\{^1H\}$ NMR pattern of this complex is very similar to the spectrum of $[RhCl_2(\kappa^4\text{-}rac\text{-et,ph-}$

P4)]$^{+}$ prepared and characterized via NMR and single crystal structures by Clinton Hunt.[10] Since this complex does not form immediately after filling the tube with gas, it is assumed that it is a product of the degradation of the active catalyst. This complex is also relatively stable because it remains in the NMR tube after release of gas pressure.

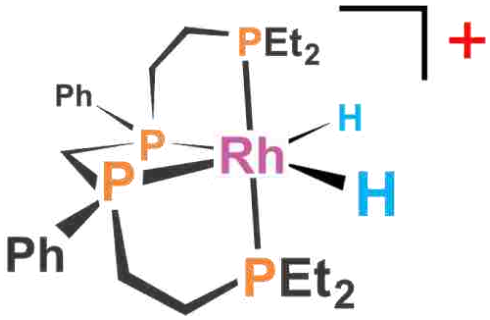


**Figure 2.2.** The monometallic degradation product [$RhH_2$($\kappa^4$-*rac*-et,ph-P4)]$^{+}$.

We believe that another degradation product exists. The peaks at −7.9, 22.5, 61.5 and 77 ppm showed a clear correlation in the $^{31}P\{^{1}H\}$-$^{31}P\{^{1}H\}$ COSY.[8] This indicates that these peaks belong to the same complex. Also these peaks are not present immediately after filling the NMR tube with gas, which support the assumptions that the complex is a degradation product of the catalyst.

Rhonda Matthews performed broad-band and selective decoupling experiments in order to determine whether the complex contains hydride ligands. During broad-band $^{1}H\{^{31}P\}$ NMR decoupling the doublet of quartets in the hydride region of $^{1}H$ NMR spectrum collapsed into a doublet of doublets with a large coupling constant 164 Hz (Figure 2.3).[7a] It was also shown that the hydride pattern was the same on 250 and 700 MHz spectrometer.[8]

A narrow-band $^{1}H\{^{31}P\}$ NMR decoupling experiment (Figure 2.4) showed that there is a correlation between this doublet of quartet hydride resonances and $^{31}P$ resonances 77.0 ppm, 61.5 ppm and −7.9 ppm. The correlation to the −7.9 ppm $^{31}P\{^{1}H\}$ peak was particularly surprising.

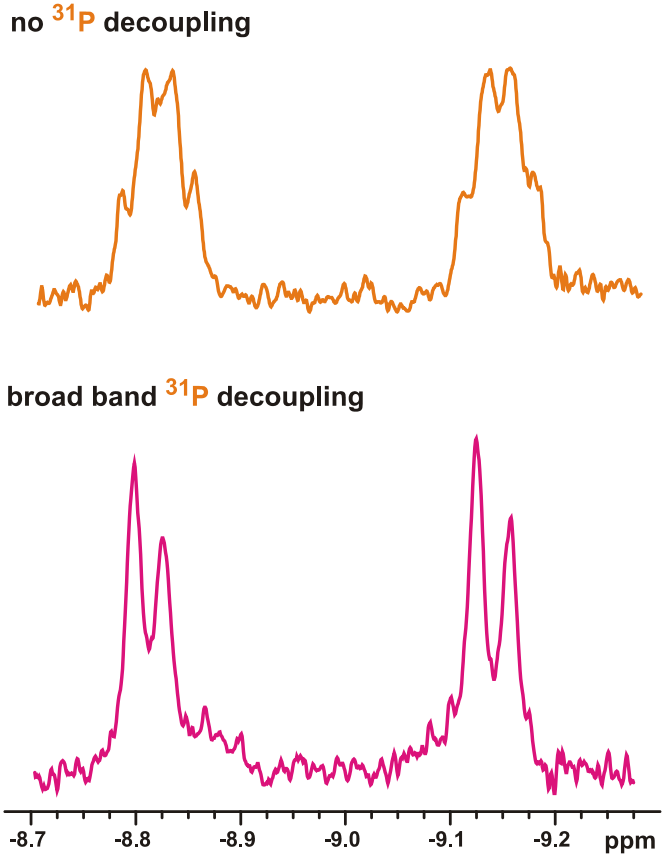


**Figure 2.3.** $^{1}$H NMR spectrum (500 MHz) of $[Rh_2(nbd)_2(rac\text{-et,ph-P}_4)](BF_4)_2$ under 200 psig $H_2$/CO in dichloromethane (selected hydride region).[7a]

Petia Greguorieva suggested $[Rh(\kappa^4\text{-}rac,rac\text{-et,ph-P4})_2RhH_2]^{2+}$ for the structure of the complex (Figure 2.5). The complex contains Rh(I) and Rh(III) atoms bridged and chelated by two et,ph-P4 ligands. The two upfield resonances in $^{31}P\{^{1}H\}$NMR were assigned to the phosphines bonded to the Rh(III) atom that also contains the hydride ligands. The signal at 22.5 ppm presumably belongs to the internal phosphines that are *trans* to the hydrides and the signal at −7.9 ppm to the external hydrides on Rh(III). Two versions of the structure were proposed - one with the external phosphorus atoms on the Rh(III) trans to each other (Figure 2.5, right) and the other structure with dangling external phosphines to suit better the upfield shift (Figure 2.5, left).

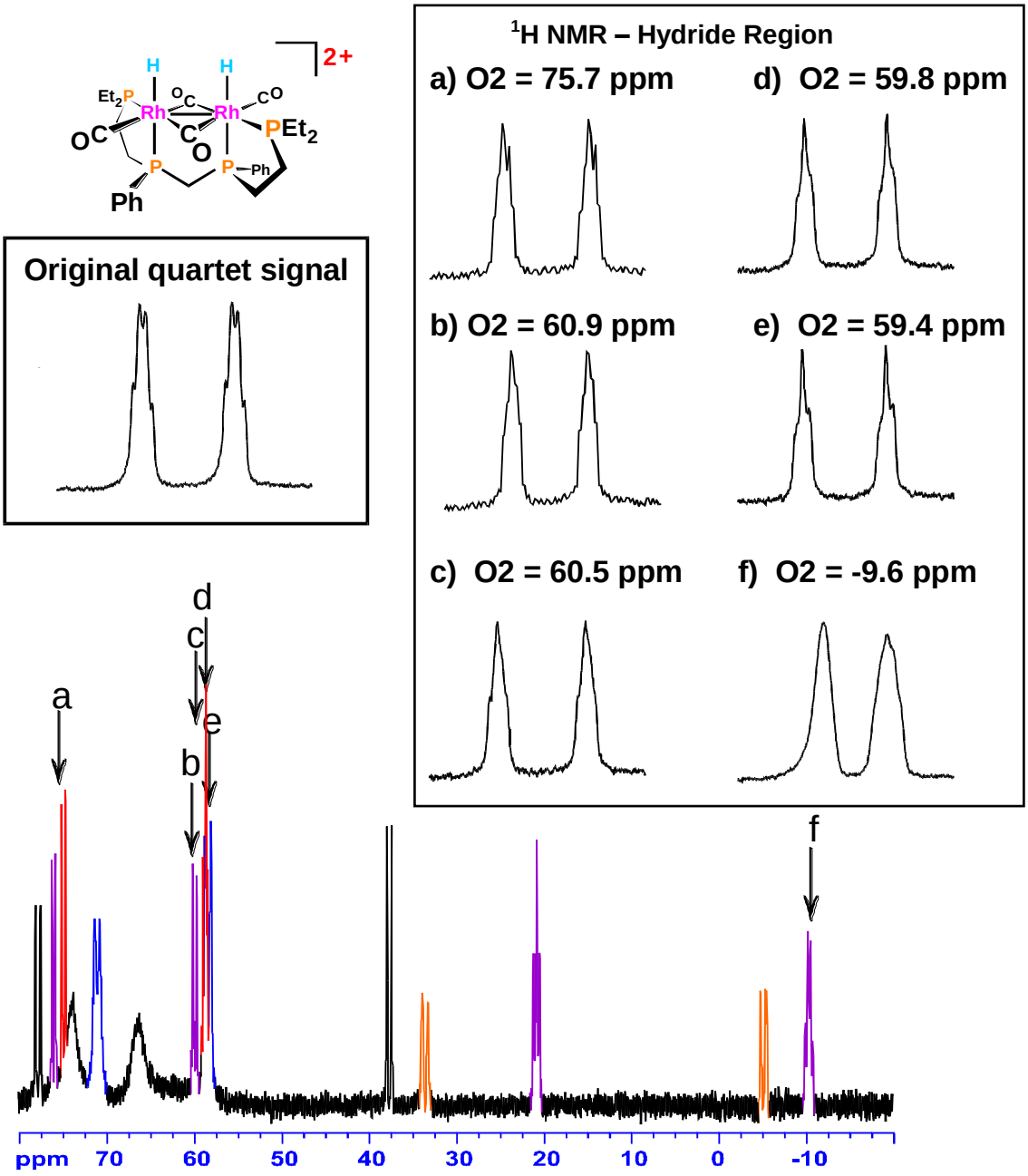


**Figure 2.4.** $^{31}P\{^{1}H\}$ NMR spectrum (500 MHz) of $[Rh_2(nbd)_2(rac\text{-et,ph-P4})](BF_4)_2$ under 250 psig of $H_2/CO$ and $^{1}H\{^{31}P\}$ spectra of the selected hydride region.[7a]

It is still not clear whether the large coupling constant 164 Hz belongs to originally assigned $^{1}J$(Rh-H) coupling or to *trans* $^{2}J$(P-H) coupling. Therefore additional $^{31}P$ decoupling $^{1}H$ and H-P HMBC experiments are needed to confirm the assignments.

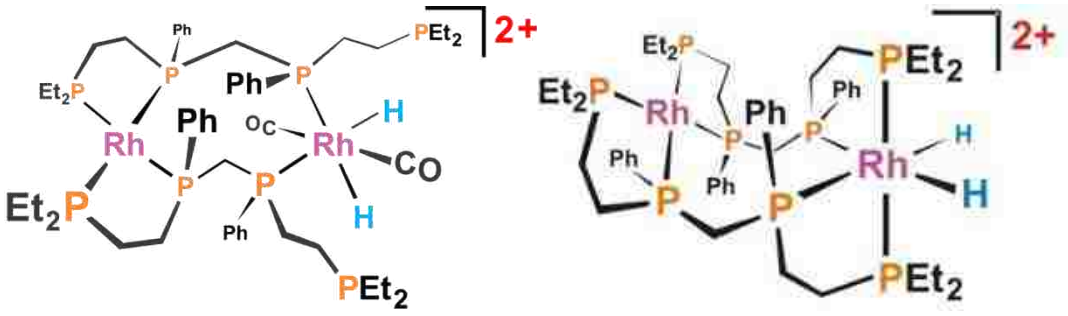

**Figure 2.5.** Previously proposed structures of the double ligand degradation product.[8]

The shifts and coupling constant for all species in the $^{31}P\{^{1}H\}$ NMR of the dirhodium catalyst at Figure 2.1 are summarized in Table 2.1.[8]

**Table 2.1.** Overview of NMR shifts and coupling constants.[8]

| Complex (all *rac*-et,ph-P4) | $^{1}H$(hydride)/ppm (J/Hz) | $^{31}P\{^{1}H\}$/ppm (J/Hz) |
|---|---|---|
| $[Rh_2(CO)_{5\text{-}6}(\kappa^4\text{-et,ph-P4})]^{2+}$ | | 72.4 ($J_{Rh\text{-}P}$ = 112.5, $J_{P\text{-}P}$=23)<br>59.9 ($J_{Rh\text{-}P}$ = 124.6,$J_{P\text{-}P}$=21.8) |
| $[Rh_2(\mu\text{-H})(\mu\text{-CO})H(CO)_3(\kappa^4\text{-et,ph-P4})]^{2+}$ | –55 °C : –9.4<br>–11.7 | 25 °C:<br>75.0 (broad exchanging)<br>66.0 (broad exchanging) |
| $[Rh_2H_2(\mu\text{-CO})_2(CO)_2(\kappa^4\text{-et,ph-P4})]^{2+}$ | 60 °C : –11.0 | 25 °C:<br>75.0 (broad exchanging)<br>66.0 (broad exchanging) |
| $[Rh_2(\mu\text{-CO})_2(CO)_2(\kappa^4\text{-et,ph-P4})]^{2+}$ | | 77.4 ($J_{Rh\text{-}P}$ = 117.7)<br>39.0 ($J_{Rh\text{-}P}$ = 116.4) |
| $[RhH_2(\kappa^4\text{-et,ph-P4})]^{+}$ | –18.3($J_{Rh\text{-}H}$ = 30,<br>$J_{H\text{-}H}$ = 15) | 35.0 ($J_{Rh\text{-}P}$ = 131.7, $J_{P\text{-}P}$ = 16.0)<br>–3.3 ($J_{Rh\text{-}P}$ = 148.6,$J_{P\text{-}P}$ = 24.8) |
| $[Rh(\kappa^4\text{-et,ph-P4})_2RhH_2]^{2+}$ | –8.8(trans$^2J_{H\text{-}P}$ = 164,<br>cis$^2J_{H\text{-}P}$ = 15) | 77.0 ($J_{Rh\text{-}P}$ = 228.0, $J_{P\text{-}P}$ = 77.5)<br>61.5 ($J_{Rh\text{-}P}$=227.9,$J_{P\text{-}P}$ = 78.6)<br>22.5 ($J_{Rh\text{-}P}$ = 137.0, $J_{P\text{-}P}$ = 24.5)<br>–7.9 ($J_{Rh\text{-}P}$ =116.1,$J_{P\text{-}P}$ = 14) |

Petia Gueorguieva attempted synthesis of complexes similar to the catalyst degradation products $RhH_2(\kappa^4\text{-}rac\text{-et,ph-P4})]^{+}$ and $[Rh(\kappa^4\text{-}rac,rac\text{-et,ph-P4})_2RhH_2]^{2+}$. More information about the structure of the degradation products could be obtained by comparison of the $^{31}P\{^{1}H\}$NMR spectra of the synthesized complexes to the *in-situ* catalyst spectrum. Single

crystal structures of rhodium monometallic or bimetallic complexes with *rac*- or *meso*-tetraphosphine ligands were previously reported but none of the them contained hydrides. Clinton Hunt was the first to synthetize the monometallic dichloride complex $[RhCl_2(\kappa^4$-et,ph-P4)]$BF_4$, which has similar $^{31}P\{^1H\}$NMR spectra as the monometallic degradation product with the suggested structure $RhH_2(\eta^4$-et,ph-P4)]$^+$.[10] Petia Gueorguieva prepared dichloride complex $[RhCl_2(\kappa^4$-et,ph-P4)]$BF_4$ by reacting one equivalent of mixed et,ph-Ph4 ligand with one and half equivalent $[Rh(nbd)_2]BF_4$, but her attempts to attach hydride via reaction with either $LiBEt_3H$ or $LiAlH_4$ were unsuccessful.[8]

Independent preparation of the proposed $[Rh(\kappa^4$-*rac*,*rac*-et,ph-P4)$_2RhH_2]^{2+}$ complex has so far failed. Crystals of $[Rh_2($*rac*,*rac*-et,ph-P4)$_2](BF_4)_2$ (Figure 2.6), $[Rh_2($*meso*,*meso*-et,ph-P4)$_2](Cl)_2$.1.5MeOH/$H_2O$, $[Rh_2($*meso*,*meso*-et,ph-P4)$_2](PF_6)_2$ and $[Rh_2($*rac*,*meso*-et,ph-P4)$_2]$-$(BF_4)_2$[11] were previously characterized by X-ray crystallography.[12] These structures provide clear evidence for the "double-ligand" dirhodium structural motif.

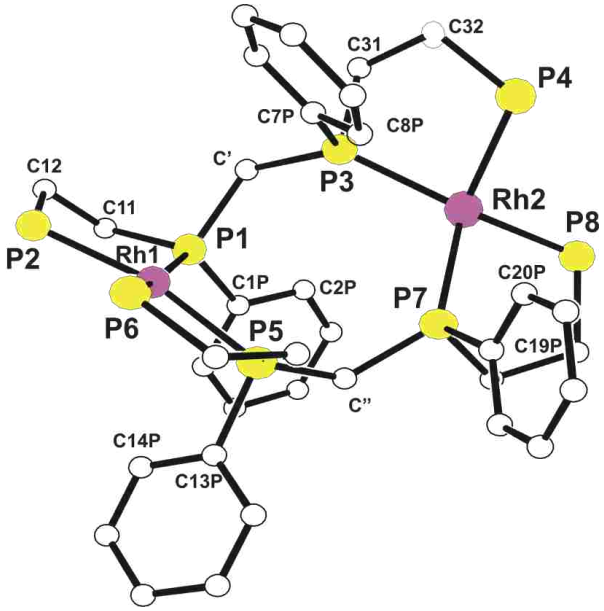


**Figure 2.6.** Crystal structure of $[Rh_2($*rac*,*rac*-et,ph-P4)$_2](BF_4)_2$.[12]

## 2.2 Current Studies in Acetone

### 2.2.1 One-dimensional NMR

Since the previous experiments in acetone did not unambiguously answer questions about the structure of all complexes in the acetone NMR spectra, I repeated some of the previous experiments in acetone. I worked at lower pressures (90-100 psig $H_2$/CO gas instead of 250 psig) in order to get closer to the conditions of a real hydroformylation run, which is usually performed at 90 psig and 90°C.

Figure 2.7 shows $^{31}P\{^1H\}$NMR spectrum of the dirhodium catalyst under 100 psig $H_2$/CO at room temperature the same day the sample was prepared (bottom) and two days later (top). Degradation products grew in time and were clearly visible in the spectrum of the two days old sample. The degradation products seem to be the same as in previous studies at high pressures.

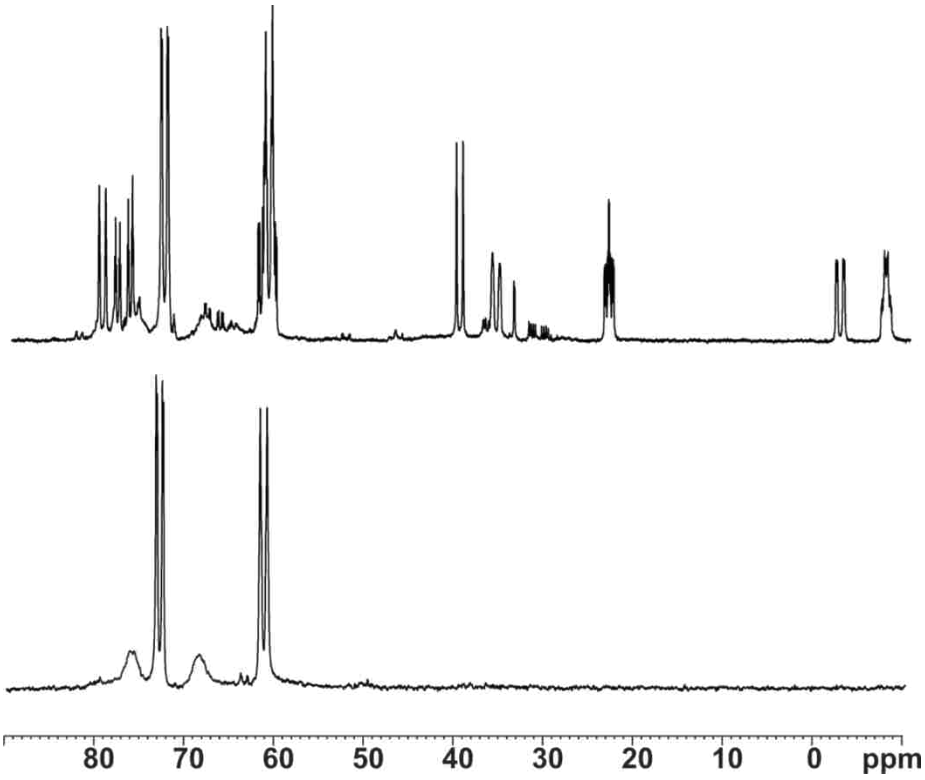


**Figure 2.7.** $^{31}P\{^1H\}$NMR of $[Rh_2(nbd)_2(rac\text{-et,ph-P4})](BF_4)_2$ in acetone under 100 psig $H_2$/CO. The bottom spectrum shows the sample two hours after preparation while the top shows the sample two days after preparation.

The hydride region in a $^{1}$H NMR spectrum of $[Rh_2(nbd)_2(rac\text{-et,ph-P4})](BF_4)_2$ is shown in Figure 2.8. It is similar to previously observed spectra at higher pressure. The resonances at −8.8 ppm and −18.4 ppm belong to the degradation products. The detail of the central area of the hydride region in dependence on temperature is shown in Figure 2.9.

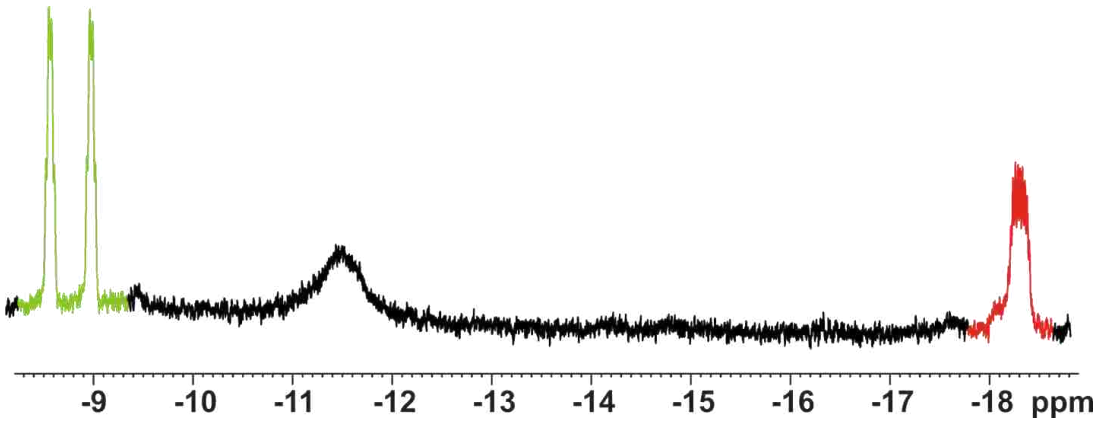


**Figure 2.8.** Hydride region in the $^{1}$H NMR of $[Rh_2(nbd)_2(rac\text{-et-ph,P4})](BF_4)_2$ in acetone.

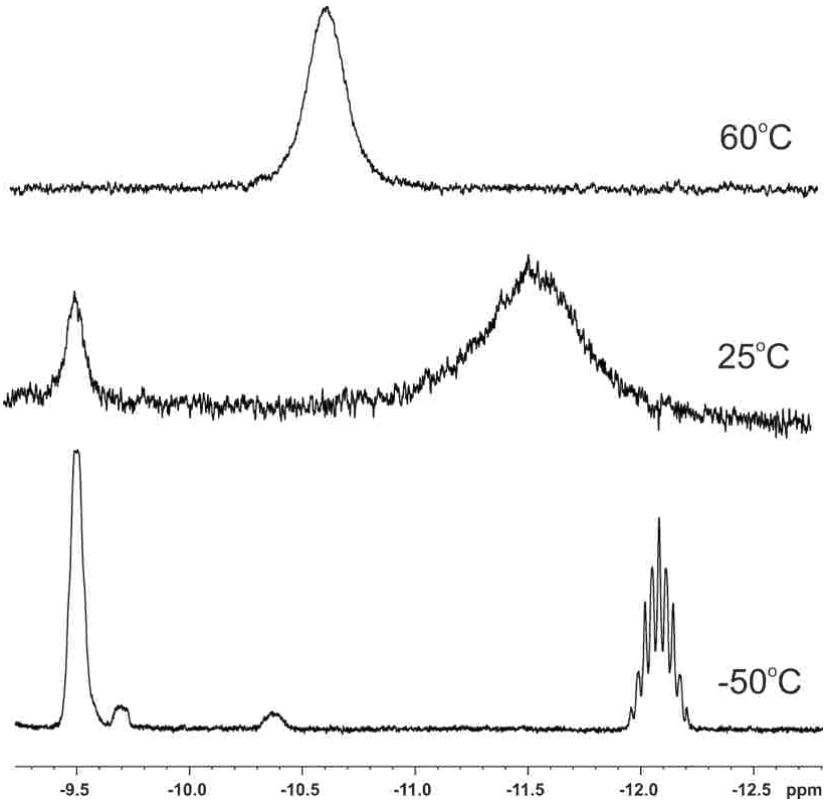


**Figure 2.9.** Variable temperature $^{1}$H NMR of $[Rh_2(nbd)_2(rac\text{-et-ph,P4})](BF_4)_2$ in acetone (selected hydride region) under 90 psig of $H_2$/CO.

Figure 2.9 shows that the two broad hydride peaks originally present at room temperature coalesce into one peak at higher temperatures. At low temperatures the two peaks stay separate and one of them resolves into a nonet. This behavior was previously interpreted as dynamic exchange between several hydride complexes. It was proposed that at lower temperatures the complex $[Rh_2(\mu\text{-}H)(\mu\text{-}CO)H(CO)_3(\textit{rac}\text{-et,ph-P4})]^{2+}$ (number 2* at Figure 2.10) prevails with one terminal (–9.5 ppm) and one bridging hydride (–12.1 ppm). At higher temperatures (> 60 °C) the symmetrical terminal hydride complex $[Rh_2H_2(\mu\text{-}CO)_2(CO)_x(\textit{rac}\text{-et,ph-P4})]^{2+}$ (number 2 at Figure 2.10) dominates, where x = 0, 1, 2. This assignment was supported by previous observations that high hydroformylation activity is observed only at higher temperatures and under such conditions bridging CO bands are present in the FT-IR spectra with the highest intensity.[8]

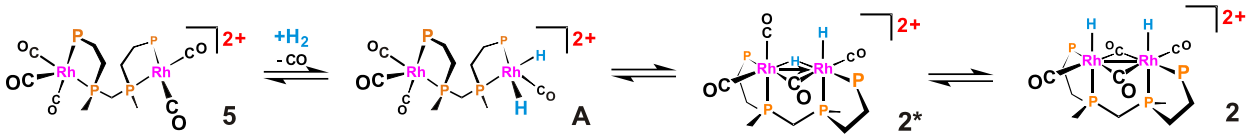


**Figure 2.10.** Formation of hydrides in the proposed hydroformylation mechanism.[13]

### 2.2.2 Two-dimensional NMR and Selective Decoupling

A $^{31}P\{^1H\}$-$^{31}P\{^1H\}$ COSY was performed at room temperature in order to show connectivity among phosphorus atoms (Figure 2.10). The green regions belong to the dirhodium double ligand degradation product and the red regions to the monorhodium degradation product. The results confirmed the previous observations by Petia Gueorguieva.[8]

Due to some inconsistencies in previous broad band and narrow band decoupled spectra of $[Rh_2(nbd)_2(\textit{rac}\text{-et-ph,P4})](BF_4)_2$, additional selective decoupling experiments were undertaken with focus on the double ligand degradation complex. The results of the current selective decoupling experiments are shown at Figure 2.12.

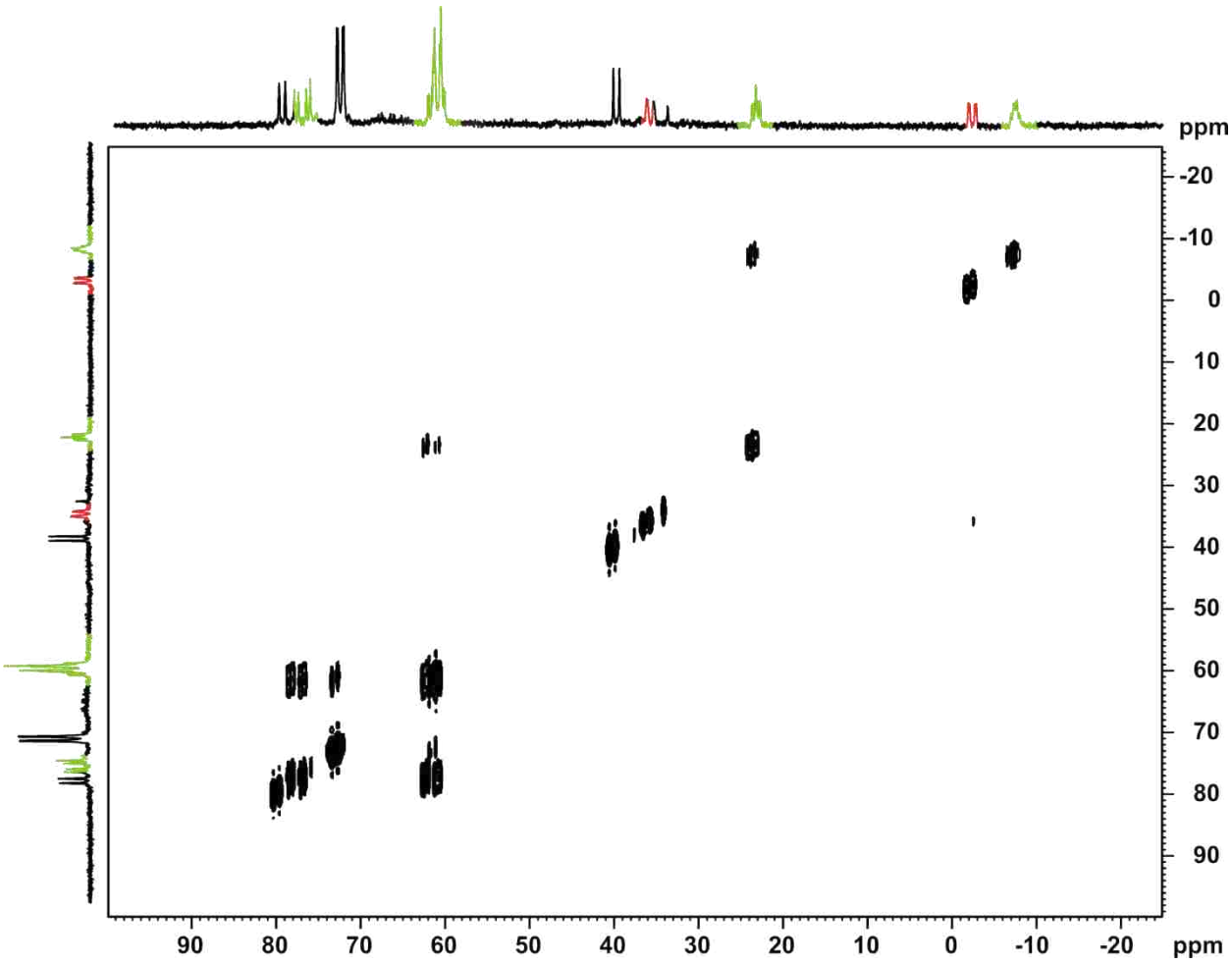


**Figure 2.11.** $^{31}P\{^{1}H\}$-$^{31}P\{^{1}H\}$ COSY of $[Rh_2(nbd)_2(rac\text{-et-ph,P4})](BF_4)_2$ in acetone under 100 psig $H_2/CO$ at room temperature.

While we know from $^{31}P\{^{1}H\}$ COSY (Figure 2.11) that the peaks at –8, 22, 61 and 74 ppm belong to the same species, $^{31}P$ coupling to the doublet of pseudo-quartets hydride area was observed during decoupling in the above regions of $^{31}P\{^{1}H\}$ spectrum except for the resonance at 22 ppm (Figure 2.12). This was confirmed by multiple decoupling experiments. The selective decoupling experiments agrees with the observation of Rhonda Matthews that the most negative $^{31}P$ peak is coupled to the –8.8 ppm hydride resonance (Figure 2.4), but she did not do selective decoupling for the 20 ppm $^{31}P$ peak. I attempted to confirm the results via gs-HMBC, which is

another technique capable to show connectivity between hydride and phosphorus atoms, but the experiment did not produce useful results.

Figure 2.12 shows the collapse of the two hydride peaks into one broad resonance (spectrum a) upon decoupling the –9 ppm $^{31}$P signal. This is important for disproving the original assignment of the large 164 Hz coupling constant as Rh-H coupling. Prof. Stanley initially proposed (and published) that the 164 Hz coupling belonged to $^{1}$J(Rh-H) based on the inability to change the 164 Hz coupling with either selective or broad-band $^{31}$P decoupling. Based on this he proposed that the 164 Hz coupling was characteristic of a Rh(II) dihydride complex[7b], but later assignments of the NMR spectrum suggested that it was more likely due to *trans* $^{2}$J(H-P) coupling.[8] If the collapse is real, it would confirm the *trans* $^{2}$J(H-P) assignment. Unfortunately, this result was not duplicated in a new set of selective decoupling experiments.

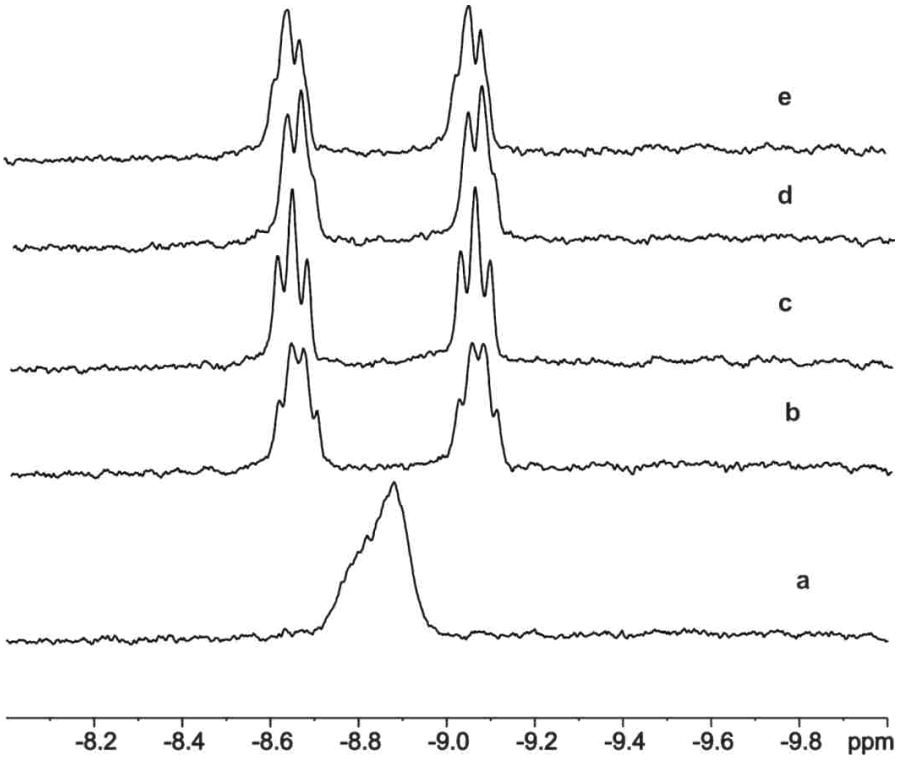


**Figure 2.12.** $^{1}$H NMR of hydride region for $[Rh_2(nbd)_2(rac\text{-et,ph-P4})](BF_4)_2$ under 90 psig of $H_2$/CO at room temperature. (a) Decoupling at –9 ppm in $^{31}$P{$^{1}$H} NMR, (b) decoupling at 22 ppm, (c) decoupling at 61 ppm, (d) and (e) decoupling around 74 ppm.

The collapse of the –8.8 ppm hydride pattern shown in Figure 2.11, therefore, is the only time we have seen $^{31}P$ decoupling have an impact on the large 164 Hz coupling. This inconsistency in our NMR data is extremely frustrating and is keeping us from a firm structural assignment of the double-P4 ligated dirhodium hydride complex.

A doublet of pseudo-quartets in the hydride region of the $^{1}H$ NMR spectrum seems unusual, but similar patterns have been reported in connection to monometallic rhodium phosphine complexes. Schrock and Osborn[14] and Clegg *et al.*,[15] for example, reported a doublet of quartets with a large *trans* J(H-P) coupling constant of 136.6 Hz for $[RhH_2(PMe_3)_4]^+$. The crystal structure of this complex has two hydrides oriented *cis* to each other in a distorted octahedral environment. Lorenzini *et al.*[16] reported similar pattern for *cis,mer*-$Rh(H)_2Cl(PMePh_2)_3$ with a $J_{H\text{-}P}$ = 163.4 Hz (Figure 2.13).

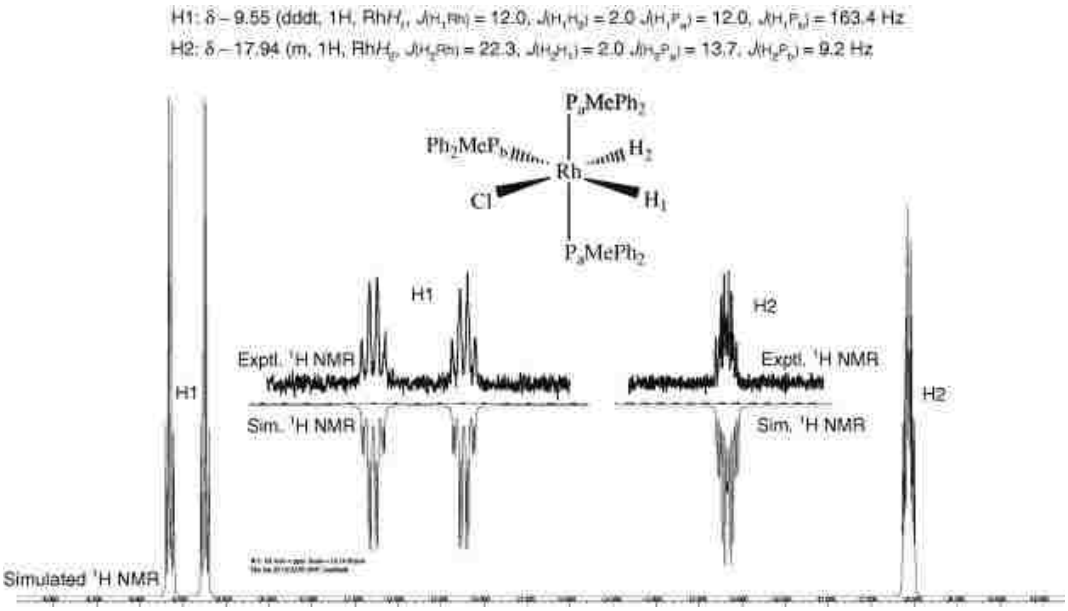


**Fig. 2.13.** $^{1}H$ NMR of *cis,mer*-$Rh(H)_2Cl(PMePh_2)_3$ measured and simulated by F. Lorenzini.[16]

The previously proposed structures for the double ligand dirhodium complex (Figure 2.5) were based on shifts and coupling constants in $^{31}P\{^{1}H\}$ NMR and connectivities in $^{31}P\{^{1}H\}$-$^{31}P\{^{1}H\}$ COSY, where the resonance at 77.0 ppm showed correlations with the peaks at 61.5

ppm. The former was suggested to be external phosphine and the later internal phosphines, both bonded to the Rh(I) atom and *trans* to each other in a square planar orientation due to the large P-P coupling constant. The other two upfield signals were assigned to phosphines at a Rh(III) center containing hydride ligands. The resonance at 22.5 ppm was assigned to the internal phosphines located *trans* to the hydrides and the resonance at −7.9 to the internal phosphines located mutually trans.

The related patterns in $^{31}P\{^{1}H\}$NMR of the double ligand degradation complex are rather complicated and the areas are in detail shown in Figures 2.14, 2.15, 2.16 and 2.17. The corresponding shifts and best estimates of coupling constants are summarized in Table 2.2.

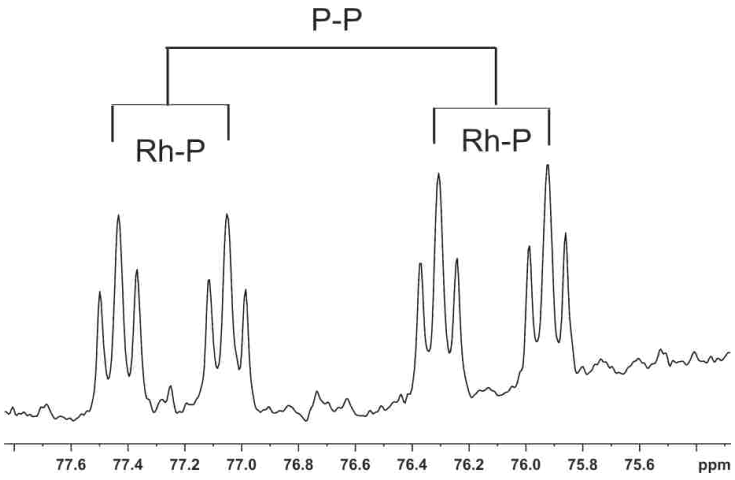


**Figure 2.14.** Selected area in $^{31}P\{^{1}H\}$ NMR of a double ligand degradation product.

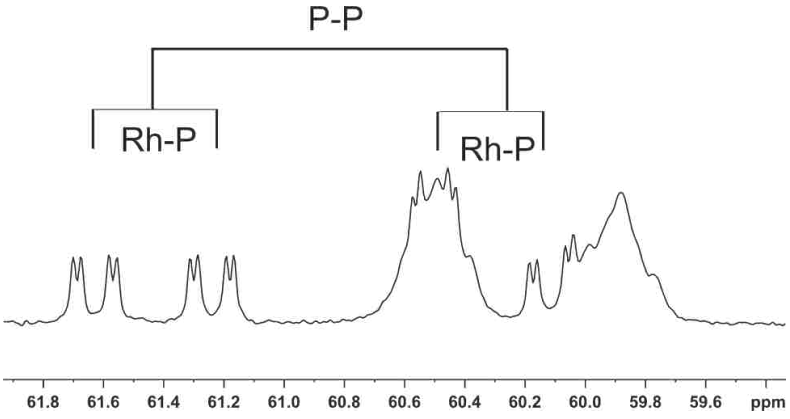


**Figure 2.15.** Selected area in $^{31}P\{^{1}H\}$ NMR of a double ligand degradation product.

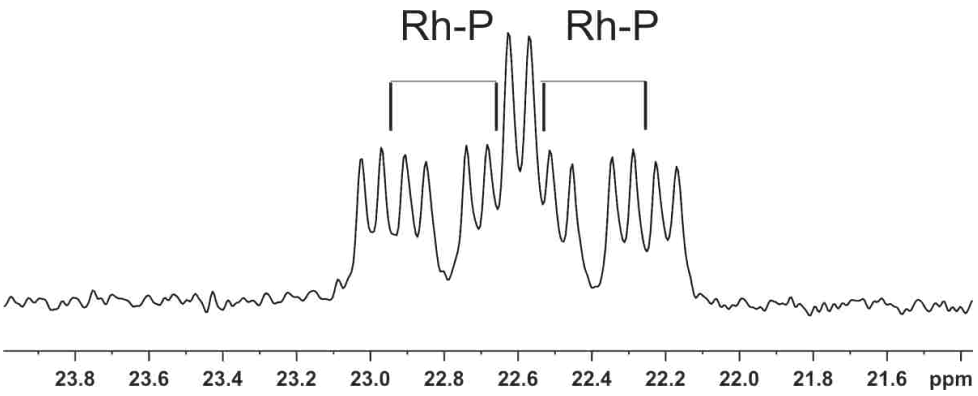


**Figure 2.16.** Selected area in $^{31}P\{^{1}H\}$ NMR of a double ligand degradation product.

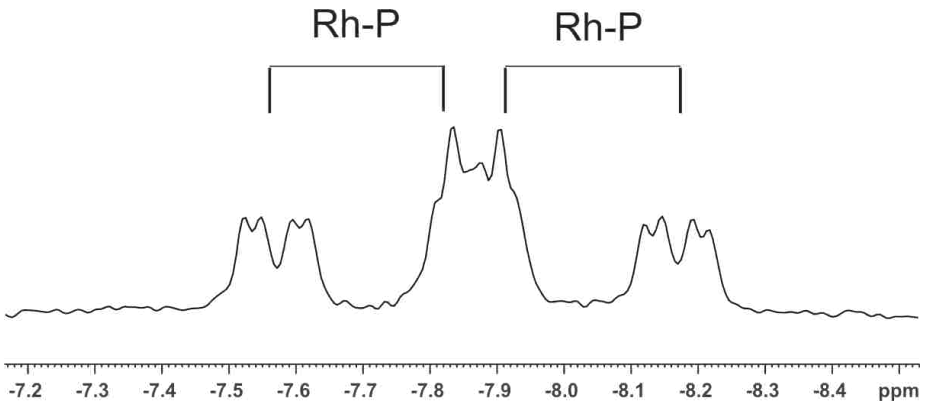


**Figure 2.17.** Selected area in $^{31}P\{^{1}H\}$ NMR of a double ligand degradation product.

**Table 2.2.** Shifts and couplings of the dirhodium double ligand complex.

| $^{1}H$ (hydride)/ppm (J/Hz) | $^{31}P\{^{1}H\}$/ppm (J/Hz) |
|---|---|
| –8.8 (*trans* $J_{H-P}$ = 164, *cis* $J_{H-P}$ = 11) | 77.0 ($J_{P-P}$ = 228.3, $J_{Rh-P}$ = 77.3)<br>60.9 ($J_{P-P}$ = 229.9, $J_{Rh-P}$ = 79.0)<br>22.5 ($J_{Rh-P}$ = 58.0, $J_{P-P}$ = 12.2)<br>–7.9 ($J_{Rh-P}$ = 53.5, $J_{P-P}$ = 14) |

The selective decoupling experiments do not support the assignment that placed both hydrides *trans* to the internal phosphines and oriented towards the outside of the complex. When looking for a different structure in order to explain the results of the decoupling experiments, I found literature on a dicationic heterobimetallic complexes that contained rhodium and iridium metal centers connected via two bridging diphenylphosphinomethane (dppm) ligands and two

semibridging hydrides (Figure 2.12).[17] The $^{1}H$ NMR of this complex does not show large *trans* $J_{H-P}$ coupling because it does not contain any hydride trans to phosphine. The NMR data are summarized in table 2.3.

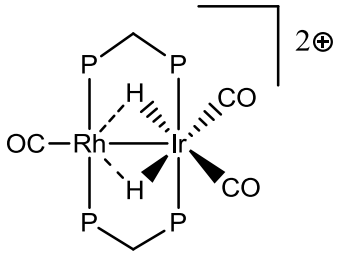


**Figure 2.18.** A dicationic heterobimetallic complex with two bridging dppm and hydrides.[17]

**Table 2.3.** NMR data for $[RhIr(CO)_3(\mu\text{-}H)_2(dppm)_2][BF_4]_2$.[17]

| $\delta(^{31}P\{^{1}H\})$ | $^{1}J_{Rh-P}$ | $\delta(^{1}H)$ |
|---|---|---|
| 21.9 (Rh-P)<br>− 10.2 (Ir-P) | 102.7 | 7.57-7.33 (mult, 40H)<br>4.63 (mult, 4H)<br>–11.18 (mult, 2H, $^{2}J_{P(Ir)-H}$ = 11.1 Hz, $^{2}J_{P(Rh)-H} \leq 7$ Hz, $^{1}J_{Rh-H}$ = 17.3 Hz |

A similar structure can possibly explain the unusual results of the selective decoupling experiments (Figure 2.19). The new structure has basically the same arrangement on Rh(I) as the previously suggested structures (Figure 2.5) but Rh(III) differs significantly. The internal phosphines are proposed to be oriented *trans* to each other while the external phosphines are oriented *trans* to hydrides. The hydrides points inwards so they can be semibridging to the Rh(I) center and this could explain the coupling between both phosphines on the Rh(I) center that are in the downfield region of the $^{31}P\{^{1}H\}$ NMR spectrum (77 and 61 ppm). This corresponds well with the coupling constants in table 2.2. The couplings for the phosphine resonances around 77 and 61 ppm have large couplings assigned to *trans* P-P coupling. The resonance at –7.9 ppm have smaller coupling 53 Hz assigned to Rh-P coupling. The area at 22.5 ppm shows somewhat similar pattern with Rh-P 58 Hz. The two internal phosphines oriented *trans* to each other do not

show large *trans* coupling since they are chemically equivalent. It is not fully clear why irradiation of the resonance at 22.5 ppm does not show collapse of the hydride pattern during selective decoupling experiments. It might be related to the *cis* orientation of those phosphines to the hydrides. This assignment is still tentative and more NMR experiments are needed (selective decoupling NMR and HMBC) to confirm phosphine-hydride correlations and to verify the assignments. Attempts should be continued to isolate crystals of the degradation products and characterize them by x-ray analysis.

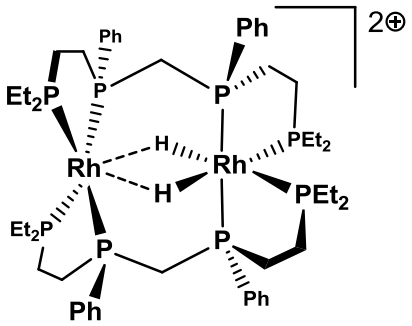


**Figure 2.19.** Suggested structure for the double ligand degradation product.

### 2.3 Studies in Water/Acetone

Hydroformylation studies by David Aubry and Novella Bridges showed significant improvement for the $[Rh_2(nbd)_2(rac\text{-et-ph,P4})](BF_4)_2$ catalyst in water/acetone relative to pure acetone solvent.[18] It would be useful to study the catalyst in both solvent systems by high pressure NMR spectroscopy in order to explain the hydroformylation activity difference. So far, the only spectrum recorded in acetone/water was a $^{31}P\{^1H\}$ spectrum at 200 psig $H_2$/CO 48-96 hours after filling with gas (Figure 2.14).[8] Figure 2.14 shows that the main difference in water/acetone compared to acetone solvent are taller peaks around 66 and 75 ppm and missing peaks 20 ppm and -7.9 ppm that are characteristic of the double P4-ligand dirhodium catalyst degradation product. A $^1H$ NMR spectrum of the sample was not recorded.

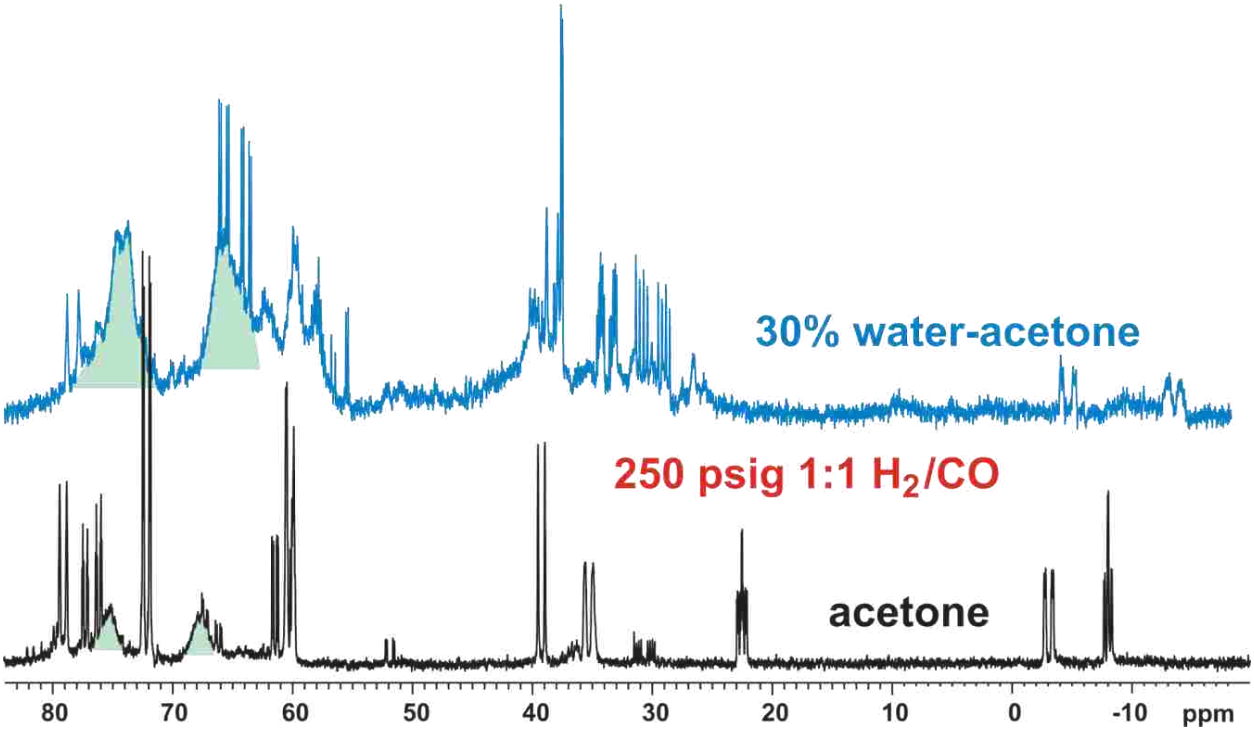


**Figure 2.20**. $\{^1H\}^{31}P$ NMR spectrum of $Rh_2$ in acetone and acetone/water at room temperature.[8] Green highlighted broad peaks are assigned to $[Rh_2H_2(\mu\text{-}CO)_2(CO)_x(rac\text{-et,ph-P4})]^{2+}$ and $[Rh_2H(\mu\text{-}H)(\mu\text{-}CO)(CO)_x(rac\text{-et,ph-P4})]^{2+}$ (x = 1-3) in dynamic equilibrium. Although this is still the proposal for the acetone solvent, our studies have indicated a different set of catalyst complexes in water-acetone.

It would be interesting to study the catalyst at increased temperature since it is known that the catalyst is active at higher temperatures from the previous hydroformylation studies.[11] The $^{31}P\{^1H\}$ NMR spectra at 60 ºC are shown at Figure 2.15, the bottom spectrum was taken in acetone while the top spectrum is in water/acetone. Both samples were one day old. There are no observed degradation products in water/acetone. Interestingly, the penta/hexacarbonyl peaks, assigned to the resting state of the catalyst in acetone, are missing in water/acetone solvent. In both spectra the broad peaks at 67 ppm seem to be resolving. Both broad peaks resolve at around 80 °C.

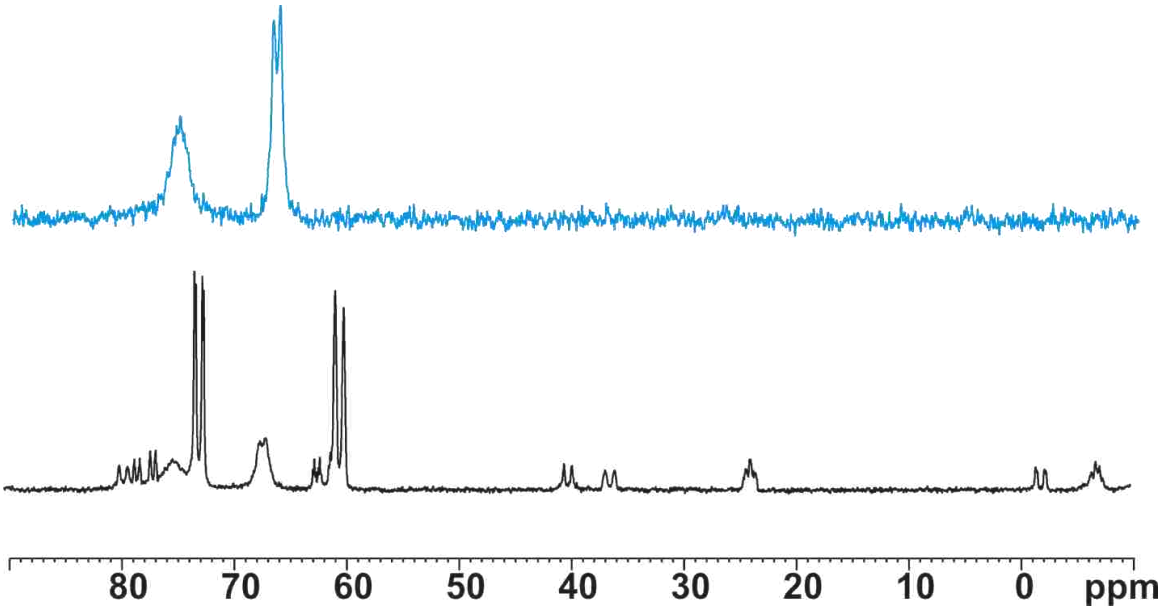


**Figure 2.21**. $\{^1H\}^{31}P$ NMR spectra of $[Rh_2(nbd)_2(rac\text{-et,ph-P4})](BF_4)_2$ under 100 psig $H_2/CO$ in acetone (bottom) and 30% acetone/water (top) at 60ºC.

The increased degradation in acetone compared to acetone/water shown in Figure 2.15 is clearly one of the reasons for better catalyst performance in the water/acetone. It is in agreement with hydroformylation studies of David Aubry, who varied the soaking time of the catalyst under 45-75 psig $H_2/CO$ and 90 °C prior to the injection of the alkene. In acetone, soaking for 50 minutes led to 80% catalyst deactivation and soaking for 80 minutes resulted in a completely inactive catalyst. In marked contrast, 2 hours of soaking of the $Rh_2$ catalyst prior to hydroformylation in 30% water/acetone led to only 10% loss of activity of the catalyst.[18]

Samples for $^1H$ NMR spectra had to be prepared in $d_6$-acetone with non-deuterated water. In $d_6$-acetone/$D_2O$, no hydrides were observed by $^1H$ NMR due to hydrogen/deuterium exchange with water. Figure 2.16 shows selected hydride area in the $^1H$ NMR of $Rh_2$ at low temperature in acetone and water/acetone. The peak around –12 ppm is present in both spectra. However, the peak at around –9.5 ppm is missing in water/acetone. Previous interpretation in acetone presumed that the peak at –9.5 is due to the terminal hydride while the other peak due to

bridging hydride. In case of water/acetone system, it could mean the presence of just one hydride, which is assigned as bridging due to the similarities in the coupling patterns.

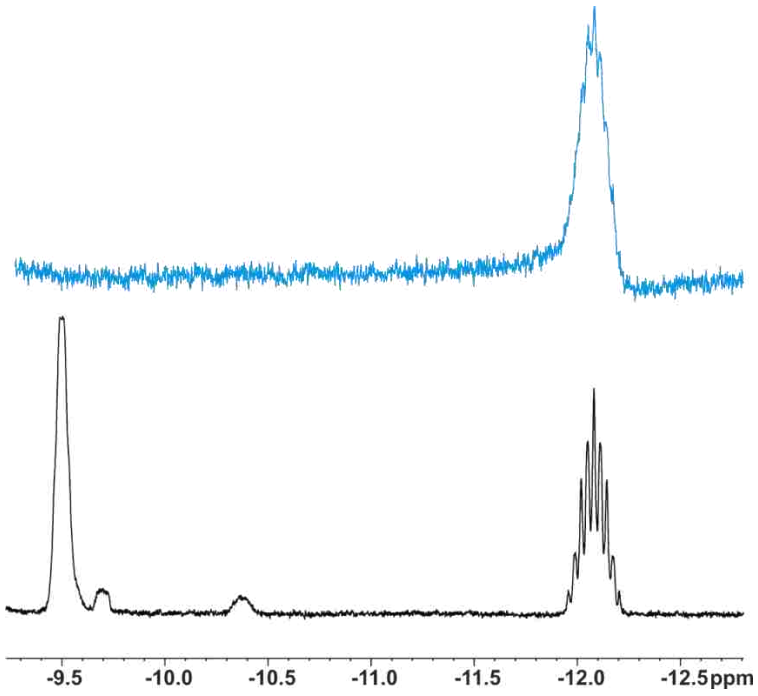


**Fig. 2.22.** $^{1}$H NMR's of the hydride region of $Rh_2$ at low temperature under 90 psig of $H_2$/CO: bottom spectrum is in acetone at –50 °C, the top spectrum in in 30% water/acetone at –35 °C (sample froze at lower temperature).

### 2.4 Summary and Future Experiments

The $^{31}P\{^{1}H\}$ and $^{1}$H NMR in acetone are very similar to previous experiments at higher pressures. A selective decoupling for the dirhodium double P4-ligand degradation product confirmed the previously observed response of the hydride region at –8.8 ppm to the most of the phosphine resonances, but failed to show any coupling to a signal at 22 ppm in $^{31}P\{^{1}H\}$. One $^{31}$P decoupling study showed a collapse of the 164 Hz coupling for the –8.8 ppm hydride resonance. This supported our suspicion that the coupling is due to *trans* P-H coupling through the Rh center. Unfortunately, this decoupling study has not been reproduced. A new dirhodium double P4-ligated structure with Rh(I)/Rh(III) centers and semi-bridging hydrides was suggested for the

degradation complex. It is only a tentative assignment and more experiments are needed to confirm it, for example, $^{31}$P-$^{1}$H HMBC. But it is currently our best structural assignment based on available data and that of previously characterized Rh-H phosphine systems. Also, experiments should be continued to attempt to isolate the degradation products, recrystallize them and characterize them by X-ray crystallography.

$^{31}$P{$^{1}$H} NMR showed that there is far less and slower degradation in water/acetone solvent. The resting state of the catalyst in acetone, the dirhodium penta/hexacarbonyl complex, is present only in small amounts in water/acetone. The two broad peaks present in both acetone and water/acetone resolve at higher temperatures. $^{1}$H NMR at low temperature showed a missing terminal hydride peak, which might indicate that the complex is a monohydride, but there is not much difference at $^{1}$H NMR between the two solvent systems at higher temperatures.

Because the hydroformylation is proposed to occur via bimetallic cooperativity between the two rhodium atoms, $^{103}$Rh NMR experiments are still worth doing on the 700 MHz NMR, particularly $^{103}$Rh-decoupled $^{31}$P and $^{1}$H as well as $^{103}$Rh-$^{1}$H NMR correlation experiments.

**2.5 References**


1. Horvath, I. T.; Millar, J. M. *Chem. Revi.* **1991,** *91* (7), 1339-1351.
2. (a) Brown, J. M.; Kent, A. G. *J. Chem. Soc. Chem. Comm.* **1982,** (13), 723-725; (b) Brown, J. M.; Kent, A. G. *J. Chem. Soc. Perkin Trans.* **1987,** (11), 1597-1607; (c) Bianchini, C.; Lee, H. M.; Meli, A.; Vizza, F. *Organometallics* **2000,** *19* (5), 849-853; (d) Bergounhou, C.; Neibecker, D.; Mathieu, R. *Organometallics* **2003,** *22* (4), 782-786.
3. (a) Jongsma, T.; Challa, G.; Vanleeuwen, P. *J. Organomet. Chem.* **1991,** *421* (1), 121-128; (b) Molina, D. A. C.; Casey, C. P.; Mueller, I.; Nozaki, K.; Jaekel, C. *Organometallics* **2010,** *29* (15), 3362-3367.
4. (a) Kranenburg, M.; Vanderburgt, Y. E. M.; Kamer, P. C. J.; Vanleeuwen, P.; Goubitz, K.; Fraanje, J. *Organometallics* **1995,** *14* (6), 3081-3089; (b) Casey, C. P.; Whiteker, G. T.; Melville, M. G.; Petrovich, L. M.; Gavney, J. A.; Powell, D. R. *J. Am. Chem. Soc.* **1992,** *114* (14), 5535-5543; (c) van der Veen, L. A.; Boele, M. D. K.; Bregman, F. R.; Kamer, P. C. J.; van Leeuwen, P.; Goubitz, K.; Fraanje, J.; Schenk, H.; Bo, C. *J. Am. Chem. Soc.* **1998,** *120* (45), 11616-11626.

5. (a) Bianchini, C.; Frediani, P.; Meli, A.; Peruzzini, M.; Vizza, F. *Chem. Ber. Recueil* **1997,** *130* (11), 1633-1641; (b) Kiss, G.; Horvath, I. T. *Organometallics* **1991,** *10* (11), 3798-3799.

6. Brown, J. M.; Canning, L. R. *J. Organomet. Chem.* **1984,** *267* (2), 179-190.

7. (a) Matthews, R. C., PhD Thesis, Louisiana State University, 1999; (b) Matthews, R. C.; Howell, D. K.; Peng, W. J.; Train, S. G.; Treleaven, W. D.; Stanley, G. G. *Angew. Chem. Int. Ed.* **1996,** *35* (19), 2253-2256.

8. Gueorguieva, P. G., PhD Thesis, Louisiana State University, 2004.

9. Garrou, P. E. *Chem. Rev.* **1981,** *81* (3), 229-266.

10. Hunt, C.; Fronczek, F. R.; Billodeaux, D. R.; Stanley, G. G. *Inorg. Chem.* **2001,** *40* (20), 5192-5198.

11. Laneman, S. A., PhD Thesis, Louisiana State University, 1990.

12. Hunt, C.; Nelson, B. D.; Harmon, E. G.; Fronczek, F. R.; Watkins, S. F.; Billodeaux, D. R.; Stanley, G. G. *Acta Crystallogr., Sect. C: Cryst. Struct. Commun.* **2000,** *56,* 546-548.

13. Wilson, Z., PhD Thesis, Louisiana State University, 2004.

14. Schrock, R. R.; Osborn, J. A. *J. Am. Chem. Soc.* **1971,** *93* (10), 2397-2407.

15. Clegg, W.; Elsegood, M. R. J.; Scott, A. J.; Marder, T. B.; Dai, C. Y.; Norman, N. C.; Pickett, N. L.; Robins, E. G. *Acta Crystallogr., Sect. C: Cryst. Struct. Commun.* **1999,** *55,* 733-739.

16. Lorenzini, F.; Patrick, B. O.; James, B. R. *Inorg. Chim. Acta* **2008,** *361* (7), 2123-2130.

17. McDonald, R.; Cowie, M. *Inorg. Chem.* **1990,** *29* (8), 1564-1571.

18. Aubry, D. A.; Bridges, N. N.; Ezell, K.; Stanley, G. G. *J. Am. Chem. Soc.* **2003,** *125* (37), 11180-11181.

# CHAPTER 3: FT-IR AND ACID-BASE STUDIES

## 3.1 Introduction

Fourier transform infrared spectroscopy (FT-IR) is, next to high-pressure NMR spectroscopy, one of the most useful tools for investigation of metal-carbonyl catalysts. FT-IR is extremely useful for hydroformylation studies where M-CO stretching frequencies provide considerable information about how electron-rich or deficient the metal center is. The CO absorption bands are generally strong, easily observed by FT-IR, and can generally be found in the 1700 to 2100 $cm^{-1}$ region.[1] Information about the binding mode of the carbonyl ligands (e.g., terminal or bridging) can also be easily gained from the spectra.

Infrared spectroscopy has been employed for studies of a number of metal/ligand catalysts. Cobalt carbonyl complexes were investigated under hydroformylation conditions either in presence of phosphine ligands or without them.[2] Reports were published on the IR investigation of unmodified rhodium carbonyl catalysts[3] as well as rhodium in the presence of phosphine,[4] diphosphine,[5] phosphite,[6] and mixed phosphine-phosphite[7] ligands. Moreover, the possibility of bimetallic cooperativity between two rhodium centers was also investigated employing FT-IR on dirhodium complexes with bridging thiolate ligands.[8] In many cases information about the active forms of a catalyst can be gained by these studies, as well as information about additional complexes present in the catalysis, either as part of the catalytic cycle, off-cycle equilibria, or degradation products.

An autoclave modified for IR measurements was first reported by Noack[9] in 1968 and since that time various IR cell designs have been constructed. The most common instruments[10] are based either on autoclaves containing an infrared transmittance windows[9] or autoclaves with built in cylindrical crystal from materials as silicon or ZnSe.[11]

When a catalytic system is being investigated, both FT-IR and high pressure NMR have their benefits and inconveniences. NMR is used with significantly higher concentration of catalyst, for example 5 to 100 times more than what is used during a catalytic run.[12] This can affect the equilibria among various catalyst species. Catalytic species in low concentration can easily be missed. Another limitation is absence of stirring and relatively small volume of gas above the liquid.[12] FT-IR conditions might be closer to an actual hydroformylation run, due to proper stirring and lower catalyst concentrations depending on the design of the particular IR cell.

**3.2 Former Experiments**

FT-IR experiments were employed to study the dirhodium tetraphosphine catalyst precursor $[Rh_2(nbd)_2(rac\text{-et,ph-P4})](BF_4)_2$. Prior to these experiments it was originally proposed that the main catalytic species that forms under addition of $H_2$/CO gas was the neutral complex $Rh_2H_2(CO)_2$(*rac*-et,ph-P4). This was proposed in analogy to monometallic $Rh/PPh_3$ catalyst systems where neutral complexes are generated under $H_2$/CO.[13]

In our early studies in acetone 8% isomerization was observed. Prof. Stanley proposed that the rather high isomerization could be caused by a release of two equivalents of strong $HBF_4$ acid when $[Rh_2(nbd)_2(rac\text{-et,ph-P4})](BF_4)_2$ reacts with $H_2$/CO.[13] If this was really the case then a neutral bimetallic catalyst that does not release $HBF_4$ under exposure to $H_2$/CO should be more suitable. Based on this reasoning, r*ac*-$Rh_2(\eta^3\text{-allyl})_2$(et,ph-P4) was prepared by reaction of allylmagnesium chloride with the dicationic precursor $[Rh_2(nbd)_2(rac\text{-et,ph-P4})](BF_4)_2$.[14] Unfortunately, $Rh_2(\eta^3\text{-allyl})_2$(*rac*-et,ph-P4) performed extremely poorly as a hydroformylation catalyst with an initial turnover frequency 35 $h^{-1}$, a very low 2.4:1 linear to branched ratio, 14% olefin isomerization, and 5% olefin hydrogenation.[14] For comparison, $[Rh_2(nbd)_2$(*rac*-et,ph-

P4)](BF$_4$)$_2$ is far more active with a 600 h$^{-1}$ initial turnover frequency, 28:1 linear to branched ratio, 8% isomerization and 3.4% hydrogenation.[13-14]

After addition of two equivalents of HBF$_4$ to the neutral catalyst precursor, similar hydroformylation performance was observed as with the dicationic precursor.[14] This indicates that the active catalyst generated from the dicationic precursor was not a neutral species as originally thought, but a dicationic complex instead.[14] More information was obtained by FT-IR spectroscopic studies (Figure 3.1).

Figure 3.1 shows FT-IR spectra of the two catalyst precursors - neutral and dicationic. The spectra are either of a pure catalyst precursor, two precursors mixed together or a precursor with addition of an acid or a base. All spectra were recorded at 90 °C, 90 psig $H_2$/CO and acetone or THF was used as solvent. The top spectrum belongs to the neutral catalyst precursor. The carbonyl bands appear at approximately 100 cm$^{-1}$ lower frequencies than the carbonyls generated from the dicationic precursor (the bottom spectrum), which supports the idea that the active catalyst generated from the dicationic precursor is a dicationic complex.

Figure 3.1 also shows FT-IR spectra of the neutral dirhodium catalyst precursor with the added one equivalent of HBF$_4$ (the second spectrum from top), mixture of equimolar amounts of the dirhodium neutral and dicationic precursors (the middle spectrum) and the dicationic dirhodium catalyst with addition of two equivalents of NEt$_3$ (the second spectrum from the bottom). All three spectra show that the terminal carbonyls are located at intermediate stretching frequencies between the terminal carbonyl bands for the neutral and dicationic precursors. This indicates that the generated species are monocationic. Some of the three spectra contain a bridging carbonyl band at 1797 cm$^{-1}$ while for the neutral precursor with one equivalent of HBF$_4$

this band is absent. Therefore, several different monocationic species might be generated depending on the catalyst precursor and exact reaction conditions.[14]

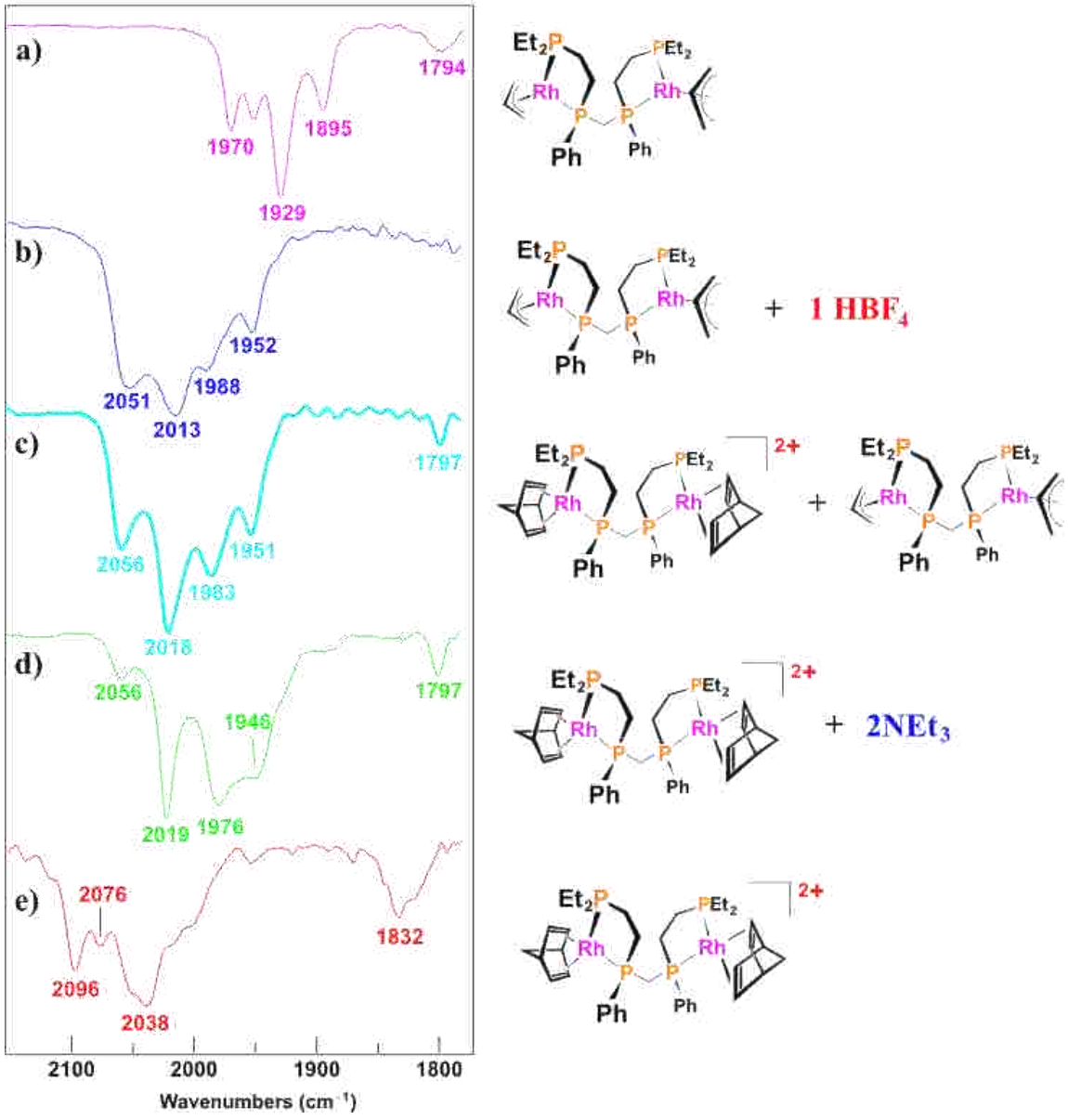


**Figure 3.1.** Neutral and dicationic dirhodium tetraphosphine catalysts in acetone under $H_2/CO$.[14]

When two equivalents of base are added to the dicationic precursor, the generated monocationic species are active for hydroformylation (Table 3.1). The addition of base had

positive effect on L:B ratio (increase). It also suppressed side reactions, which is desirable. Unfortunately, the rate of hydroformylation decreased.[14]

**Table 3.1**. Hydroformylation of 1-hexene with $[Rh_2(nbd)_2(rac\text{-et,ph-P4})](BF_4)_2$ in acetone with addition of $HBF_4$ or $NEt_3$ (90 ºC, 90 psig $H_2$/CO).[14]

| Additive | TOF (TO/h) | Aldehyde L:B | Isomerization | Hydrogenation |
|---|---|---|---|---|
| - | 636 | 28:1 | 8 | 3 |
| 2-4 eq $HBF_4$ | not available | 21:1 | 12 | 6 |
| 2 eq $NEt_3$ | 215 | > 30:1 | < 1.5 | < 1.5 |

All of the above experiments were performed in acetone. Catherine Alexander[15] was the first to study the dirhodium tetraphosphine catalyst with $H_2$/CO in 30% acetone/water via FT-IR (Figure 3.2). Figure 3.2 shows comparison of the FT-IR spectra for the dirhodium tetraphosphine catalyst $[Rh_2(nbd)_2(rac\text{-et,ph-P4})](BF_4)_2$ in acetone and acetone/water (the top two spectra). Catherine Alexander noted that both the spectra contain terminal CO bands at 2094, 2075 and 2035 $cm^{-1}$ (slightly shifted to 2021 $cm^{-1}$ in water/acetone). There are also bridging CO bands at approximately 1834 and 1818 $cm^{-1}$ in both spectra. A correlation between these bridging carbonyl bands and hydroformylation activity has been previously observed. Based on her data Catherine Alexander concluded "that there are not any structural differences between the species formed under a 1:1 $H_2$/CO ratio (90 psig) at 90 °C, and the 30% water/acetone studies."[15]

The band at 2094 $cm^{-1}$ in Figure 3.2, however, is significantly smaller in water/acetone than in pure acetone solvent. This band has been previously assigned to a hexa/pentacarbonyl complex $[Rh_2(CO)_{5\text{-}6}(rac\text{-et,ph-P4})]^{2+}$ that is considered the resting state of the catalyst. In order to explain the difference in hexa/pentacarbonyl complex formation between the two solvent systems, an FT-IR comparison with just CO gas would be beneficial in order to get more information about the carbonyl complex formation.

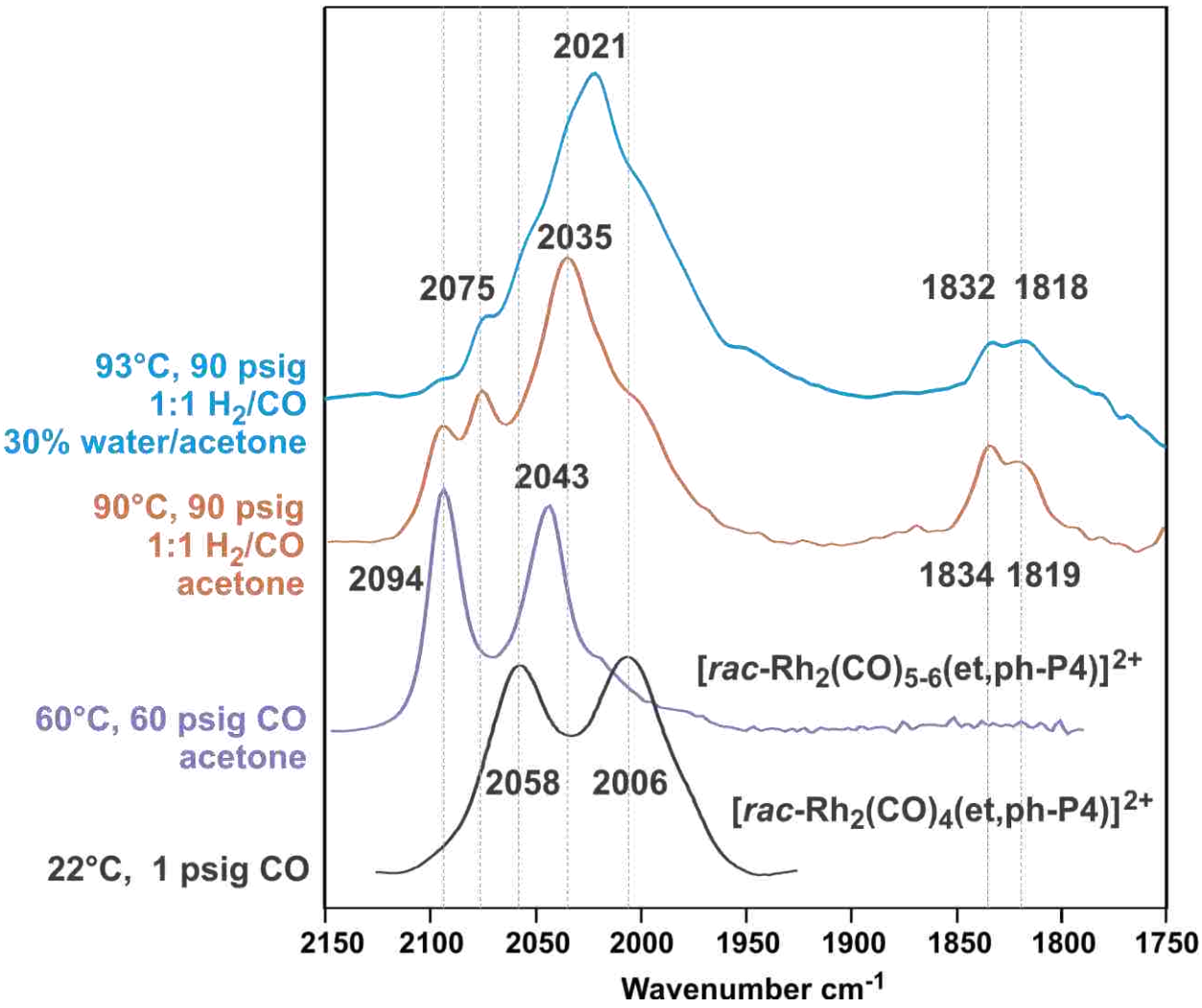


**Figure 3.2.** $[Rh_2(nbd)_2(rac\text{-et,ph-P4})](BF_4)_2$ under $H_2/CO$ pressure.[15]

Figure 3.3 shows how $[Rh_2(nbd)_2(rac\text{-et,ph-P4})](BF_4)_2$ responds when exposed to CO in acetone. At room temperature and low CO pressure the dominant band appears at 2015 $cm^{-1}$. This peak decreases with time, increasing CO pressure and temperature while peaks at 2043 and 2095 $cm^{-1}$ increase. This observation can be explained by an equilibrium among several carbonyl complexes shown in Figure 3.3. A $[Rh_2(CO)_2(nbd)_2(rac\text{-et,ph-P4})]^{2+}$ complex forms (band at 2015 $cm^{-1}$) as CO binds to the dirhodium complex $[Rh_2(nbd)_2(rac\text{-et,ph-P4})]^{2+}$. With increasing CO pressure, the norbornadiene ligands are displaced from the rhodium atoms. This leads to the

formation of a tetracarbonyl complex that, with increasing gas pressure and temperature, adds more carbonyl ligands and forms the penta/hexacarbonyl complex.[15]

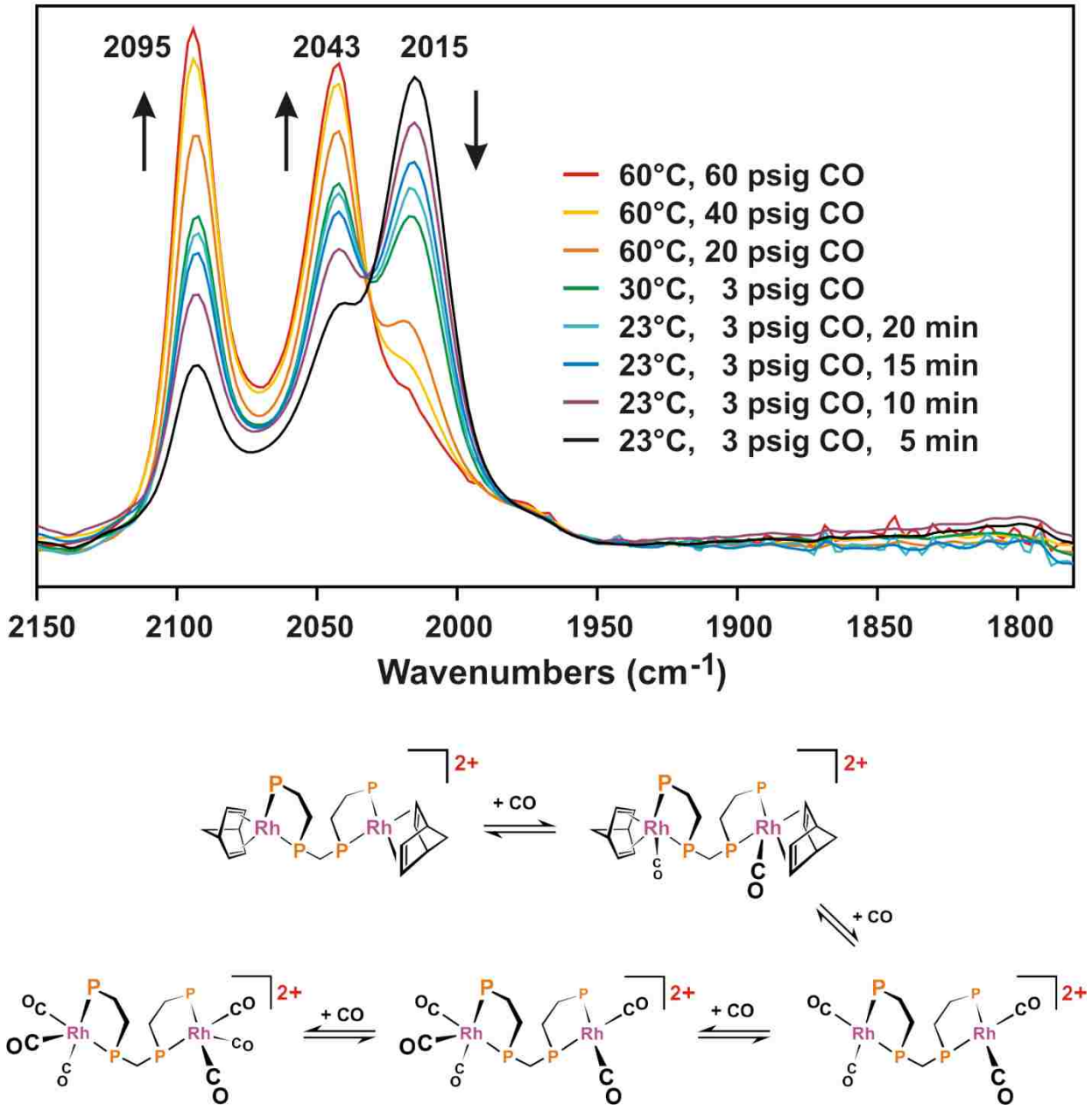


**Figure 3.3.** $[Rh_2(nbd)_2(rac\text{-et,ph-P4})](BF_4)_2$ in acetone under CO at various temperatures.[15]

In order to have a comparison among the two solvent systems reacting with CO, a new analogous experiment was performed in water/acetone. The results are described in section 3.3.1.

### 3.3 Current Studies in Water/Acetone

#### 3.3.1 FT-IR Studies

FT-IR spectra of the dirhodium catalyst in water/acetone were recorded on a newly purchased ReactIR instrument from Mettler-Toledo. Some experiments were also performed on the "old" Spectratech Circle Reaction Cell using a silicon crystal rod on a Bruker platform that was commonly used during former experiments. Prof. Stanley found that the ZnSe rod used in previous high pressure FT-IR experiments was reacting with the dirhodium complexes causing precipitation of metallic Rh onto the crystal rod. The silicon rod appears to be unreactive to the rhodium complexes, is easily cleaned, and far more resistant to breakage. It has lower IR throughput relative to the ZnSe rod, but new focusing mirrors on the cell holder boosted the IR throughput so we are getting better detector counts than with the ZnSe rod. The equipment is described in more detail in Chapter 7.

Spectra similar to Alexander's FT-IR spectra in Figure 3.2 were obtained independently for $[Rh_2(nbd)_2(rac\text{-et,ph-P4})](BF_4)_2$ in acetone as well as water/acetone under $H_2$/CO. Also the recorded spectrum of $[Rh_2(nbd)_2(rac\text{-et,ph-P4})](BF_4)_2$ under CO in acetone confirmed the previous observations. However, spectrum of $[Rh_2(nbd)_2(rac\text{-et,ph-P4})](BF_4)_2$ in water/acetone under CO pressure was not previously recorded. This measurement can be important for explanation of why significantly smaller amount of the penta/hexacarbonyl complex formed in water/acetone under $H_2$/CO compared to acetone. Therefore, this experiment was undertaken (Figure 3.4.). Figure 3.4 shows that a band forms at 2020 $cm^{-1}$ when $[Rh_2(nbd)_2(rac\text{-et,ph-P4})]^{2+}$ is placed under CO in water/acetone. When CO pressure and temperature are increased, the main band shifts slightly to higher wavenumbers and broadens, but still remains dominant. This is quite different from acetone, where the originally major peak of the bis(norbornadiene)-

dicarbonyl complex at 2015 $cm^{-1}$ diminishes with increasing temperature and CO pressure while two bands of comparable size grows in the spectrum.

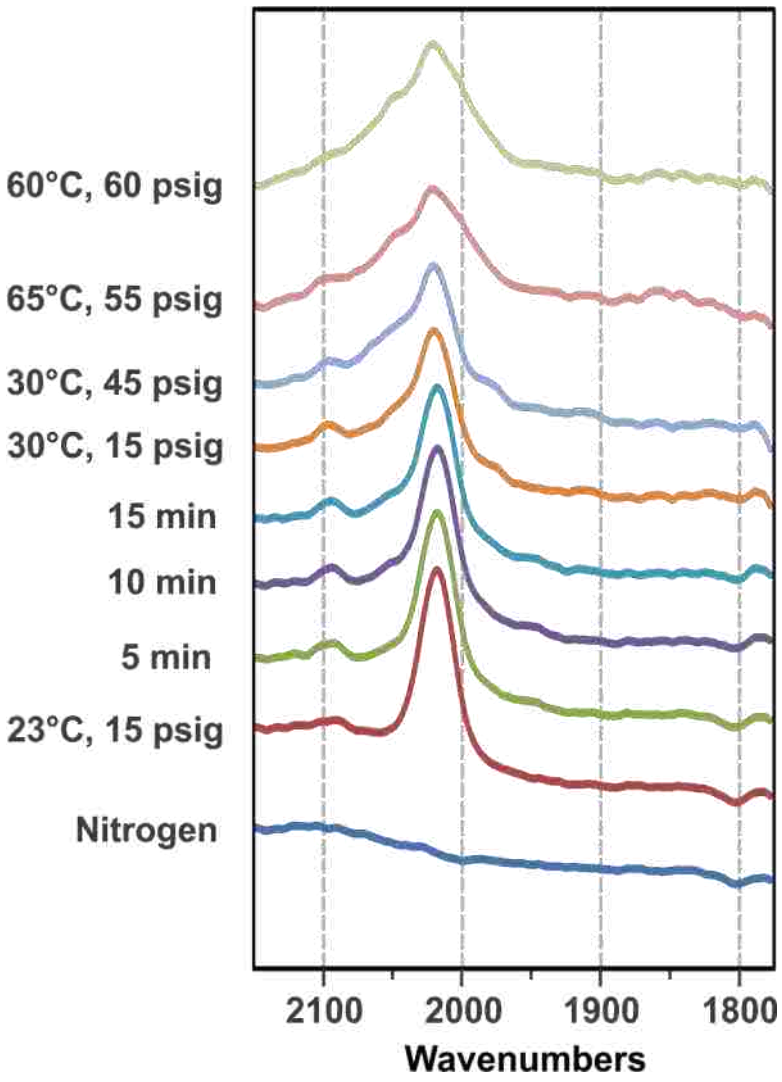


**Figure 3.4.** $[Rh_2(nbd)_2(rac\text{-et,ph-P4})](BF_4)_2$ in water/acetone under CO pressure.

Norbornadiene is readily displaced from the bis(norbornadiene)dicarbonyl complex and tetracarbonyl and penta/hexacarbonyl complexes form in acetone, in water/acetone the norbornadiene seems to be replaced slower than in acetone, probably due to the hydrophobic nature of norbornadiene. Contrary to acetone, the spectrum at Figure 3.4 shows a minimal tendency for formation of penta/hexacarbonyl complexes in water/acetone. This was already

indicated by the high-pressure NMR studies. The signals for the pentacarbonyl complex that are present in the $^{31}P\{^{1}H\}$NMR spectrum in acetone seem absent in water/acetone (Figure 2.21 in Chapter 2). It is also worth mentioning that in FT-IR spectra for monocationic dirhodium complexes in acetone (Figure 3.1) the band at 2094 $cm^{-1}$ related to formation of penta/hexacarbonyl complex has very low intensity.

The reason for less formation of the pentacarbonyl/hexacarbonyl complex could be caused by water inhibiting CO and alkene coordination. If water would coordinate to a metal complex, it would also stabilize the loss of CO from the complex. Molarity of the $H_2O$ in the acetone solution is 16.7 while acetone is 12 M, i.e. molarity of water is higher than molarity of acetone. On the other hand, since in water/acetone there is significantly less catalyst present in its resting state, the inhibition caused by water might not be observed as decrease in catalysis. According to DFT calculations performed by Prof. Stanley the lone pair of $H_2O$ has an energy –8.13 eV, which is lower than that of acetone at –6.88 eV. This means that acetone is a better donor and should coordinate easier than water to a metal complex. Water can also affect hydroformylation through formation of hydrogen bonds with carbonyl ligands which have a slightly negative charge. Water can draw CO electron density and since CO is a poor donor ligand, this can help CO to dissociate.

All the experiments above were performed in the absence of an alkene. An FT-IR hydroformylation experiment in presence of 1-hexene (2 M) in water/acetone under $H_2$/CO showed no significant changes in the carbonyl bands. Unfortunately no information could be gained from the aldehyde region around 1700 $cm^{-1}$ since possible changes were hidden by an acetone band which appears in the same area. This is the same as observed in pure acetone where

the addition of 1-hexene initiates hydroformylation, but does not change the Rh-CO bands seen in the FT-IR.

Figure 3.5 shows comparison of $[Rh_2(nbd)_2(rac\text{-et,ph-P4})]^{2+}$ in water/acetone exposed to CO or $H_2$/CO (2 M 1-hexene was present during the $H_2$/CO experiment). Under CO atmosphere, a band forms immediately at 2020 $cm^{-1}$ that broadens with increasing temperature. The position of the band is very close to the dominant band at 2021 $cm^{-1}$ in water/acetone under $H_2$/CO. It is also relatively close to band 2015 $cm^{-1}$ in acetone under CO that was assigned to the bis-(norbornadiene)dicarbonyl complex (Figure 3.3). We believe that the hydrogen bonding of water to the carbonyl ligands is causing the shift of frequency to higher energies relative to the band in acetone.

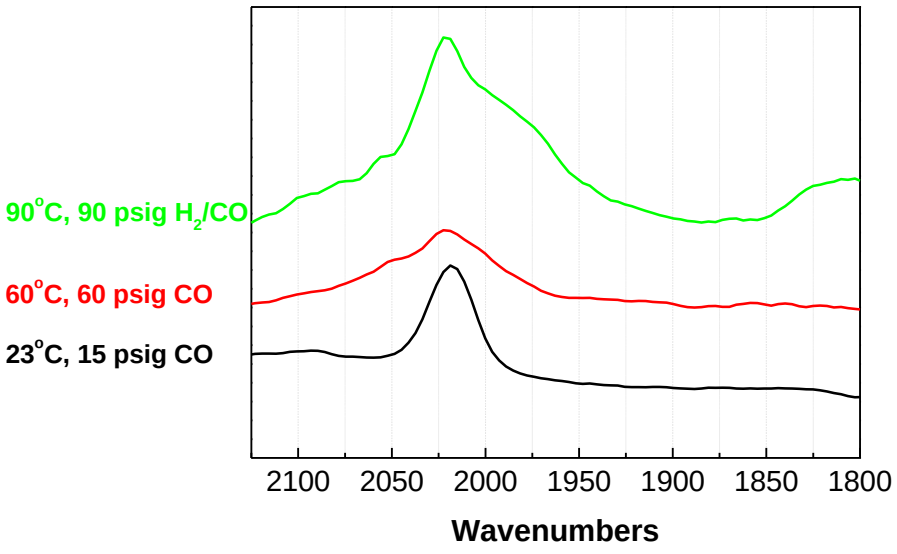


**Figure 3.5.** $[Rh_2(nbd)_2(rac\text{-et,ph-P4})](BF_4)_2$ in water/acetone under CO and $H_2$/CO pressure.

### 3.3.2 Acidity of Catalyst Solution

Since the solvent currently used for hydroformylation is 30% water/acetone, pH of the catalyst solution after hydroformylation was measured. The results are shown in Table 3.2. The

catalyst solutions are acidic, with the pH directly dependent on the molarity of $[Rh_2(nbd)_2$(*rac*-et,ph-P4)$](BF_4)_2$. The results indicate that the dirhodium catalyst behaves as a strong acid.

**Table 3.2.** pH values of water/acetone solution after hydroformylation.

| Molarity | pH |
|---|---|
| 1 mM | 3.1 |
| 10 mM | 2.2 |

To further investigate the deprotonation equilibria in water/acetone, hydroformylation reactions were performed in a Parr autoclave with addition of an acid or a base analoguously to the previous experiments in acetone by Spencer Train.[14] Triethylamine is not a strong base but it is stronger than water. The results are shown in Table 3.3.

**Table 3.3.** Hydroformylation of 1-hexene in 30% water /acetone with addition of acid and base (after 2 h at 90 ºC, 90 psig $H_2$/CO).

| Additive | Initial Rate | Aldehyde L:B | Isomerization |
|---|---|---|---|
| None | 24 $min^{-1}$ | 29 | 2.7% |
| 5 eq $HBF_4$ | 12.5 $min^{-1}$ | 23 | 8.8% |
| 2 eq $NEt_3$ | 4.2 $min^{-1}$ | 15 | 1.3% |

Hydroformylation slowed down with the addition of base and isomerization decreased. The same trend was observed previously in acetone. While the L:B ratio increased in acetone (Table 3.1) when base was present in the solution, a decrease in L:B ratio was observed in water/acetone. The increase in acetone was explained by formation of a monocationic monohydride complex when the base is added. This complex was proposed to be slower than the dicationic dihydride but more selective.[14] The decrease in the L:B ratio in water/acetone might indicate the presence of a monocationic monohydride species (Figure 3.6) that are being

further deprotonated with added $NEt_3$ to form a neutral complex that we have already demonstrated is a very poor hydroformylation catalyst.

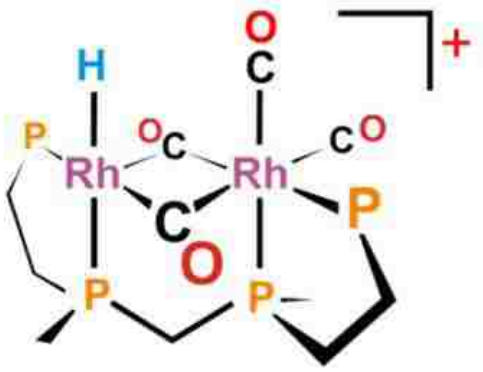


**Figure 3.6.** Monocationic monohydride dirhodium complex.

An equilibrium between dihydride and monohydride species that is affected by addition of an acid or a base was previously reported in literature. Schrock and Osborne studied rhodium hydrogenation catalyst $[Rh(nbd)L_n]^+ PF_6^-$, where L is a tertiary phosphine.[16] They proposed the equilibrium:

$$[RhH_2L_nS_x]^+ \rightleftharpoons RhHL_nS_y + H^+$$

between the neutral hydride and cationic dihydride. Bianchini investigated hydroformylation of 1-hexene with rhodium in presence of linear triphosphine $PhP(CH_2CH_2PPh_2)_2$.[17] When hydroformylation was performed in presence of $NEt_3$, less isomerization was observed than in the absence of the base. This was explained by possible existence of a different catalyst species, probably "a monohydride species formed by heterolytic splitting of $H_2$ as generally occurs in base-assisted hydroformylations catalyzed by phosphane-modified rhodium complexes."[17] However, *in-situ* $^{31}P$ NMR experiment did not show any different complexes in the presence of a base.[17]

Joo investigated rhodium(I), iridium(I) and ruthenium(II) hydrides in aqueous solutions in order to determine effect of water on hydrogenation and discovered that some equilibria

between hydride complexes were dependent on the pH of the solution.[18] For ruthenium complexes with the water soluble phosphine ligand $PPh_2(C_6H_4SO_3Na)$ (tppms), the following equilibria were proposed:

$$\tfrac{1}{2}\,[\{RuCl_2(tppms)_2\}_2] + H_2 + tppms \rightleftharpoons [HRuCl(tppms)_3] + H^+ + Cl^-$$

$$[HRuCl(tppms)_3] + H_2 + tppms \rightleftharpoons [H_2Ru(tppms)_4] + H^+ + Cl^-.$$

In an acidic solution the dominant species was $[HRuCl(tppms)_3]$, while in neutral and basic environment the main complex was $[H_2Ru(tppms)_4]$ as confirmed by $^1H$ and $^{31}P$ NMR spectroscopy.[18]

For the dirhodium tetraphosphine catalyst, the pH measurements and hydroformylation with added $NEt_3$ indicate a deprotonation equilibrium. Does spectroscopy support this assumption? Figure 3.7 shows the comparison of several FT-IR spectra at different conditions. A FT-IR spectrum of $[Rh_2(nbd)_2(et,ph\text{-}P4)](BF_4)_2$ at 90 ºC and 90 psig $H_2$/CO did not show much difference between water/acetone and acetone except the height of the 2094 $cm^{-1}$ peak. However, there is an almost exact match of the catalyst mixture at 25 ºC and 75 psig $H_2$/CO in water/acetone with the monocationic complexes generated by two different routes at 90 ºC and 90 psig $H_2$/CO in acetone.

$^1H$ NMR spectra of $[Rh_2(nbd)_2(rac\text{-}et,ph\text{-}P4)](BF_4)_2$ under $H_2$/CO showed considerable differences between acetone and water/acetone solvents (Figure 2.22 in Chapter 2). In acetone, there are two peaks present at low temperatures that were assigned to the bridging and terminal hydride of the dicationic dirhodium catalyst. However, only one peak is observed in the water/acetone spectrum, which might indicate presence of only one type of hydride and supports deprotonation to form monocationic monohydride complexes.

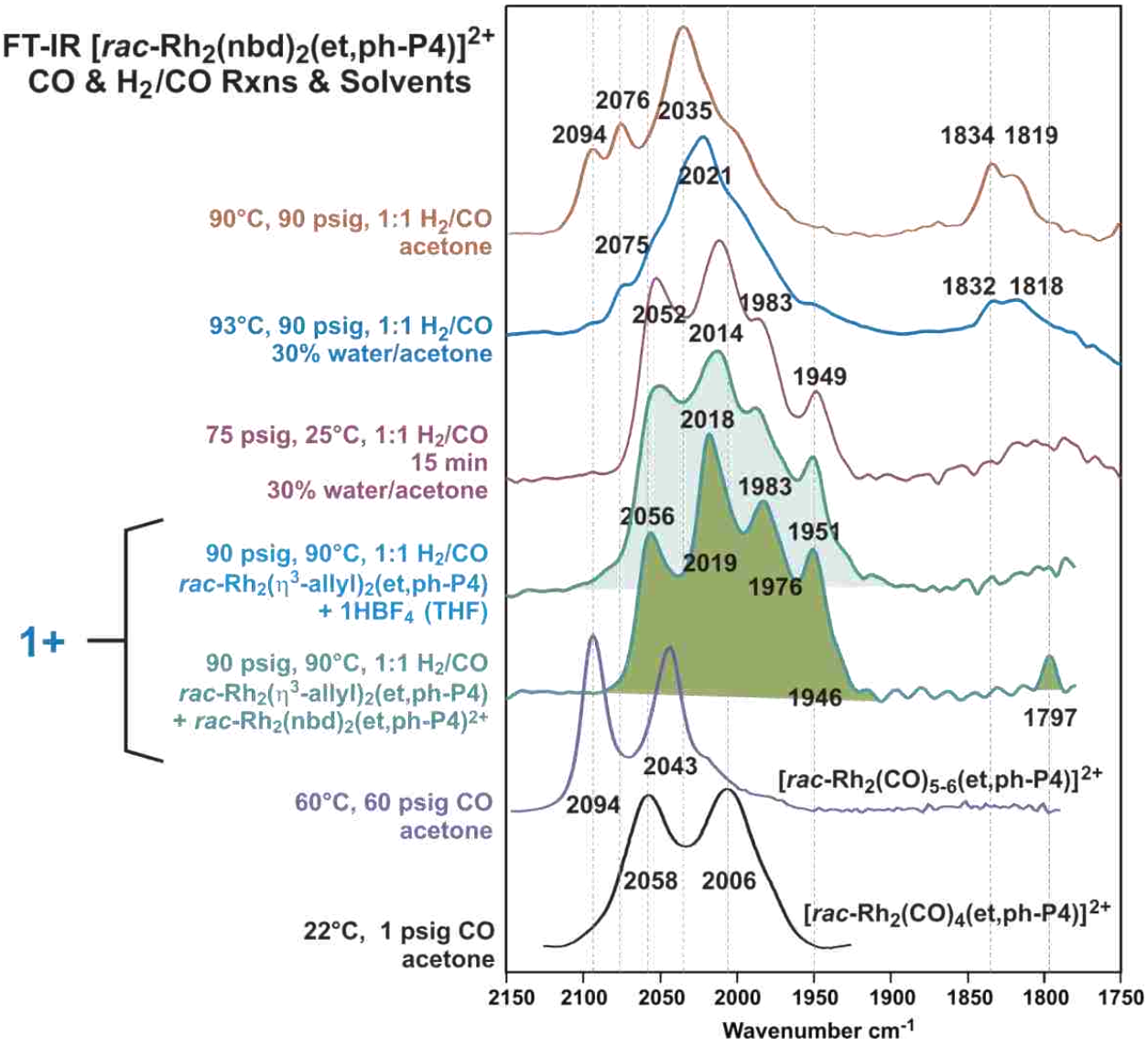


**Figure 3.7** Comparison of FT-IR spectra under various conditions.

Figure 3.8 shows $^{31}P\{^{1}H\}$NMR spectra of aged samples of $[Rh_2(nbd)_2$(*rac*-et,ph-P4)$](BF_4)_2$ under $H_2$/CO in acetone (top), water/acetone (bottom) and water/acetone with addition of $HBF_4$ (middle spectrum). The typical peaks of the degradation products are present in acetone. The two most clearly visible peaks are found around 22 ppm and –8 ppm and were assigned to the dirhodium double ligand complex. These peaks are very small/almost nonexistent in water/acetone. However, in water/acetone in the presence of $HBF_4$ (11 equivalents) these

peaks are present in a substantial amount. Therefore degradation of the catalyst seems to be also affected by the acid/base equilibrium.

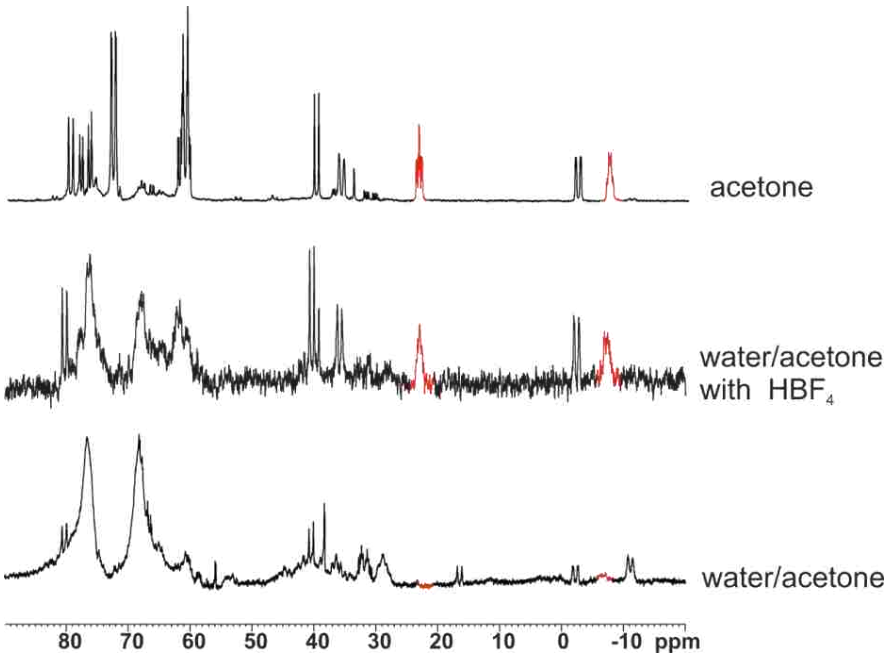


**Figure 3.8** $^{31}P\{^{1}H\}$NMR of $[Rh_2(nbd)_2(rac\text{-et,ph-P4})](BF_4)_2$ after several days under 90 psig $H_2/CO$ in acetone (top spectrum), in 30% water/acetone with addition of $HBF_4$ (middle spectrum) and in 30% water/acetone (bottom spectrum).

### 3.4 Summary and Future Experiments

FT-IR experiment showed that the dirhodium catalyst precursor reacts with CO gas in water/acetone. However, the resulting species containing carbonyl ligands is not the same as in acetone. There is significantly less formation of penta/hexacarbonyl complexes and, therefore, less of the catalyst is in its resting state. The decrease of pH after hydroformylation as well as the lower L:B ratio with the addition of base indicates the presence of a monocationic monohydride species as the principal active hydroformylation catalyst in water/acetone.

pH measurements were performed on samples in water/acetone after pressure was released from the autoclave. For future experiments it would be ideal to monitor pH during the actual hydroformylation run. Parr, the manufacturer of autoclaves that we use for

hydroformylation reactions, already addressed the issue of a pH measurement in pressure vessels.[19] A special electrode (Spectra pH sensor) was developed that contains a pressure compensating device and can be used up to 34 bar and 135 ºC. Parr offers to attach the pH sensor to autoclaves smaller than 1 L through the bottom of the cylinder.[19]

### 3.5 References


1. Crabtree, R. H., *The Organometallic Chemistry of the Transition Metals*. Wiley 2005.
2. (a) Mirbach, M. F. *J. Organomet. Chem.* **1984,** *265* (2), 205-213; (b) Pino, P.; Major, A.; Spindler, F.; Tannenbaum, R.; Bor, G.; Horvath, I. T. *J. Organomet.Chem.* **1991,** *417* (1-2), 65-76; (c) Whyman, R. *J. Organomet. Chem.* **1974,** *81* (1), 97-106; (d) Whyman, R. *J. Organomet. Chem.* **1974,** *66* (1), C23-C25; (e) Vanboven, M.; Alemdaroglu, N.; Penninger, J. M. L. *J. Organomet. Chem.* **1975,** *84* (1), 65-74.
3. Fyhr, C.; Garland, M. *Organometallics* **1993,** *12* (5), 1753-1764.
4. Moser, W. R.; Papile, C. J.; Weininger, S. J. *J. Mol. Catal.* **1987,** *41* (3), 293-302.
5. (a) Bronger, R. P. J.; Kamer, P. C. J.; van Leeuwen, P. *Organometallics* **2003,** *22* (25), 5358-5369; (b) Silva, S. M.; Bronger, R. P. J.; Freixa, Z.; Dupont, J.; van Leeuwen, P. *New J. Chem.* **2003,** *27* (9), 1294-1296.
6. Kamer, P. C. J.; van Rooy, A.; Schoemaker, G. C.; van Leeuwen, P. *Coord. Chem. Rev.* **2004,** *248* (21-24), 2409-2424.
7. Nozaki, K.; Matsuo, T.; Shibahara, F.; Hiyama, T. *Organometallics* **2003,** *22* (3), 594-600.
8. (a) Bayon, J. C.; Esteban, P.; Real, J.; Claver, C.; Polo, A.; Ruiz, A.; Castillon, S. *J. Organom. Chem.* **1991,** *403* (3), 393-399; (b) Dieguez, M.; Claver, C.; Masdeu-Bulto, A. M.; Ruiz, A.; van Leeuwen, P.; Schoemaker, G. C. *Organometallics* **1999,** *18* (11), 2107-2115.
9. Noack, K., An infrared high-pressure cell. *Spectrochim. Acta* **1968,** *24* (12), 1917.
10. Damoense, L.; Datt, M.; Green, M.; Steenkamp, C. *Coord. Chem. Rev.* **2004,** *248* (21-24), 2393-2407.
11. Moser, W. R.; Cnossen, J. E.; Wang, A. W.; Krouse, S. A. *J. Catal.* **1985,** *95* (1), 21-32.
12. Caporali, M.; Frediani, P.; Salvini, A.; Laurenczy, G. *Inorg. Chim. Acta* **2004,** *357* (15), 4537-4543.
13. Broussard, M. E.; Juma, B.; Train, S. G.; Peng, W. J.; Laneman, S. A.; Stanley, G. G. *Science* **1993,** *260* (5115), 1784-1788.
14. Train, S. G., PhD Thesis, Louisiana State University, 1994.
15. Thomas Alexander, C. L., PhD Thesis, Louisiana State University, 2009.
16. Schrock, R. R.; Osborn, J. A. *J. Am. Chem. Soc.* **1976,** *98* (8), 2134-2143.

17. Bianchini, C.; Frediani, P.; Meli, A.; Peruzzini, M.; Vizza, F. *Chem. Ber. Recueil* **1997,** *130* (11), 1633-1641.

18. Joo, F.; Kovacs, J.; Benyei, A. C.; Katho, A. *Angew. Chem. Int. Ed.* **1998,** *37* (7), 969-970.

19. Parr, Bulletin No.203.

# CHAPTER 4: CATALYST ACTIVATION WITHOUT HYDROGEN

## 4.1 Background

Previous chapters compared properties of dirhodium tetraphosphine in acetone and acetone/water solvent under $H_2$/CO pressure. The water/acetone solvent system is interesting because in theory activation of the catalyst for hydroformylation could occur just in presence of CO and water without the addition of any $H_2$ gas. This general process is called water gas shift reaction (WGSR) where hydrogen and carbon dioxide are formed from water and CO

$$CO\ (g) + H_2O\ (l) \longrightarrow CO_2\ (g) + H_2\ (g).$$

WGSR is an important for industry because it enables the use of coal for hydrogen production.[1] Both heterogeneous or homogeneous catalysts can be used.[2] Transition metal complexes belong to homogeneous catalysts and their advantage compared to the heterogeneous catalysts is that they are active for WGSR at lower temperatures. The transition metal complexes are usually dissolved in a mixture of water and an organic solvent due to their limited solubility in water.[2]

Rhodium phosphine complexes $[RhHL_3]$ (L = $PEt_3$ or $P^iPr_3$), $[Rh_2H_2(\mu\text{-}H_2)(PCy_3)_4$, trans-$[RhH(N_2)\{PPh(^tBu)_2\}_2]$,$[RhH(P^tBu_3)_2]$ are among the most active homogeneous catalysts for WGSR.[3] $RhH[(P^iPr)_3]_3$ is presumably activated in a neutral environment by oxidative addition of water on the rhodium atom.[4] WGSR can be coupled with other processes as hydrogenation or hydroformylation and serve as a source of $H_2$ for those reactions.[3]

The dirhodium cationic monohydride complex $[Rh_2(\mu\text{-}H)(\mu\text{-}CO)(CO)_2(dppm)_2]^+A^-$, where dppm is bis(diphenylphosphino)methane and $A^-$ is *p*-$CH_3C_6H_4SO_3^-$ or $PF_6^-$, is an active WGSR catalyst.[5] The catalysis rate of 2.5 turnovers/h was reported in *n*-PrOH with 2 equivalents LiCl under 1 atm CO and at 90 °C.[5a]

$[Rh_2(\mu\text{-}H)(\mu\text{-}CO)(CO)_2(dppm)_2]^+$ is somewhat similar to our dirhodium tetraphosphine complex and therefore sparked my interest about its WGSR activity. Prof. Stanley presumed that the complex might be capable of WGSR, but it has never been demonstrated. It might be important for our research on aldehyde-water shift reaction, which is currently investigated by research group member Rider Barnum. During the aldehyde-water shift catalysis, aldehyde and water are transformed into $H_2$ and carboxylic acid. The active catalyst for this has been proposed to be $[Rh_2(\mu\text{-}CO)_2(CO)_2(rac\text{-et,ph-P4})]^{2+}$. A small amount of $H_2$ must be present from the beginning of the reaction in order to form closed-mode bridged carbonyl complexes. Therefore experiments with the tetraphosphine dirhodium catalyst in water/acetone under CO to investigate the possibility of WGSR have been performed.

**4.2 Results and Discussion**

$^{31}P\{^1H\}$ NMR spectra of the dirhodium catalyst under 50 psig CO in 30% water/acetone were recorded and are shown in Figure 4.1. The bottom spectrum was taken 70 minutes after filling the NMR tube with gas. The spectrum is different from the spectra obtained so far with $H_2$/CO. The top spectrum in the figure was taken after the sample was left on the bench for 2 days at room temperature and then heated to 90°C for 20 minutes (the sample darkened during heating). The $^{31}P\{^1H\}$ NMR spectrum is very similar to that of the dirhodium catalyst under $H_2$/CO.

The next step was to determine if any hydrides formed in the sample. There are indeed several hydride peaks present as shown in Figure 4.2. A hydride peak around −11 ppm was previously correlated to the hydroformylation activity under $H_2$/CO conditions. However, other hydrides peaks are also present that resemble degradation products under $H_2$/CO conditions. The

peaks around −9 ppm were assigned as a dirhodium double ligand complex while the signal around −18 ppm is related to a monometallic degradation product.

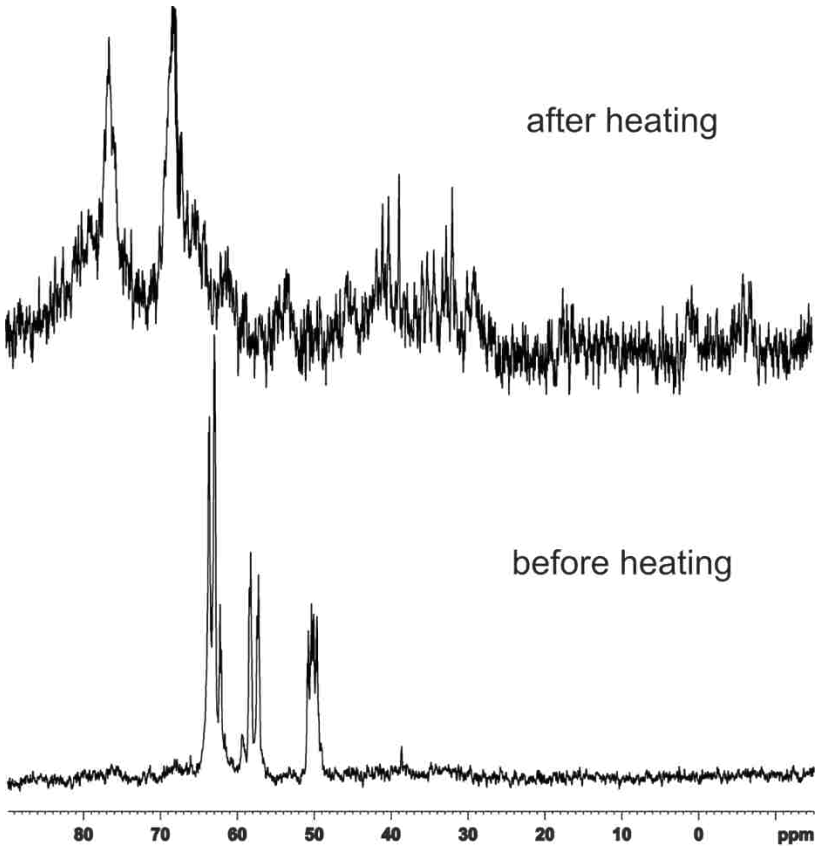


**Figure 4.1.** $^{31}P\{^{1}H\}$NMR spectra of $[Rh_2(nbd)_2(rac\text{-et,ph-P4})]^{2+}$ in acetone/water under 50 psig CO at room temperature (bottom) and after heating to 90°C for 20 mins (top).

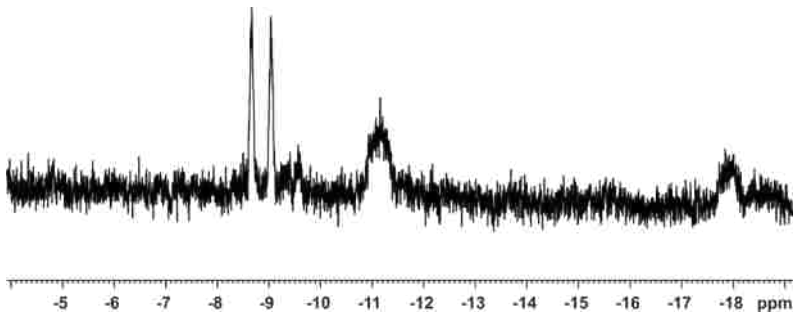


**Figure 4.2.** $^{1}H$ NMR spectrum of $[Rh_2(nbd)_2(rac\text{-et,ph-P4})]^{2+}$ in acetone/water under 50 psig CO after heating.

Two things are important for WGSR catalytic cycle - the presence of hydride on a rhodium complex and release of $H_2$. Previously, WGSR was investigated with a catalyst precursor that already contained hydride, for example Yoshida investigated WGSR with the catalyst precursor $[RhH(PEt_3)_3]$.[6] It is also possible to use a precursor that does not contain hydrides as Kubiak's $[Rh_2(\mu\text{-}CO)(CO)_2(dppm)_2]$ in presence of p-toluenesulfonic acid.[5b] Here, NMR showed hydride formation from the dirhodium tetraphosphine catalyst precursor without addition of any acid. Initial presence of hydride on the rhodium catalyst precursor might not be necessary since Yoshida reported formation of $H_2$ when $Rh_2(CO)_3(P^iPr_3)_3$ reacted with water.[7] We do not have any direct evidence of $H_2$ release for our dirhodium tetraphosphine catalyst precursor $[Rh_2(nbd)_2(rac\text{-et,ph-}P_4)](BF_4)_2$, i.e., proof that a complete cycle of WGSR really takes place. Release of $H_2$ from the metal complex can be possibly very slow step, for example Sutherland and Cowie reported that complex $[Ir_2(CO)_4(\mu\text{-}H)_2(dppm)_2]^{2+}$ released $H_2$ slowly when left under CO for two weeks.[8]

It is surprising that dirhodium double ligand degradation product is present in substantial amount in the solution, since this complex is characteristic for acetone solvent system. This can be explained by equilibrium between the dirhodium dihydride and dirhodium monohydride complexes in the solution where the former complex is more prone to degradation. Degradation can also occur from an open mode carbonyl complex with subsequential addition of hydrogen to the degradation products. Regardless, hydrogen must be present in order for hydride containing degradation products to be formed.

Figure 4.3 shows $^{19}F$ NMR of the sample in order to possibly explain the effect of the $BF_4^-$ anion on the process. It is known that the reaction of $BF_4^-$ with water leads to the defluorination of the anion which results in the formation of $BF_3(OH)^-$ and HF.[9] In the spectrum

are several peaks visible. The two peaks around −151 ppm should correspond to free $BF_4^-$ ion. The signal around −145 ppm could belong to a coordinated $BF_4^-$. Somewhat similar shift and pattern was observed for a complex $[Re(\eta^1\text{-}BF_4)(CO)_3\{PPh(OMe)_2\}_2]$.[10] The origin of the signal at −169 ppm is so far unknown.

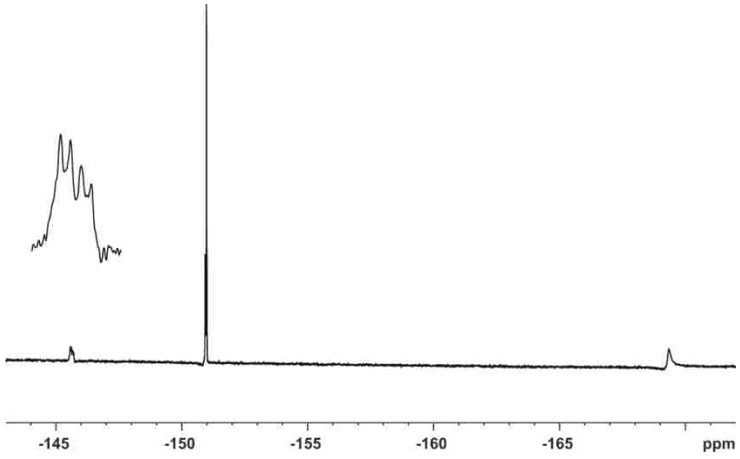


**Figure 4.3.** $^{19}F$ NMR of dirhodium catalyst under CO after heating.

Since the NMR spectra above indicated water-gas shift reaction, an experiment was performed attempting to use WGSR as a hydrogen source for hydroformylation. A reaction was performed in a Parr autoclave under usual hydroformylation conditions (1mM catalyst, 1M 1-hexene, 30% water-acetone), but CO gas was used instead of $H_2$/CO mixture. During the first hour of the experiment 50 psig CO was used, followed by 90 psig CO for the second hour and for the last hour 90 psig $H_2$/CO mixture was introduced into the autoclave. The results are summarized in table 4.1. No hydroformylation occurred after one hour at 50 psig CO. Aldehyde was absent also when pressure was increased to 90 psig CO and the autoclave was kept at this pressure for one hour. After a total two hours under CO gas, it was switched to $H_2$/CO gas and hydroformylation resumed. Even though higher isomerization than usual was observed, the fact

that hydroformylation occurred indicates that the catalyst did not fully degrade under CO pressure in water/acetone.

**Table 4.1.** Hydroformylation of 1-hexene in water/acetone with CO (first two hours) and $H_2$/CO gas (last hour).

| Time | % Unreacted | Aldehyde L:B | % Isomerization |
|---|---|---|---|
| 10 min | 100 | - | - |
| 1 h | 100 | - | - |
| 2 h | 95.8 | - | 4.2 |
| 3 h | 35.7 | 29.3 | 21.1 |

It would be beneficial to let the reaction run longer under CO, since in the literature WGSR runs are reported as long as 70 hours.[5b] Also acid/base addition, salt addition, varying CO pressure and temperatures might potentially have beneficial effect on the process and should be investigated.

In conclusion, NMR studies indicated that it is possible to form hydride in water with the dirhodium tetraphosphine catalyst under CO pressure and therefore WGSR in theory can serve as a source of hydrogen for other reactions such as hydroformylation. However, the preliminary experiment showed that WGSR is not a sufficient source of hydrogen for this reaction since no hydroformylation was observed within 2 hours. Possible future experiments should be allowed to run longer in order to determine if it is possible to observe hydroformylation at all. Reaction conditions should also be optimized.

### 4.3 References


1. Okano, T.; Kobayashi, T.; Konishi, H.; Kiji, J. *Bull. Chem. Soc. Jpn* **1981,** *54* (12), 3799-3805.
2. Doi, Y.; Yokota, A.; Miyake, H.; Soga, K. *Inorg. Chim. Acta* **1984,** *90* (1), L7-L9.

3. Simpson, M. C.; ColeHamilton, D. J. *Coord. Chem. Rev.* **1996,** *155*, 163-207.

4. Laine, R. M.; Crawford, E. J. *J. Mol. Catal.* **1988,** *44* (3), 357-387.

5. (a) Kubiak, C. P.; Eisenberg, R. *J. Am. Chem. Soc.* **1980,** *102* (10), 3637-3639; (b) Kubiak, C. P.; Woodcock, C.; Eisenberg, R. *Inorg. Chem.* **1982,** *21* (6), 2119-2129.

6. Yoshida, T.; Okano, T.; Ueda, Y.; Otsuka, S. *J. Am. Chem. Soc.* **1981,** *103* (12), 3411-3422.

7. Yoshida, T.; Okano, T.; Otsuka, S. *J. Am. Chem. Soc.* **1980,** *102* (18), 5966-5967.

8. Sutherland, B. R.; Cowie, M. *Organometallics* **1985,** *4* (9), 1637-1648.

9. Wiench, J. W.; Michon, C.; Ellern, A.; Hazendonk, P.; Iuga, A.; Angelici, R. J.; Pruski, M. *J. Am. Chem. Soc.* **2009,** *131* (33), 11801-11810.

10. Carballo, R.; Castineiras, A.; Garcia-Fontan, S.; Losada-Gonzalez, P.; Abram, U.; Vazquez-Lopez, E. M. *Polyhedron* **2001,** *20* (18), 2371-2383.

# CHAPTER 5: CATALYST IMMOBILIZATION

## 5.1 Background

Homogeneous catalysis is not common in industry because separation of the products from the catalyst is difficult.[1] Hydroformylation is, therefore, both unusual and one of the largest homogeneous processes carried out in industry. Immobilization of the catalyst on a solid material has been investigated for quite some time in order to separate the catalyst from the hydroformylation products.[1] The solid support can be inorganic, polymer, or it can be a supported liquid phase. In general these methods, so far, have not been successful due to problems with stability, reaction rates and selectivity.[1] Carbon monoxide is an extremely efficient ligand at displacing other ligands and leaching later transition metals like Rh and Co from supports.

Novella Bridges and David Aubry[2] attempted to improve the separation of the dirhodium tetraphosphine catalyst from the aldehyde product by the addition of water. It led to the formation of a separate aldehyde phase, but this approach was not successful because the dirhodium catalyst unexpectedly proved to be more soluble in the aldehyde phase than the water/acetone layer. Attachment of the dicationic dirhodium catalyst to a solid material might work better than that for neutral monometallic systems leading to successful and easy catalyst separation.

Several ways on how to attach phosphines to silica have been previously published. Phosphines that contain an ethoxysilane group can be attached to oxide surfaces.[3] Introducing the ethoxysilane group into the tetraphosphine ligand et, ph-P4, however, might be synthetically challenging, even though attachment of the ethoxysilane group to a bis(diphenylphosphino)-

methane (dppm) ligand has been accomplished.[4] Alternate routes for the immobilization of phosphines that do not contain the ethoxysilane groups have been achieved.[5]

Immobilization of a phosphine/rhodium complexes was reported by Lorenzini et al,[6] who employed a sol-gel method for the immobilization of the bimetallic hydrogenation catalyst $[Rh_2(COD)_2(dppm)(\mu\text{-}Cl)]BF_4$. The cationic complex [(R,R)-Me-(DUPHOS)Rh(COD)]$CF_3SO_3$, where Me-DUPHOS is 1,2-bis(2,5-dimethylphosphacyclopentyl)ethane (Figure 5.1), was immobilized on a silica surface through the hydrogen bonding of the triflate anion with the silanol groups on the silica surface.[7] Even though this is a non-covalent immobilization, the bond was stable enough for use as a hydrogenation catalyst at 8 psi $H_2$ at room temperature. Moreover, the catalyst was recyclable.[7] The complex $[Pd(dppp)(dtc)]BF_4$, where dppp is 1,3-bis(diphenylphosphino)propane and dtc = N,N-diethyldithiocarbamate, was attached to silica surface on a similar principle via the $BF_4^-$ anion.[8]

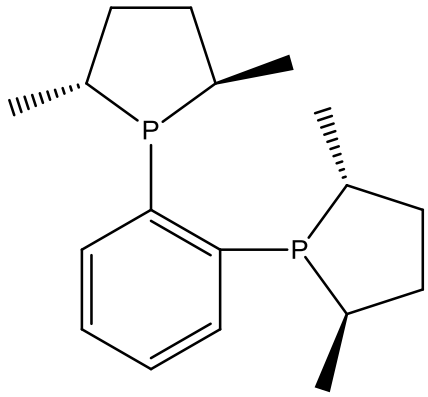


**Figure 5.1.** (R,R)-Me-DUPHOS.

Since our dirhodium tetraphosphine system is mono- or dicationic(depending on solvent), it should be possible to attach it to a silica surface analogously to the above two cationic complexes. The main advantage of this approach is that the ligand does not have to be synthetically modified. The potential problem is that CO is a far stronger leaching agent relative to hydrogen.

## 5.2 Results

The dirhodium catalyst precursor (0.051g) in dichloromethane (DCM) was added to one gram of silica gel (Sorbent Technologies, 32-63 μm particle size). The mixture was stirred for one hour under nitrogen atmosphere, then the liquid was removed and the remaining solid was dried. The obtained product was a yellow powder shown in Figure 5.2. NMR characterization of the product was attempted, but the solid state NMR was not successful due to the low loading of the catalyst on the silica surface.

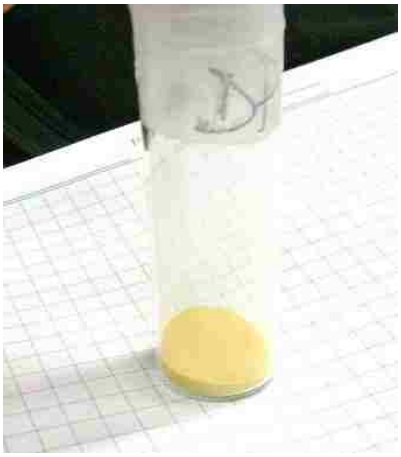

**Figure 5.2.** Silica gel with attached dirhodium catalyst.

In order to test catalyst leaching, some modified silica was dispersed in DCM and mixed. After several days of occasional shaking, the solution was still colorless with light orange solid at the bottom, as shown at Figure 5.3. This indicates that the catalyst is not leaching to DCM solution.

**Figure 5.3.** Supported catalyst after 3 days in DCM showing no leaching into the solvent.

The catalyst attached to silica was tested under hydroformylation conditions, even though the amount of the catalyst was much smaller than usually used (1mM). The autoclave was charged with the catalyst inside the glovebox and hydroformylation was performed in acetone at 90°C and 90 psig $H_2$/CO. The color of the solution after hydroformylation was orange (Figure 5.4), which means that the attachment of the catalyst was not strong enough during the hydroformylation conditions and was released from the silica gel.


**Figure 5.4.** Catalyst after hydroformylation.

In conclusion, the dirhodium catalyst was attached to silica gel via ionic attraction of the $BF_4^-$ anions. It was strong enough to keep the catalyst on silica in a DCM solution at room temperature, but under the actual hydroformylation conditions in acetone the catalyst was released into the solution. It would be worthwhile to repeat the experiment in a nonpolar solvent. For further experiments, immobilization of the dirhodium complex via the sol-gel method might be more suitable. It is also possible to modify the silica surface with a long-chain alkyl halide and attach the tetraphosphine ligand et,ph-P4 via deprotonation of the methylene bridge as previously suggested by Frederick Koch (Figure 5.5).[9] Both methods will be more laborious than

the attempted simple immobilization via the anion method and will be a good challenge for the next student on this project.

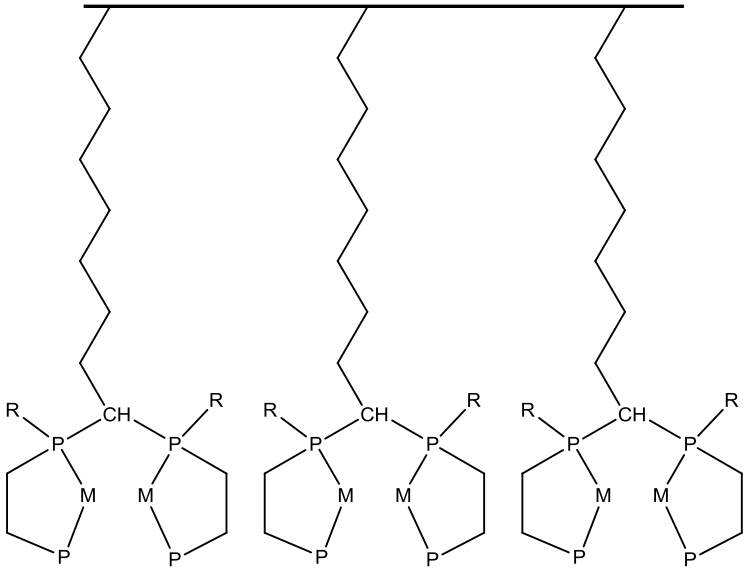


**Figure 5.5.** Scheme of a solid supported et,ph-P4.

### 5.3 References


1. Ding, H.; Hanson, B. E. *J. Mol. Catal. A* **1995,** *99* (3), 131-137.
2. Aubry, D. A.; Bridges, N. N.; Ezell, K.; Stanley, G. G. *J. Am. Chem. Soc.* **2003,** *125* (37), 11180-11181.
3. Merckle, C.; Haubrich, S.; Blumel, J. *J. Organomet. Chem.* **2001,** *627* (1), 44-54.
4. Bogza, M.; Oeser, T.; Blumel, J. *J. Organomet. Chem.* **2005,** *690* (14), 3383-3389.
5. (a) Yang, Y.; Beele, B.; Blumel, J. *J. Am. Chem. Soc.* **2008,** *130* (12), 3771-3773; (b) Sommer, J.; Yang, Y.; Rambow, D.; Blumel, J. *Inorg. Chem.* **2004,** *43* (24), 7561-7563; (c) Blumel, J. *Inorg. Chem.* **1994,** *33* (22), 5050-5056.
6. Lorenzini, F.; Hindle, K. T.; Craythorne, S. J.; Crozier, A. R.; Marchetti, F.; Martin, C. J.; Marr, P. C.; Marr, A. C. *Organometallics* **2006,** *25* (16), 3912-3919.
7. de Rege, F. M.; Morita, D. K.; Ott, K. C.; Tumas, W.; Broene, R. D. *Chem. Comm.* **2000,** (18), 1797-1798.
8. Wiench, J. W.; Michon, C.; Ellern, A.; Hazendonk, P.; Iuga, A.; Angelici, R. J.; Pruski, M. *J. Am. Chem. Soc.* **2009,** *131* (33), 11801-11810.
9. Koch, H. F., PhD Thesis, Louisiana State University, 1997.

# CHAPTER 6: SUMMARY AND FURTHER EXPERIMENTS

## 6.1. Summary

The dirhodium catalyst precursor $[Rh_2(nbd)_2(rac\text{-et,ph-P}_4)](BF_4)_2$ was spectroscopically studied in acetone and 30% water/acetone at various temperatures in order to explain previously reported better hydroformylation results in the water/acetone solvent. Even though NMR studies were performed at significantly lower pressure, the results in acetone were similar to results obtained in previous studies. Facile fragmentation of the dirhodium catalyst in acetone under $H_2$/CO pressure, even at room temperature, occurs to form monometallic, $[RhH_2(\kappa^4\text{-}rac\text{-et,ph-P4})]^+$, and double-ligand dirhodium complexes that are inactive for hydroformylation. Uncertainty in the structure of the double ligand dirhodium degradation product hindered publishing of the spectroscopic studies for many years. Here, a new structure was suggested for the double ligand complex (Figure 6.1) that fits better the results of selective decoupling experiments, $^{31}P\{^1H\}$ NMR and $^{31}P\{1H\}$-$^{31}P\{^1H\}$ COSY. The main difference from the previously suggested structures is that here the hydrides are oriented inwards. We believe that this structure offers the best correlation with the NMR data and previous work with Rh-H phosphine complexes. This will finally allow Prof. Stanley to publish the spectroscopic work of our system in acetone.

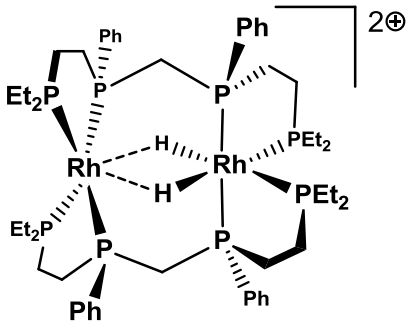


**Figure 6.1.** Suggested structure for the double ligand degradation product.

The NMR and FT-IR experiments in water/acetone have shed considerable light on the differences between the catalyst species present in the two solvent systems. *In-situ* NMR spectroscopy ($^{31}P\{^{1}H\}$NMR and $^{1}H$ NMR) showed slower degradation in water/acetone than in pure acetone. Both $^{31}P\{^{1}H\}$NMR and FTIR spectra demonstrated that $[Rh_2(nbd)_2$(*rac*-et,ph-$P_4)](BF_4)_2$ under $H_2$/CO in water/acetone forms only small amounts of the open-mode hexa/pentacarbonyl complexes, which are the resting state of the catalyst in acetone solution. This is also supported by FT-IR experiment under CO in 30% water/ acetone which shows considerably less penta/hexacarbonyl complexes compared to acetone. The reason might be water blocking coordination of CO to a metal complex or, more likely, interaction of water with bonded CO via hydrogen bonding that enhances CO dissociation from the metal complex. This is supported by the 6 $cm^{-1}$ shift to higher energies of the $\nu_{CO}$ in water/acetone solvent relative to acetone. Moreover, it was observed that norbornadiene under CO atmosphere is released slower from the complex in water/acetone than in acetone, perhaps due to a hydrophobic effect.

The shifting of the catalyst terminal carbonyl bands in water/acetone under $H_2$/CO to lower wavenumbers match up almost perfectly with previous studies of a monocationic monohydride dirhodium catalyst species that could be generated from $[Rh_2H_2(\mu\text{-}CO)_2$(*rac*-et,ph-P4)$]^{2+}$ and $Rh_2(\eta^3$- allyl$)_2$(*rac*-et,ph-P4) via a variety of methods. Also, pH measurements of the catalyst solution in water/acetone are consistent with the dicationic dihydride catalyst, $[Rh_2H_2(\mu$-$CO)_2$(*rac*-et,ph-P4)$]^{2+}$, acting as a strong acid and dissociating one $H^+$ to generate a monocationic monohydride dirhodium catalyst species that is also an effective and more robust hydroformylation catalyst.

All the above contribute to the better hydroformylation performance of the dirhodium catalyst in water/acetone relative to acetone. Our suggested hydroformylation mechanism is

shown in Figure 6.2. The proposed active catalytic species is a monocationic dirhodium monohydride complex. Both rhodium atoms are in +1 oxidation state. This is different from the mechanism in acetone where both rhodium centers in the dicationic dihydride complex are in +2 oxidation state. Another important difference is that there is most likely no formal Rh-Rh bond in the monocationic monohydride, except possibly in one step, while Rh-Rh bonds were previously proposed for several of the key steps for the dicationic dihydride complex.

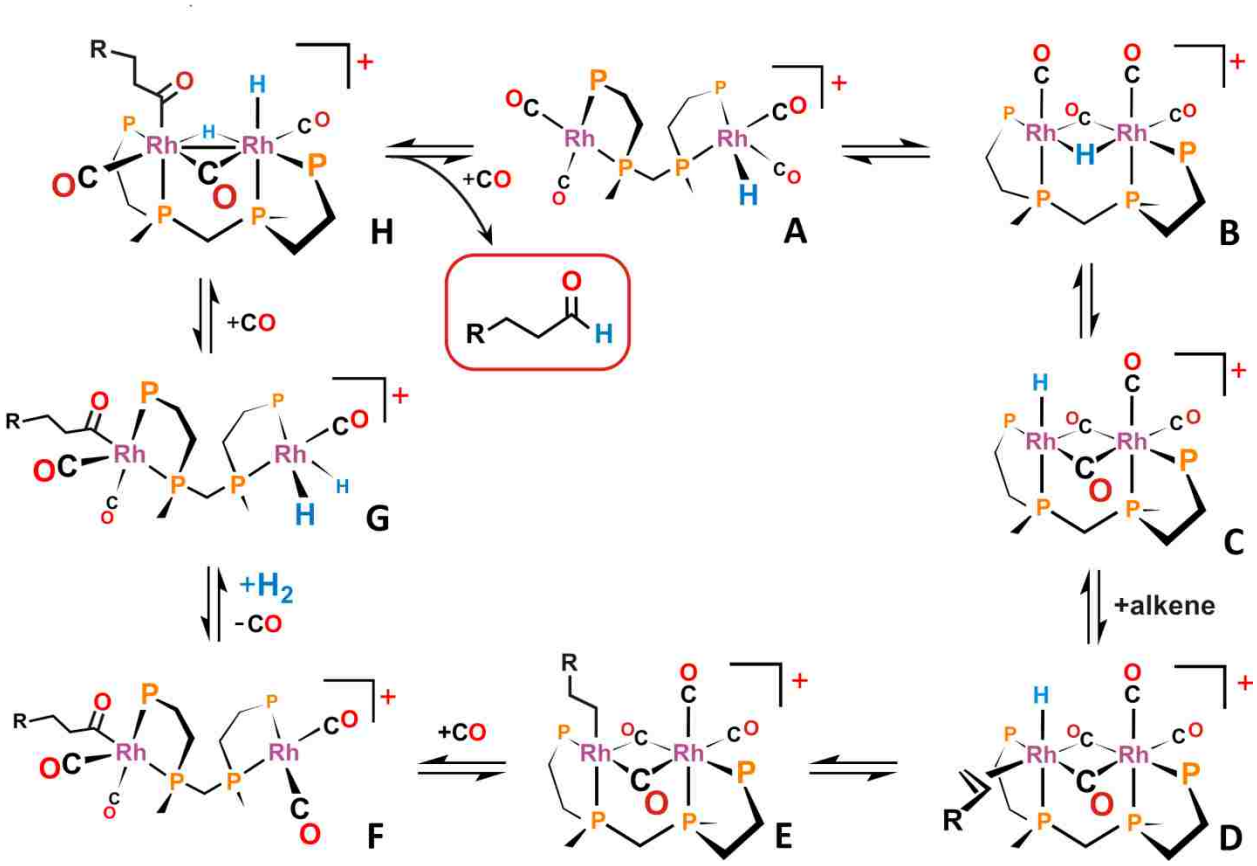


**Figure 6.2.** Suggested mechanism for hydroformylation in acetone/water.

The mechanism in Figure 6.2 starts with the open-mode monocationic dirhodium monohydride complex A. The rhodium atom with the hydride ligand is neutral while the other rhodium center in the molecule is cationic. This complex can readily form a closed-mode

complex B as a result of the interaction between the hydride ligand and the cationic Rh. NMR data indicates a facile equilibrium between the bridged-hydride species B and terminal hydride species C. The lower intensity of the bridging carbonyl bands in the FT-IR also supports the presence of this mono-carbonyl bridged complex in the catalyst mixture.

Alkene can coordinate to the terminal hydride complex, most likely to the rhodium center that contains the hydride ligand. DFT calculations by Zakiya Wilson on the dicationic catalyst demonstrated that the migratory insertion reaction between an alkene and terminal hydride has a considerably lower activation energy relative to the same insertion with a bridging hydride. So we favor the terminal hydride C as the key catalyst species that reacts with alkene. An alkyl group is formed by the migratory insertion of the alkene into the Rh-H bond, which we have shown as the linear alkyl (complex E). In the next step, acyl forms via migratory insertion of CO into the newly formed alkyl and an open mode of the catalyst is shown (complex F). Although the catalyst could stay in a closed-mode structure after the CO migratory insertion, the DFT studies on the dicationic catalyst indicated that the complexes without a Rh-Rh bond could easily convert to open-mode structures. So it is likely that there is an equilibrium between open and closed-mode structures throughout the cycle. Hydrogen can attach to the rhodium center that does not contain the acyl group via oxidative addition (complex G).

This actually would be more favorable for a closed-mode structure where the two interacting filled $d_{z^2}$ orbitals would cause a weak bonding/antibonding set of orbitals. The higher energy MO formed would be more susceptible to $H_2$ oxidative addition, relative to an open-mode complex with two non-interacting Rh centers. One of the two newly formed hydride ligands on the $Rh^{III}$ can do an intermolecular hydride transfer to the $Rh^{I}$ center (complex H), allowing reductive elimination of the aldehyde. This step represents bimetallic cooperativity between the

two rhodium atoms. The dirhodium complex returns to the starting monocationic monohydride open mode form A and the catalytic cycle can start again. A key point in the proposed cycle is that one Rh center is always cationic and will have more facile CO dissociation. This can allow substrate to coordinate, especially $H_2$.

Another possible reaction not shown in the mechanism in Figure 6.2, concerns the excess $H^+$ floating around, which could directly protonate the acyl ligand and release aldehyde from the catalyst. Protons in this case work as a co-catalyst. It is interesting however, that hydrogenation is significantly reduced in water/acetone. So protonation of the alkyl species is clearly slow relative to CO insertion. This could also indicate that protonation of the acyl ligand is slow relative to intramolecular hydride transfer. More studies will be necessary to probe this further.

Due to the deprotonation, it is likely that there are several catalyst species present at the same time in the water/acetone solution. The overview of some of the possible complexes is shown in Figure 6.3. The deprotonated monocationic complexes are highlighted. The dicationic species are also present and the equilibrium can be affected by addition of $H^+$.

In acetone, the dicationic complexes are expected to be dominant and one of the external phosphine arms is expected to fall off a rhodium metal center in the molecule, which results in a loss of one rhodium atom from the complex. In water/acetone, the arm on-off process is slower and less important than in acetone. The reason might be smaller charge on the rhodium in the monocationic complexes compared to the dicationic complexes.

This is similar to observations of Cotton and Pedersen who electrochemically oxidized complex $Re_2Cl_4(PR_3)_4$ into +1 and +2 complexes $[Re_2Cl_4(PR_3)_4]^+$ and $[Re_2Cl_4(PR_3)_4]^{2+}$ with the +2 complex being less stable.[1] Moreover, while studying the same complex, Walton et al. observed formation of new complexes with different number of chlorine and phosphine ligands.[2]

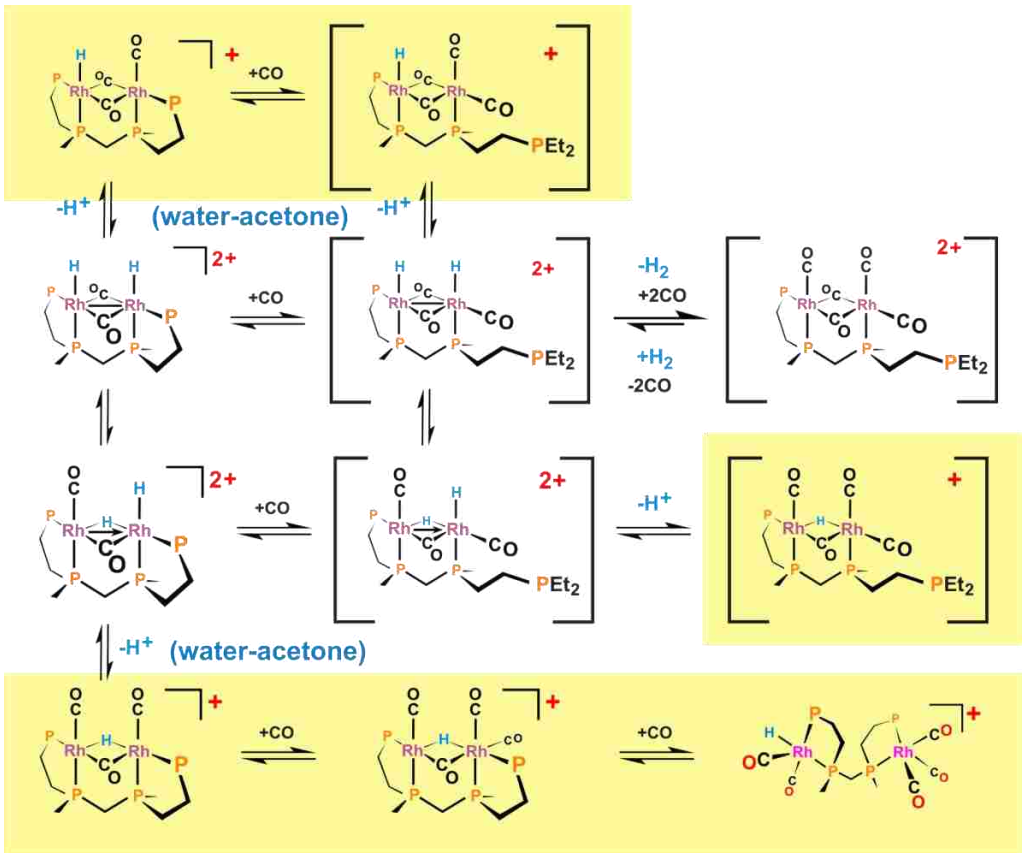


**Figure 6.3.** Some of the possible species present in $[Rh_2(nbd)_2(rac\text{-et,ph-P}_4)](BF_4)_2$ solution exposed to $H_2$/CO in water/acetone.

Reaction scheme of electrochemical oxidation of $Re_2Cl_4(PR_3)_4$ and the corresponding products can be expressed by the following set of equations[3]

$$Re_2Cl_4(PR_3)_4 - 2e^- \longrightarrow [Re_2Cl_4(PR_3)_4]^{2+}$$

$$[Re_2Cl_4(PR_3)_4]^{2+} + Cl^- \longrightarrow [Re_2Cl_5(PR_3)_3]^+ + PR_3$$

$$[Re_2Cl_5(PR_3)_3]^{2+} + Cl^- \longrightarrow Re_2Cl_6(PR_3)_2 + PR_3.$$

These equations demonstrate a tendency of phosphine ligands to dissociate when the complex is oxidized to +1 and +2 ions. Our dirhodium catalyst complex in acetone has charge +2. The phosphine ligands donate electron pairs to the Rh centers that increase the net positive charge on the phosphorus atoms. The electrostatic repulsion between the partial positive charge on the metal center and the partial positive charge on the phosphine ligand weakens the dative bonding.

In the monocationic complexes, there is less electrostatic repulsion that does not promote dissociation as much as in the dicationic system.

Water as a co-solvent enabled activation of the dirhodium tetraphosphine complex when exposed to CO without addition of $H_2$ gas. This was demonstrated by formation of hydride species that were detected by $^1H$ NMR spectroscopy. However, the subsequent experiment in a Parr autoclave showed that the process was not fast and efficient enough for any practical application in hydroformylation.

The dirhodium catalyst was attached to the surface of silica gel in order to enable easy separation of the catalyst from the reaction mixture after hydroformylation. The cationic character of the tetraphosphine dirhodium catalyst was utilized and the catalyst was attached via hydrogen bonding of the $BF_4^-$ anions to the Si-OH groups on silica gel, but unfortunately leaching of the catalyst occurs during hydroformylation conditions in acetone.

**6.2. Future Experiments**

Currently synthesis of a new far stronger chelating tetraphosphine ligand is under way that should be more stable than et,ph-P4 and therefore it should be possible to avoid significant degradation of the catalyst during hydroformylation (Figure 6.4). It might be also advantageous for WGSR that takes longer time than hydroformylation and increased stability of the catalyst is required.

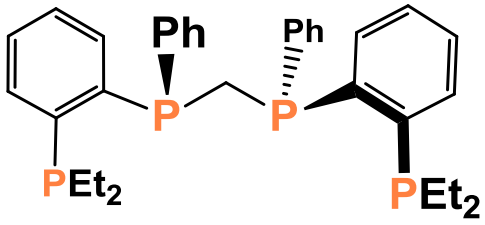


**Figure 6.4.** The new tetraphosphine ligand *rac*-et,ph-P4-Ph.

More NMR experiments of the current hydroformylation catalyst $[Rh_2(nbd)_2(rac\text{-et,ph-}P_4)](BF_4)_2$ would be useful. The structure of the double ligand degradation product in acetone is still speculative due to the inconsistent $^{31}P$ decoupling experiments on the hydride resonances. $^{31}P$-$^{1}H$ HMBC should be attempted again in order to verify correlation of the hydride peaks with the corresponding phosphine atoms. Separation of the degradation products from the reaction mixture after hydroformylation and their crystallization should also be attempted again in order to obtain their crystal structure. However, it is not an easy task since it seems that these hydride containing compounds are rather unstable at atmospheric pressure. Petia Gueorguieva in our group spent a lot of time during her research on trying to isolate degradation products from catalytic mixtures. Since the largest amounts of the double-ligand dirhodium complex are seen in NMR tube experiments, it might be best to focus on high-concentration studies where maximum amounts of this complex are produced.

$^{103}Rh$ NMR experiments would also be useful because rhodium atoms are crucial centers of activity for the hydroformylation process. $^{103}Rh$-decoupled $^{31}P$ and $^{1}H$ and more sophisticated experiments could verify the assignment of the coupling constants and structural assignments.

Since the monocationic monohydride complex is now our primary proposed catalyst for hydroformylation in water/acetone solvent, it would be beneficial to perform theoretical studies on this complex via density functional theory methods. Calculating its electronic structure and relative energy and to compare the results to the dicationic dihydride that is the main catalytic species in acetone should provide some very useful information.

Analogous high pressure NMR and FTIR experiments, as well as DFT computational studies, should be performed on the $[Rh_2(nbd)_2(meso\text{-et,ph-}P_4)](BF_4)_2$ precursor in order to explain its significantly lower hydroformylation activity.

Finally, the water gas shift reaction experiments could be attempted again. Longer duration of the experiment, perhaps one week, would be more suitable. Also the reaction conditions could be optimized by increasing temperature, CO gas pressure and addition of an acid or a salt.

### 6.3. References


1. Cotton, F. A.; Pedersen, E. *J. Am. Chem. Soc.* **1975,** *97* (2), 303-307.
2. Salmon, D. J.; Walton, R. A. *J. Am. Chem. Soc.* **1978,** *100* (3), 991-993.
3. Brant, P.; Salmon, D. J.; Walton, R. A. *J. Am. Chem. Soc.* **1978,** *100* (14), 4424-4430.

# CHAPTER 7: EXPERIMENTAL

## 7.1 General

The tetraphosphine ligand et,ph-P4 was prepared according to previously reported procedures.[1] After the separation of at least 80% *rac*-et,ph-P4 via fractional crystallization in cold hexane, the dirhodium catalyst precursor $[Rh_2(nbd)_2(rac\text{-et,ph-P4})](BF_4)_2$ was synthesized.[1] All reactions were performed under nitrogen atmosphere in a glove box or on a Schlenk line. A NMR spectrum of the product after each synthetic step was recorded on a Bruker DPX-250 or Bruker DPX-400 spectrometer. Anhydrous and deuterated solvents were used as received from the manufacturer.

Hydroformylation experiments were performed in a Parr autoclave and the products were analyzed via GC-MS using an Agilent Technologies 6890N Network GC System. Both Bruker Tensor 27 FT-IR instrument and a React-IR instrument from Mettler-Toledo were employed for in-situ FT-IR experiments. High-pressure NMR samples were prepared in Wilmad NMR tubes and measured on DPX-400 NMR spectrometer.

## 7.2 Hydroformylation of 1-hexene

A flask was charged in a glove box with 90 mg $[Rh_2(nbd)_2(rac\text{-et,ph-P}_4)](BF_4)_2$ and 80 mL of solution containing 70% acetone and 30% water by volume. The solution also contained 2 mL of toluene as an internal standard that was included in the total volume. When needed, $NEt_3$ or $HBF_4$ were added to the catalyst solution. 1-hexene (6.73 g) was filtered through an alumina column in order to remove peroxide impurities and placed in a vial. Both the vial and the flask with the catalyst solution were sealed with rubber septa.

Hydroformylation reactions were carried out in a stainless steel Parr autoclave (Figure 7.1) with a magnetic stirrer. After the autoclave was evacuated, the olefin was transferred into a

closed arm on the autoclave via cannula. The catalyst solution was transported via cannula directly into the autoclave.

**Figure 7.1.** The Parr autoclave.

The autoclave was pressurized to 45 psig $H_2$/CO (1:1) and consequently heated to 90 °C with stirring (1000 rpm). Temperature was monitored by a thermocouple and a pressure transducer was used to monitor pressure. The catalyst was left soaking at 90 °C for 20 minutes then 1-hexene was pressure injected from the side arm into the autoclave. While pressure in the autoclave was 90 psig during the whole run, the pressure in a gas reservoir decreased.

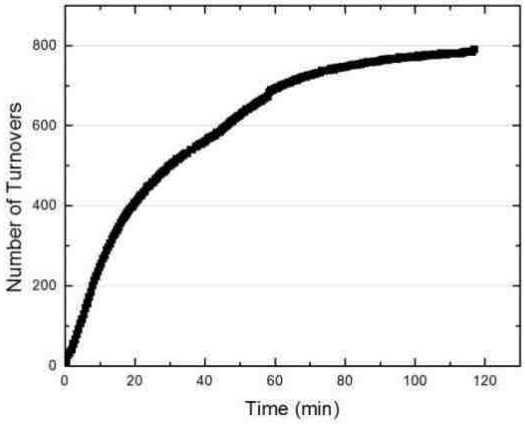


**Figure 7.2.** Aldehyde production curve.

Figure 7.2 shows an example of an aldehyde production curve. The amount of the produced aldehyde is calculated from the recorded pressure decrease. During hydroformylation, 1-2 mL samples were removed in regular intervals and analyzed by GC-MS on an Agilent

Technologies 6890N Network GC System in order to determine the L:B aldehyde ratio and the amount of side products. The column employed was HP5MS (30 m long).

### 7.3 High-pressure NMR

Since high gas pressure is applied to the catalyst sample, a special glass NMR tubes with thick walls had to be used. The Wilmad tube (524-PV-7) with a Teflon valve is shown at Figure 7.3. The threads of the valve both at the top and bottom were wrapped in Teflon tape for higher security.

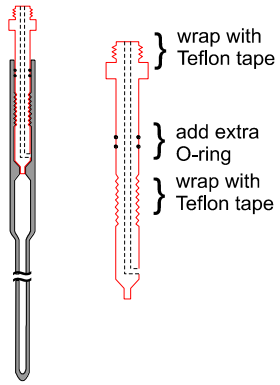


**Figure 7.3.** The scheme of a Wilmad high-pressure NMR tube.

Deuterated acetone (with TMS as internal standard) and deuterium oxide were obtained from Sigma-Aldrich and used as received. $^{31}P\{^{1}H\}$ and $^{1}H$ NMR spectra were recorded at a Bruker DPX-400 instrument.

Catalyst solution was prepared in a glove-box. The sample in the NMR tube, sealed with the Teflon valve, was removed from the glove-box and attached to a gas line. The top of the Teflon valve was flushed with small flow of $H_2$/CO gas, then the valve was opened and gas flow was increased to the desired pressure. The NMR tube was left open to the gas for at least 30 min and shook in 10 min intervals. The original concentration in acetone was 30 mM, but in water it was only 10 mM due to the limited solubility of the catalyst. Most of the samples were filled

with syngas to 90-100 psig $H_2$/CO in order to observe the catalyst at the conditions close to the real hydroformylation runs.

When $d_6$-acetone and $D_2O$ are used as solvents, hydrides might not be visible in $^1$H NMR spectra due to the hydride exchange. Therefore, $H_2O$ was used instead $D_2O$. Nevertheless, it is difficult to observe hydrides in the $^1$H NMR spectrum due to the large water signal. The problem was solved by using water suppression techniques presaturation and WATERGATE.

### 7.4 In-situ FT-IR

High pressure FT-IR studies were performed using either a Bruker Tensor 27 FT-IR instrument or a ReactIR instrument from Mettler-Toledo. The Bruker Tensor 27 FT-IR instrument contains a SpectraTech circle reaction cell (CRC) (Figure 7.4), which is basically a Parr autoclave with a cylindrical crystal (silica) leading from one side of the cell to the opposite side. The cell works on principle Attenuated Total Reflectance (ATR), where the IR beam and response of the sample are transported through the crystal while the autoclave itself is closed and pressurized. A thermocouple and a pressure transducer are employed to monitor temperature and pressure. Gas can be introduced to or released from the autoclave by a system of valves. An FT-IR spectrum is generated from the information collected from a mercury cadmium telluride (MCT) detector which is cooled with liquid nitrogen to −196 °C to minimize thermal noise.

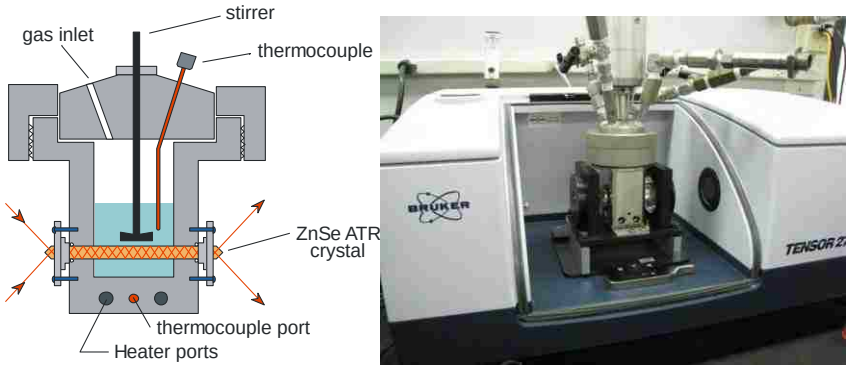


**Figure 7.4.** Spectra Tech Circle reaction cell (left) and Bruker Tensor 27 FT-IR instrument (right).

The ReactIR (Figure 7.5) is also based on a Parr autoclave, but the inner design differs from the Spectra Tech Reaction Circle cell.

**Figure 7.5.** ReactIR.

The procedure of taking spectra was similar on both instruments. Samples were prepared in a glove box and sealed in vials with septa. The concentration of the samples was 10 mM. Solution volume for ReactIR was 10 mL, while for CRC it was 13 mL.

Prior to each FT-IR experiment, the first spectrum was recorded without any solution, then background spectra of the solvent were taken under around 45 psig $H_2$/CO at room temperature and in 10 °C increments up to 90 °C. The background spectra were stored and later used for subtraction from the spectra of the sample at the corresponding temperature.

Prior to measurement of the catalyst sample, the reaction cell was purged with nitrogen to remove any traces of air. The catalyst solution was transferred inside the reaction cell via syringe and put under small pressure of gas (CO or $H_2$/CO). The sample was stirred at 400 rpm and an initial room temperature scan was taken. Afterwards the gas pressure and temperature were increased and other spectra were recorded. The highest values were commonly 90 °C and 90 psig gas.

**7.5 References**

1. Alexander, C. T., PhD Thesis, Louisiana State University, 2009.

# VITA

Darina Polakova was born in Prague, Czech Republic. She attended the Czech Technical University where she received master's degree in chemistry. She enrolled at LSU in 2006. She is currently a candidate for the Doctor of Philosophy degree at the Department of Chemistry under guidance of Prof. George G. Stanley. She married Gregory Schelonka in June 2011.